CMB ANISOTROPIES: STATUS & PROSPECTS

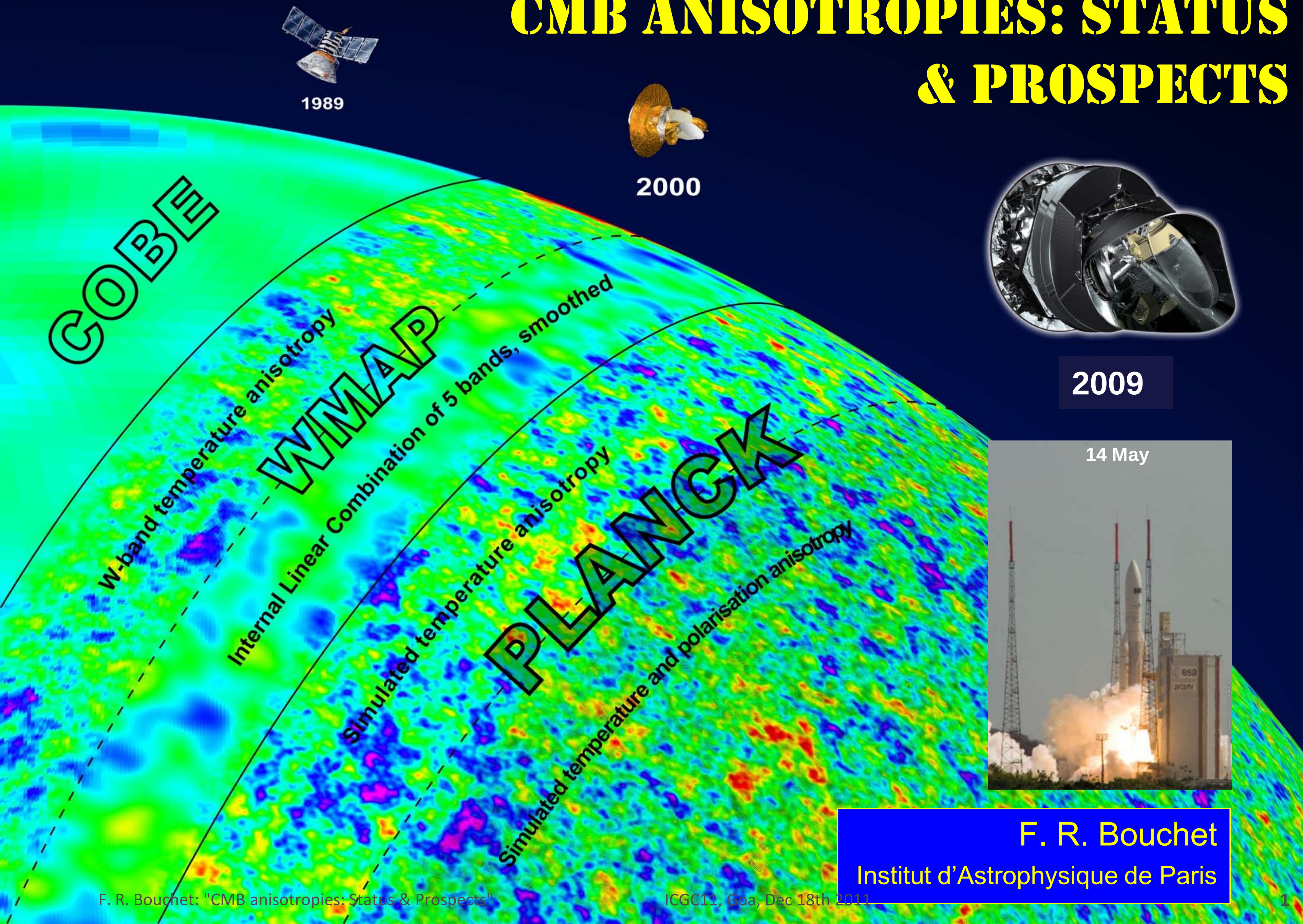

F. R. Bouchet
Institut d'Astrophysique de Paris

CMB information mine

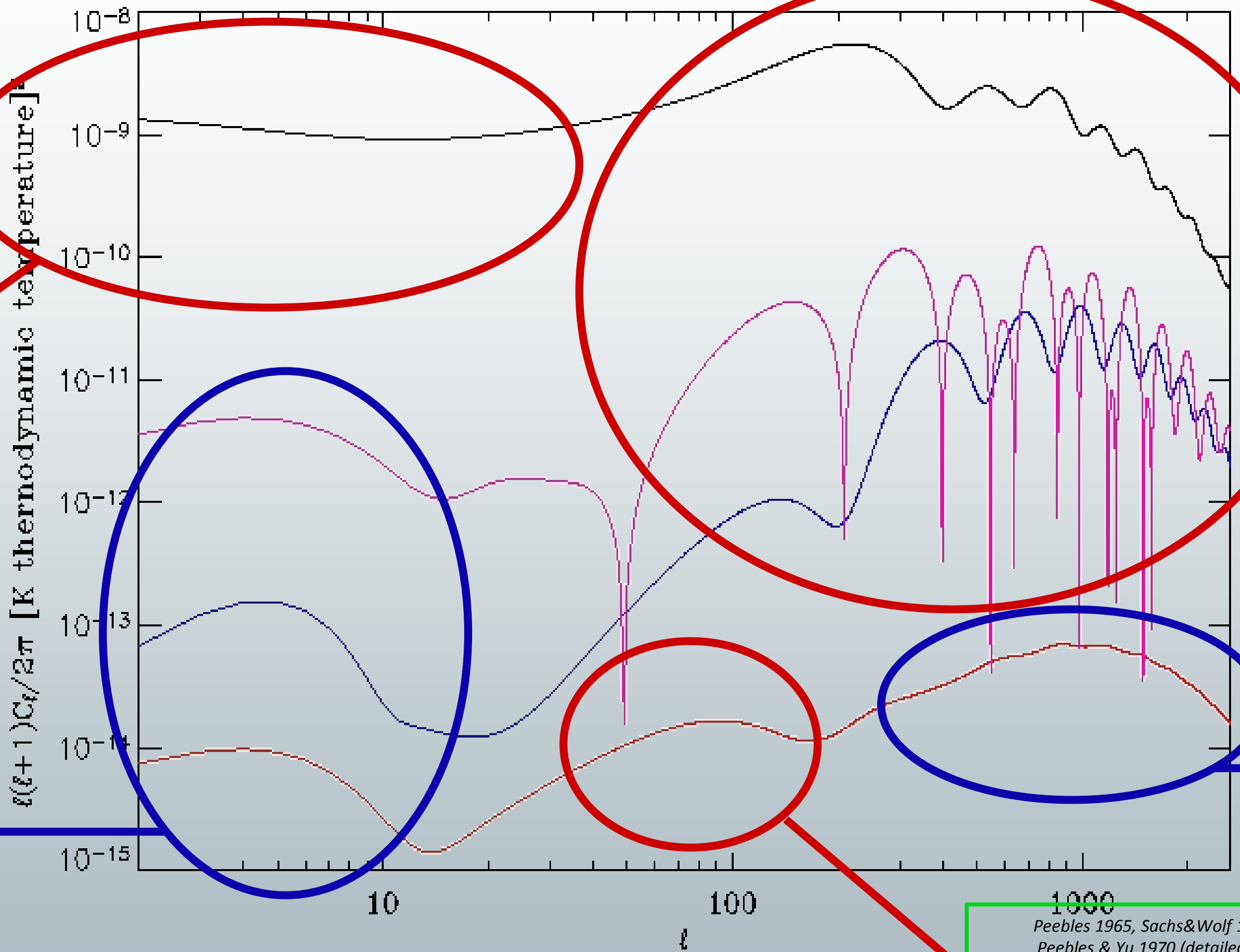

Acoustic oscillations

Primordial power

Reionisation

Lensing

Gravity waves

Note ΔT values range

Observable related to physical parameters through well-understood, mostly linear physics

Angle ≈ 200/l degrees

Peebles 1965, Sachs&Wolf 1967, Silk 1968, Sunyaev &Zeldovich 1969, Peebles & Yu 1970 (detailed rec.)… simulated maps Bond&Efstathiou 1987(Inflation) Bouchet,Bennett&Stebbins1988(strings)… public codes CMBFAST [Seljack & Zaldarriaga 96], CAMB [Lewis et al. 2000], CLASS… Kamionkowski et al 1997, Zaldarriaga & Seljak 1997 [E, B], NG…

+ all other statistical properties (NG)

THE ASTROPHYSICAL JOURNAL, 162:815–836, December 1970

PRECISION COSMOLOGY…
First numerical CMB calculation (to go through recombination)

PRIMEVAL ADIABATIC PERTURBATION IN AN EXPANDING UNIVERSE*

1965+5…

P. J. E. PEEBLES†
Joseph Henry Laboratories, Princeton University
AND
J. T. YU‡
Goddard Institute for Space Studies, NASA, New York
Received 1970 January 5; revised 1970 April 1

ABSTRACT

The general qualitative behavior of linear, first-order density perturbations in a Friedmann-Lemaître cosmological model with radiation and matter has been known for some time in the various limiting situations. An exact quantitative calculation which traces the entire history of the density fluctuations is lacking because the usual approximations of a very short photon mean free path before plasma recombination, and a very long mean free path after, are inadequate. We present here results of the direct integration of the collision equation of the photon distribution function, which enable us to treat in detail the complicated regime of plasma recombination. Starting from an assumed initial power spectrum well before recombination, we obtain a final spectrum of density perturbations after recombination. The calculations are carried out for several general-relativity models and one scalar-tensor model. One can identify two characteristic masses in the final power spectrum: one is the mass within the Hubble radius ct at recombination, and the other results from the linear dissipation of the perturbations prior to recombination. Conceivably the first of these numbers is associated with the great rich clusters of galaxies, the second with the large galaxies. We compute also the expected residual irregularity in the radiation from the primeval fireball. If we assume that (1) the rich clusters formed from an initially adiabatic perturbation and (2) the fireball radiation has not been seriously perturbed after the epoch of recombination of the primeval plasma, then with an angular resolution of 1 minute of arc the rms fluctuation in antenna temperature should be at least $\delta T/T = 0.00015$.

I. INTRODUCTION

a) Purpose

The possible discovery of radiation from the primeval fireball opens a promising lead toward a theory of the origin of galaxies. This primeval radiation would serve, first, to fix an epoch at which nonrelativistic bound systems like galaxies can start to develop (Peebles 1965*a*), and second, to impress on the power spectrum of initial density fluctuations characteristic lengths and masses (Gamow 1948; Peebles 1965*a*, 1967*a*; Michie 1967; Silk 1968). These characteristic features in the power spectrum hopefully result from all the complicated details of the evolution of the Universe *after* the initial power spectrum is arbitrarily set at some very early epoch. If one can make a reasonable argument for a coincidence of these features with observed phenomena, it will provide an important encouragement and guide to the further development of the theory. A more direct observational test of these processes might be provided by the residual small-scale fluctuations in the microwave background (Peebles 1965*b*; Sachs and Wolfe 1967; Silk 1968; Wolfe 1969; Longair and Sunyaev 1969), if we assume that this radiation has not been further scattered (Dautcourt 1969).

* Research supported in part at Princeton by the National Science Foundation and the Office of Naval Research of the U.S. Navy, and at the California Institute of Technology by the National Science Foundation [GP-15911 (formerly GP-9433) and GP-9114] and the Office of Naval Research [Nonr-220(47)].

† Alfred P. Sloan Fellow.

‡ NAS-NRC Postdoctoral Research Associate.

Initial CMB Calculations

Matter calculations

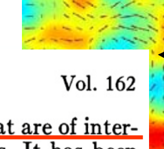

According to Zel'dovich (1967) there are two kinds of perturbations that are of interest: initial isothermal perturbations and initially adiabatic perturbations. It has been suggested that the globular clusters are the remnants of an isothermal perturbation in the early Universe (Peebles and Dicke 1968; Peebles 1969). Our purpose here is to discuss in some detail the evolution of adiabatic density fluctuations in the primeval-fireball picture.

An initially adiabatic perturbation evolves through four regimes: (*a*) When the age t of the Universe is much less than λ/c, where λ is the characteristic scale of the perturbation, a fractional perturbation $\delta\rho/\rho$ to the total mass density grows with time, but the entropy per nucleon is conserved (hence adiabatic). (*b*) When $\lambda \ll ct$, the perturbation oscillates like an acoustic wave. (*c*) As the Universe expands through the recombination phase, the photon mean free path becomes comparable to λ, and the oscillating wave is attenuated, leaving some residual perturbation in the matter distribution. (*d*) When $T \lesssim 2500°$ K, recombination is sufficiently complete that radiation drag on the matter may be neglected, and the residual perturbation may start to grow into bound systems like protogalaxies.

The above general scheme for initially adiabatic perturbations was already given by Lifshitz (1946). The very complicated regime (*c*) has been considered by a number of people in a variety of approximations, with the general conclusion that initially adiabatic perturbations on a characteristic mass scale $\lesssim 10^{11}$–$10^{13}\ \mathfrak{M}_\odot$ are strongly attenuated. This problem was first considered in approximations to first order in the photon mean free time t_c independently by Michie (1967), Peebles (1967*a*), and Silk (1968). It has since been considered by Bardeen (1968) in the first twenty moments of the radiation distribution function, and by Field (1970*a*), who solves the problem to all orders in t_c when the expansion of the Universe may be neglected. However, these approximation schemes run afoul of the enormous variation and rate of variation of the photon mean free path through the epoch of recombination. As a result, previous workers on this subject (Peebles 1967*a*; Michie 1967; Silk 1968; Field and Shepley 1968) could give only qualitative estimates of the different characteristic masses involved here. To obtain a more accurate description of the evolution through this complicated phase of recombination, we have resorted to direct numerical integration of the collision equation for the photon distribution function.

The more quantitative results of the present calculation are compared with the earlier estimates in § VII. We also discuss there the possible significance of these results. In § II we derive the differential equations to be integrated. It is impractical to integrate the collision equation numerically in the very early Universe because the photon mean free path t_c is so short, but here it becomes a good approximation to describe the radiation as a fluid with viscosity. This description of the radiation was used in all the previous work (Lifshitz 1946; Michie 1967; Silk 1968; Field and Shepley 1968), and is indeed a good approximation in this early epoch. The fluid description of radiation is equivalent to an expansion and integration of our collision equation to first order in t_c. In § III we give the resulting equations valid to first order in t_c, and we present solutions to these approximate equations under various limiting conditions. These results are used to start the numerical integration and to check numerical accuracy. In § IV we consider the residual perturbation to the microwave background. The numerical integrations are described in §§ V and VI.

b) Assumptions and Approximations

In the following calculations we use either conventional general-relativity theory, with cosmological constant Λ equal to zero, or the scalar-tensor theory (Brans and Dicke 1961). We start from a homogeneous, isotropic cosmological model, in which the present parameters are

$$H_0^{-1} = 1 \times 10^{10}\ \text{years}, \quad T_0 = 2.7°\ \text{K}. \tag{1}$$

МЕЛКОМАСШТАБНЫЕ ФЛУКТУАЦИИ РЕЛИКТОВОГО ИЗЛУЧЕНИЯ*

Я. Б. ЗЕЛЬДОВИЧ и Р. А. СЮНЯЕВ
Институт Прикладной Математики, Москва

(Received 11 September, 1969)

Аннотация. Возмущения плотности вещества в однородной и изотропной космологической модели, приводящие к образованию галактик, должны на еще более ранней стадии эволюции вызывать пространственные флуктуации реликтового излучения. Силк предположил, что между возмущениями плотности на момент рекомбинации первичной плазмы и флуктуациями наблюдаемой температуры излучения имеется адиабатическая связь $\delta T/T = \frac{1}{3}(\delta\varrho_m/\varrho_m)$.

В предлагаемой работе показано, что такая простая связь не имеет места, вследствие:

(1) немгновенности рекомбинации

(2) из-за того, что когда области с $M < 10^{15}\,M_\odot$ становятся прозрачными для излучения, еще велика оптическая толща до наблюдателя по томпсоновскому рассеянию

(3) скачкообразного увеличения $\delta\varrho_m/\varrho_m$ в ходе рекомбинации

В результате ожидаемые флуктуации температуры реликтового излучения должны быть меньше адиабатических. В статье вычислено $\delta T/T$, возникающее при рассеянии излучения на движущихся электронах; поле скоростей генерируется адиабатическими или энтропийными возмущениями плотности. Оценены также флуктуации реликтового излучения, возникающие при вторичном разогреве межгалактического газа.

Детальное исследование спектра флуктуаций в принципе может позволить выяснить природу первичных возмущений плотности; так как адиабатическим возмущениям свойственна своеобразная периодическая зависимость спектральной плотности возмущений от длины волны (массы). Практически наблюдения весьма трудны из-за малости эффекта, и из-за наличия флуктуаций, связанных с дискретными источниками радиоизлучения.

1. Введение

В современной горячей модели Вселенной предполагается, что в далеком прошлом, до рекомбинации первичной плазмы, во времена, соответствующие красному смещению $z \sim 1000$, галактик не было, а возникновение галактик связано с незначительными отклонениями от строгой однородности, существовавшими в тот период.

В первом приближении можно считать, что после рекомбинации протонов и электронов 'вещество' – нейтральные атомы – не взаимодействует с излучением, и реликтовое излучение (имеющее в настоящее время среднюю температуру 2.7 K) непосредственно приносит нам информацию о состоянии при $z \sim 1000$. В частности, отклонения температуры от средней в зависимости от направления наблюдения, проводимого сейчас с Земли, характеризуют именно отклонения от однородности, т.е. зависимость физических величин от координат в пространстве на ранней стадии.

Эти отклонения в дальнейшем (после рекомбинации) возрастают за счет гравитационной неустойчивости. За момент образования обособленных объек-

* An English translation of this paper will be published in a next issue of this journal.

Astrophysics and Space Science 6 (1970) 358–376. *All Rights Reserved*

1970Ap&SS...7....3S

SMALL-SCALE FLUCTUATIONS OF RELIC RADIATION*

R. A. SUNYAEV and YA. B. ZELDOVICH
Institute of Applied Mathematics, Academy of Sciences of the U.S.S.R., Moscow, U.S.S.R.

(Received 11 September, 1969)

Abstract. Perturbations of the matter density in a homogeneous and isotropic cosmological model which leads to the formation of galaxies should, at later stages of evolution, cause spatial fluctuations of relic radiation. Silk assumed that an adiabatic connection existed between the density perturbations at the moment of recombination of the initial plasma and fluctuations of the observed temperature of radiation $\delta T/T = \delta\varrho_m/3\varrho_m$. It is shown in this article that such a simple connection is not applicable due to:

(1) The long time of recombination;

(2) The fact that when regions with $M < 10^{15}\,M_\odot$ become transparent for radiation, the optical depth to the observer is still large due to Thompson scattering;

(3) The spasmodic increase of $\delta\varrho_m/\varrho_m$ in recombination.

As a result the expected temperature fluctuations of relic radiation should be smaller than adiabatic fluctuations. In this article the value of $\delta T/T$ arising from scattering of radiation on moving electrons is calculated; the velocity field is generated by adiabatic or entropy density perturbations. Fluctuations of the relic radiation due to secondary heating of the intergalactic gas are also estimated.

A detailed investigation of the spectrum of fluctuations may, in principle, lead to an understanding of the nature of initial density perturbations since a distinct periodic dependence of the spectral density of perturbations on wavelength (mass) is peculiar to adiabatic perturbations. Practical observations are quite difficult due to the smallness of the effects and the presence of fluctuations connected with discrete sources of radio emission.

1. Introduction

In the contemporary 'big-bang' model of the Universe it is hypothesized that in the distant past, before recombination of the initial plasma at times corresponding to a red shift $z \sim 1000$, there were no galaxies and the origin of galaxies is connected with insignificant deviations from strict homogeneity existing in that period. In the first approximation it can be considered that after recombination of protons and electrons 'matter' – neutral atoms – do not interact with radiation and relic radiation (having at present an average temperature of 2.7 K) immediately gives us information about conditions for $z \sim 1000$. In particular, the dependence of deviations of temperature on the direction of observation now being performed from the Earth characterizes the dependence of physical values, i.e. deviations of density, on the spatial coordinates at an earlier stage. These deviations grow in the future (after recombination) due to gravitation instability. For the moment of formation of separate objects it is reasonable to take the time of origin of regions with densities at least twice the average density, i.e. $\delta\varrho/\varrho \sim 1$. It is assumed that this occurred relatively recently (on a logarithmic time scale) at $z \sim 2 \approx 10$. In this case an estimate for the perturbation at the moment of recombination gives $\delta\varrho/\varrho \sim 10^{-2}$–$10^{-3}$, i.e., it is possible to speak about

* Translated from the Russian by D. F. Smith.

Astrophysics and Space Science 7 (1970) 3–19. *All Rights Reserved*

Mon. Not. R. astr. Soc. (1987) **226**, 655–687

1987: 1st detection is still 5 years away!
(Pionneering calculations 20 yrs earlier)

The statistics of cosmic background radiation fluctuations

J. R. Bond *Canadian Institute for Theoretical Astrophysics, Toronto, ON M5S 1A1, Canada*

G. Efstathiou *Institute of Astronomy, Madingley Road, Cambridge CB3 0HA and Institute for Advanced Study, Princeton, NJ 08540, USA*

Accepted 1987 January 9. Received 1986 November 25

Summary. We present computations of the radiation correlation functions and angular power spectra for microwave background anisotropies expected in $\Omega = 1$ cold dark matter dominated universes with scale-invariant adiabatic or isocurvature initial conditions. The results are valid on all angular scales. We describe the statistical properties of the radiation pattern and develop the theory of two-dimensional Gaussian random fields. A large number of properties of such fields may be derived analytically or semi-analytically, such as the number densities of hotspots and coldspots, the eccentricities of peaks and peak correlation properties. The formulae presented here provide valuable insight into the textural characteristics of the microwave background anisotropies and must be satisfied if the primordial fluctuations are Gaussian. The assumption of Gaussian initial conditions allow us to make highly specific predictions for the pattern of the temperature anisotropies. This is demonstrated by the construction of maps of the fluctuations predicted for the total intensity and the polarization.

1 Introduction

The origin of density irregularities in the Universe represents one of the most important problems in cosmology which, until recently, was largely considered intractable. The inflationary model of the early Universe has, however, led to a potentially viable mechanism for the origin of primordial density fluctuations (e.g. Starobinskii 1982; Guth & Pi 1982; Bardeen, Steinhardt & Turner 1983). Although these calculations are hardly definitive, they have succeeded in drawing attention to a particular set of initial conditions, namely scale-invariant, Gaussian fluctuations superimposed on an $\Omega = 1$ Friedman background.

In this paper, we investigate the statistical properties of the cosmic microwave background radiation (CMB), assuming that the initial fluctuations are Gaussian. The background radiation will then form a 2D Gaussian random field and should provide a clean and direct test of the statistics of the initial conditions. Given a particular cosmological model, we can compute all statistical aspects of the radiation pattern. It is unfortunate, then, that CMB anisotropies have yet

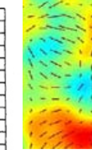

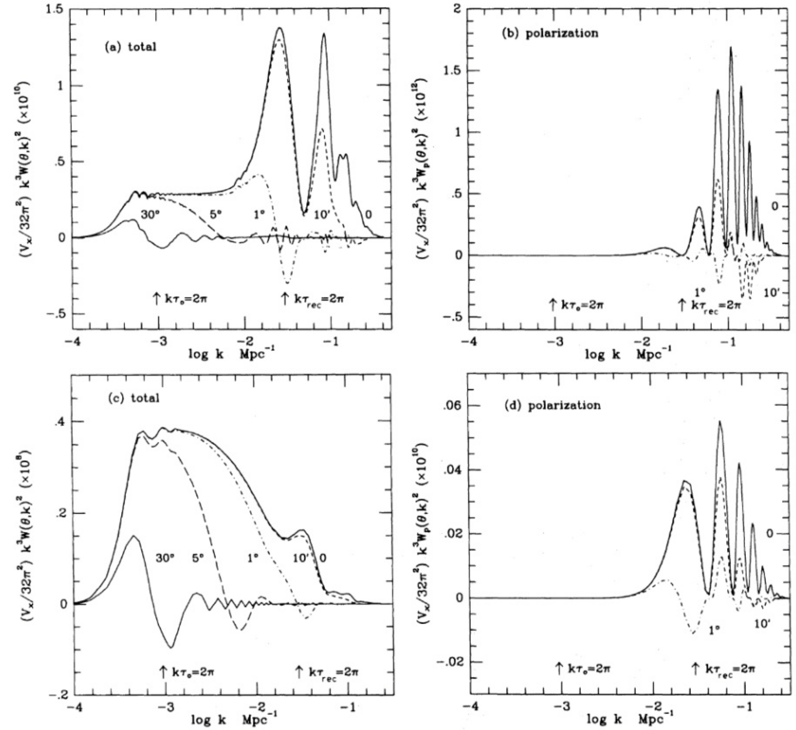

Figure 4. Integrands of the radiation autocorrelation function $k^3 W_T^2(\theta, k)$ plotted against $\log k$ for various θ. (a, b) Show the integrands for the total and polarization correlation functions, respectively for a scale-invariant adiabatic CDM model with $\Omega = 1$, $\Omega_B = 0.03$, $h = 0.75$. (c, d) Show the equivalent plots for a scale-invariant isocurvature CDM model with identical cosmological parameters. The area under each curve gives $C(\theta)$ thus it is easy to assess how fluctuations on various scales would contribute to experiments probing any particular angle. These curves have been normalized according to the prescription given in Section 4.2 with the biasing parameter $b = 1$.

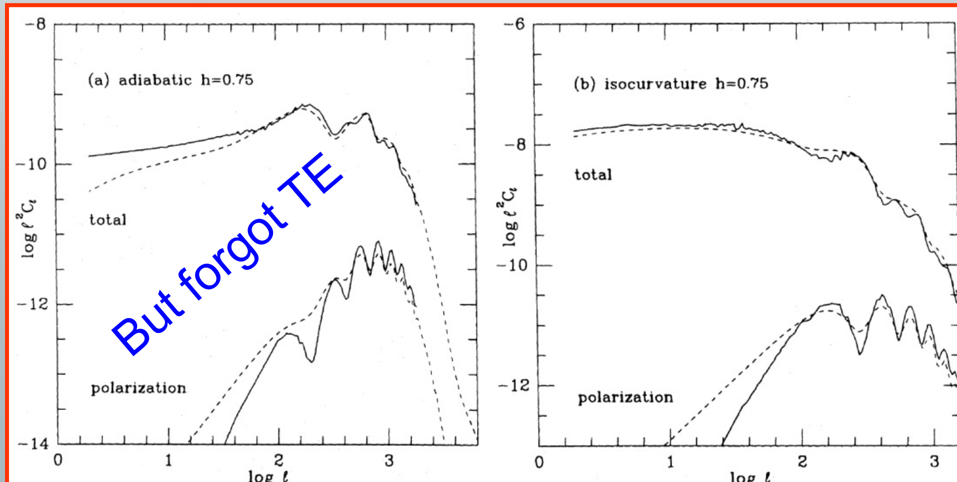

Figure 7. Power spectra for the two $h = 0.75$ scale-invariant CDM models. The solid lines show results from equation (4.17) and the dotted lines show approximate results derived from equation (4.19).

And map realisations in T & P...

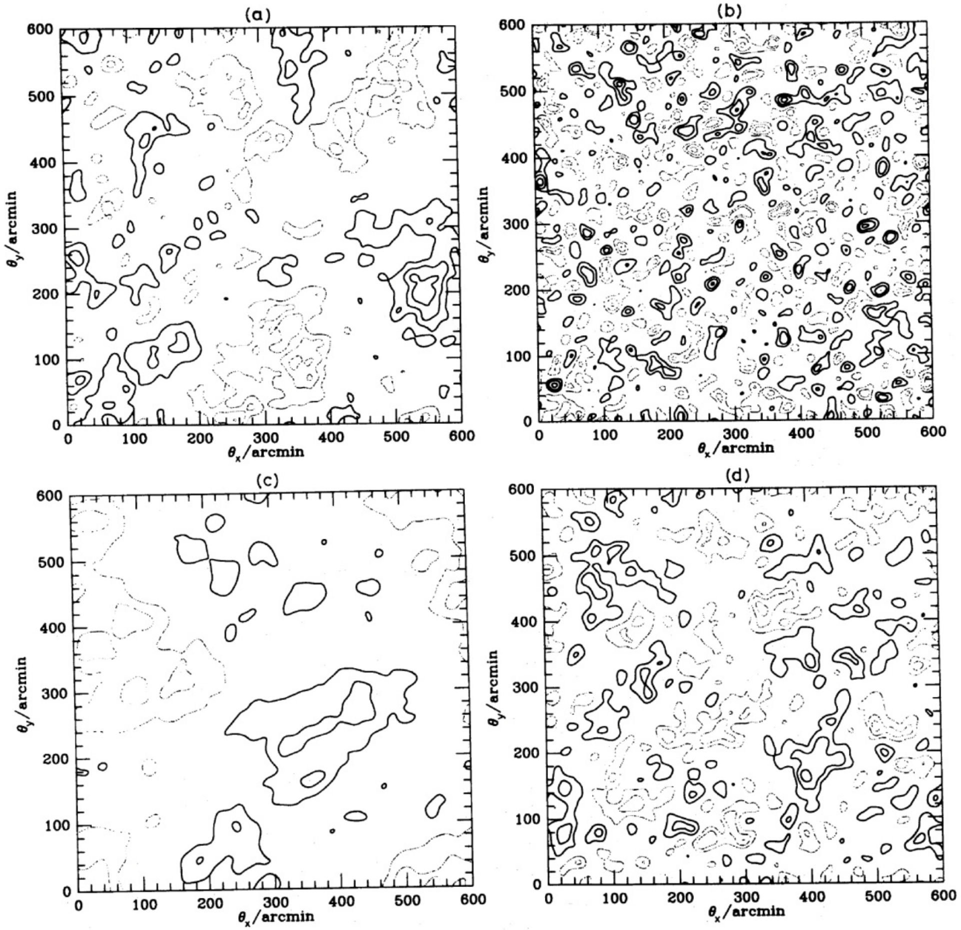

Figure 8. Realization of the Gaussian temperature and polarization fluctuations constructed using the method described in Section 5. (a, b) Show maps of the total and polarization fluctuations respectively for the $h=0.75$ scale-invariant adiabatic CDM model. (c, d) Show analogous maps for the $h=0.75$ scale-invariant isocurvature model. In constructing these plots, we used a 512×512 grid and a smoothing angle of $\theta_s=5$ arcmin. The heavy contours correspond to $\nu=1$, 2 and 3 upward fluctuations and the light lines show equivalent contours for the downward fluctuations.

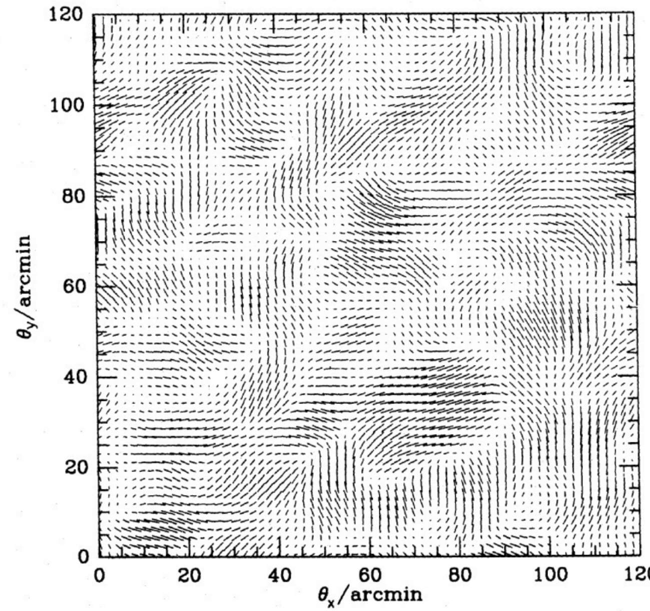

Figure 9. Simulation of the degree and spatial variation of the plane of polarization in a $2°\times2°$ patch for the $h=0$ adiabatic model simulated in Fig. 8. The length of each vector is proportional to the degree of polarization and orientation gives the plane of polarization. This picture was constructed on a 128×128 grid using a smoothing angl $\theta_s=1$ arcmin. For visual clarity, we only plot 64×64 vectors.

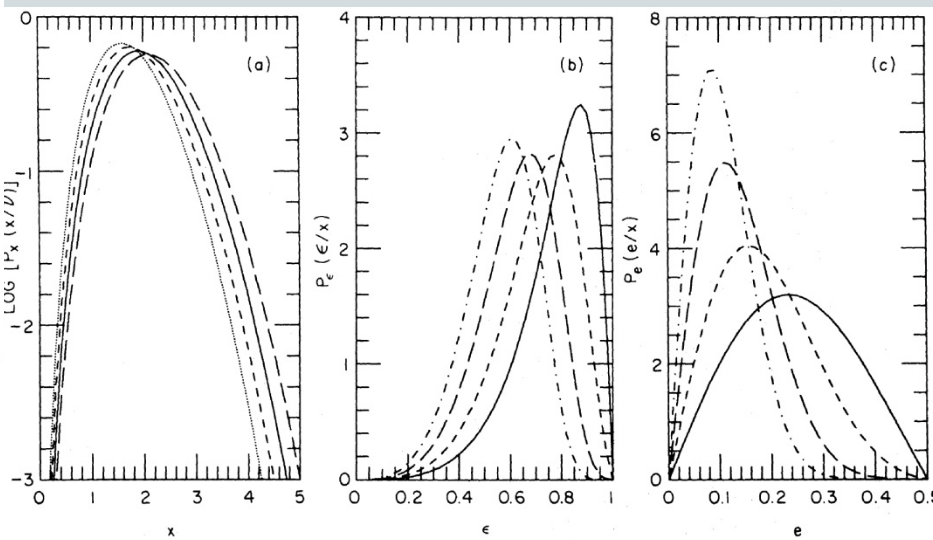

Figure 2. (a) The conditional probability of the curvature parameter $x=|\nabla^2 F/\sigma_2|$ given the height $\nu=0$ (dot), 1 (short dash), 2 (solid), 3 (long dash) of the maximum (or minimum) is plotted for $\gamma=0.347$, the value appropriate to the $h=0.75$ adiabatic CDM model. The eccentricity (b) and ellipticity (c) distributions for $x=1$ (solid), 2 (short dash), 3 (long dash) and 4 (dot-dash) are independent of the spectral parameters and ν. Integration over x gives the ϵ and e distributions for specified values of the peak height ν [equation (A2.6), Appendix 2].

Expected maps in the presence of cosmic strings

Then considered as an alternative for seeding LSS, which we know now to be sub-dominant

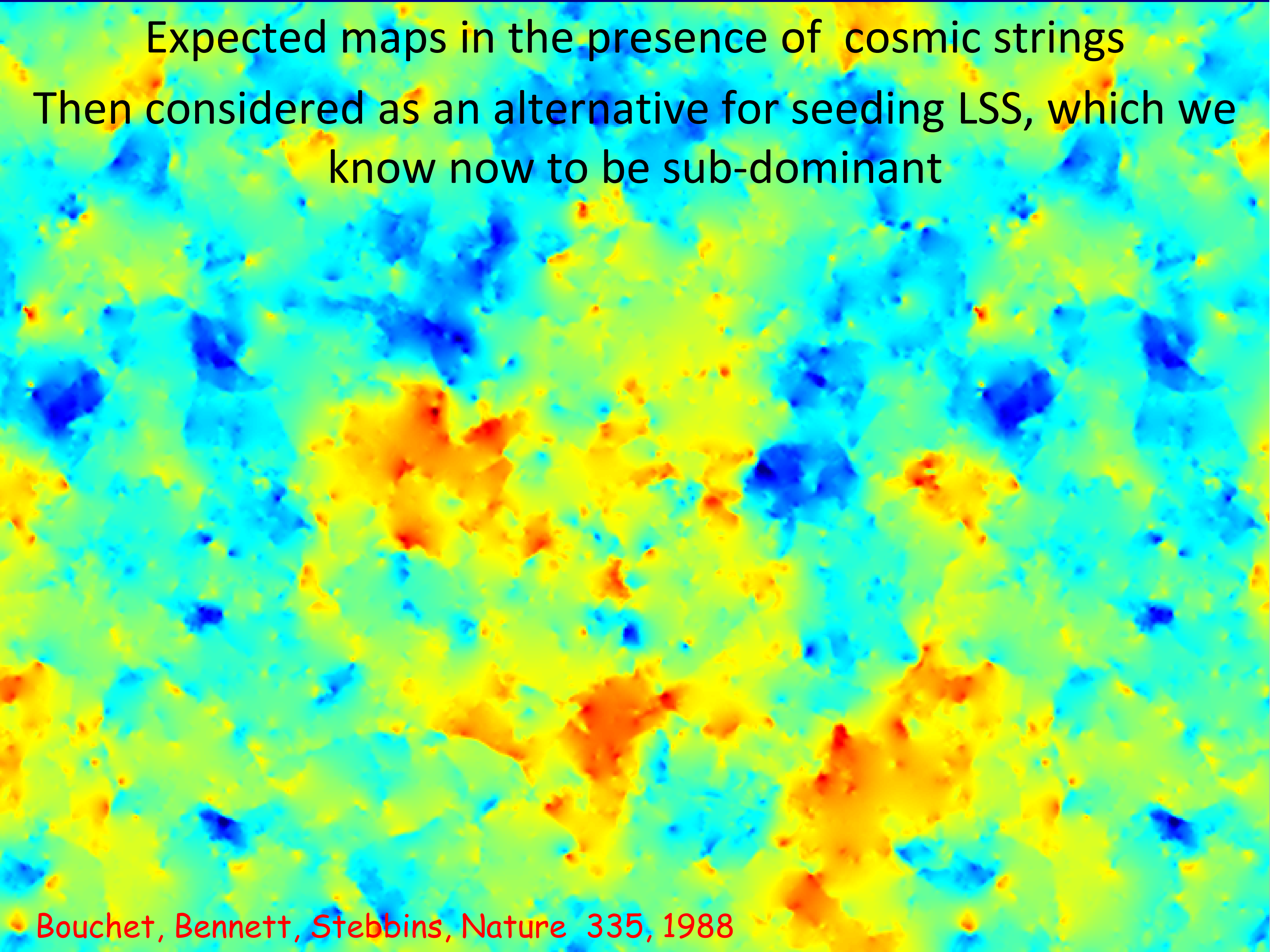

Bouchet, Bennett, Stebbins, Nature 335, 1988

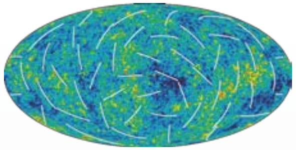

Since then…

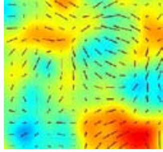

- (CMB anisotropies were discovered…)
- Angular power spectra C(l) became the norm
  - $T(n) = \Sigma_{lm}\, a_{lm}\, Y_{lm}(n)$; $a_{lm} = \int d\Omega\, T\, Y^{*}_{lm}$
  - $<a_{lm}\, a_{l'm'}> = \delta_{ll'}\, \delta_{mm'}\, C(l)$ *(If statistical isotropy)*
  - $<T_p T_{p'}> = C_{pp'} = \Sigma\, (2l+1)/4pi\, C(l)\, P_l(n_p, n_{p'})$
  - $\backslash hat\ C(l) = 1/(2l+1)\, \Sigma_m\, |a_{lm}|^2$

- $\Omega_K \neq 0$ calculations
- Elegant reformulations, introduce E & B to represent polarisation, many gauges (or absence of)…
- Precision of theoretical predictions increased ($\Delta < 1$ %)
- Speed also (tremendously).
- Off the shelf codes: CMBFAST [Seljack & Zaldarriaga 96], CAMB [Lewis et al. 2000] & CMBSLOW [Riazuelo], CMBEASY, etc
- With further options, e.g. lensing correction, isocurvature modes, reionisation… (still ongoing)
- Detailed degeneracy studies
- Improved recombination
- ...
- And more recently Non-Gaussianty botanics

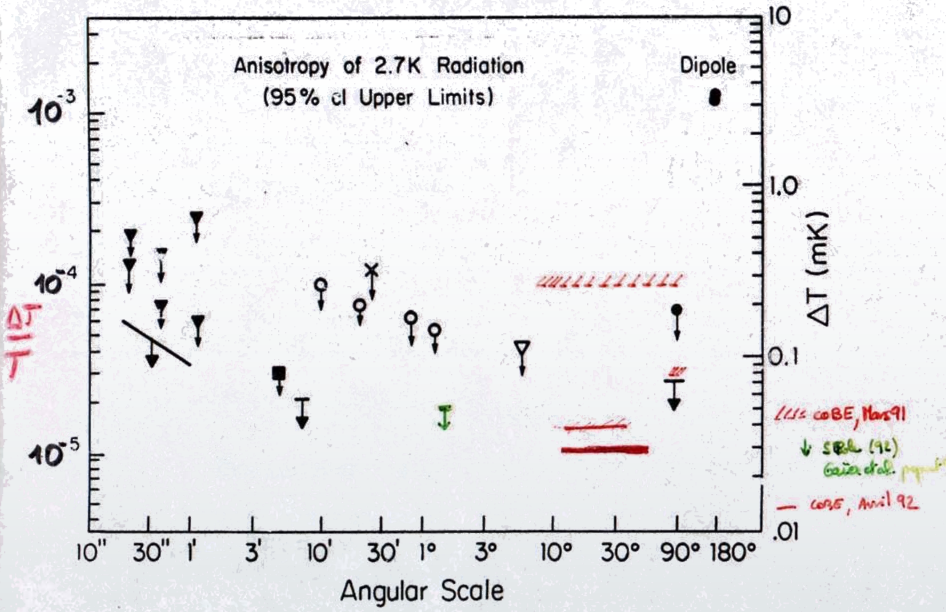

1.6: RMS variation of the CMBR temperature as a function of the angular
…n of the two antennas (from [13]).

Table 1: Primary Anisotropies for Primordial Gaussian Fluctuations

MODEL	Small Angle $10^6(\Delta T/T)$ 4.5'[7.15']	Large Angle $10^6(\Delta T/T)$ 6°
OBSERVATIONS	< 50 [< 15]	< 48 = 10
Unbiased Adiabatic B-dom		
B-dom $\Omega = \Omega_B = 0.1$	1000	-
B-dom $\Omega = \Omega_B = 1$	50	-
Unbiased Isocurvature B-dom		
B-dom ISOC 0 $\Omega = 1$ $\Omega_B = 1$	36	7
B-dom ISOC -1 $\Omega = 1$ $\Omega_B = 1$	28	14
OPEN B-dom ISOC 0 $\Omega = 0.2$ $\Omega_B = 0.2$	61	3
OPEN B-dom ISOC -1 $\Omega = 0.2$ $\Omega_B = 0.2$	84	16
OPEN ION B-dom ISOC 0 $\Omega = 0.2$ $\Omega_B = 0.2$	11	4
OPEN ION B-dom ISOC -1 $\Omega = 0.2$ $\Omega_B = 0.2$	14	31
Ω=1 biased CDM		
CDM-dom $\Omega = 1$ $\Omega_B = 0.03$	3 [5]	7
CDM-dom $\Omega = 1$ $\Omega_B = 0.1$	5 [7]	7
CDM-dom $\Omega = 1$ $\Omega_B = 0.2$	6	8
CDM+B hybrid $\Omega = 1$ $\Omega_B = 0.5$	8	15
Biased Isocurvature Axion		
CDM-dom ISOC $\Omega = 1$ $\Omega_B \ll \Omega$	-	60
Anti-biased Massive Neutrino $z_{nl} = 1$		
HOT (m_ν=24 ev) $\Omega = 1$ $\Omega = 0.1$, $b = .53$	20	20
HOT/COLD hybrid $\Omega_\nu = 0.4$ $\Omega_X = 0.5$ $\Omega_B = 0.1$	-	8
$\Omega < 1$ Unbiased CDM		
OPEN/CDM-dom $\Omega = .2$ $\Omega_X = .17$ $\Omega_B = .03$	70 [150]	40
OPEN/CDM/B $\Omega = .2$ $\Omega_X = .1$ $\Omega_B = .1$ $h = .75$	80 [170]	50
$\Lambda \neq 0$ Unbiased CDM		
VAC/CDM hybrid $\Omega = 1$ $\Omega_{vac} = .8$ $\Omega_X = .17$ $\Omega_B = .03$	20 [30]	20
VAC/CDM/B $\Omega = 1$ $\Omega_{vac} = .8$ $\Omega_X = .1$ $\Omega_B = .1$ $h = .75$	20 [30]	25
Non-Scale-Invariant IC's		
CDM-dom + Extra Power Mountain $\Omega = 1$ $\Omega_B \ll \Omega$	-	40
CDM-dom + Extra Power Plateau $\Omega = 1$ $\Omega_B \ll \Omega$	-	[illegible]

1st ICGS
In Goa

1992 vintage

The Nobel Prize in Physics 2006

"for their discovery of the blackbody form and anisotropy of the cosmic microwave background radiation"

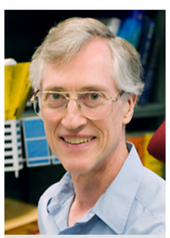
Photo: NASA

John C. Mather

1/2 of the prize

USA

NASA Goddard Space Flight Center
Greenbelt, MD, USA

b. 1946


Photo: R. Kaltschmidt/LBNL

George F. Smoot

1/2 of the prize

USA

University of California
Berkeley, CA, USA

b. 1945

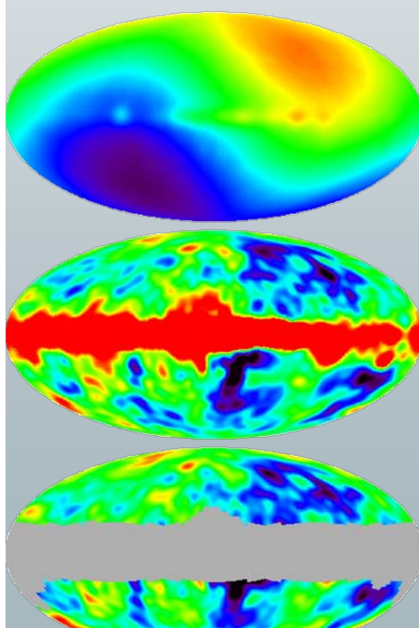

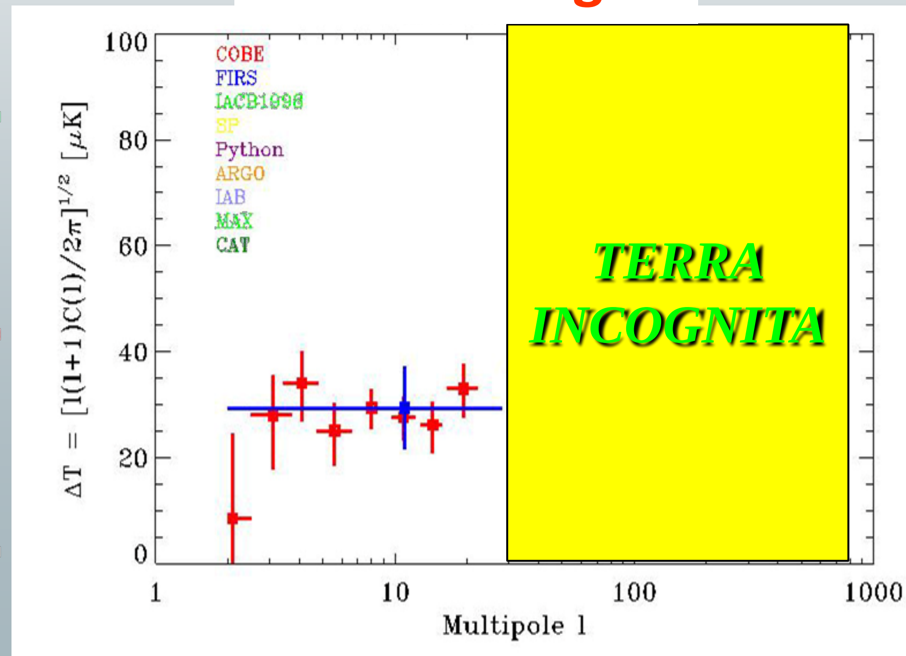

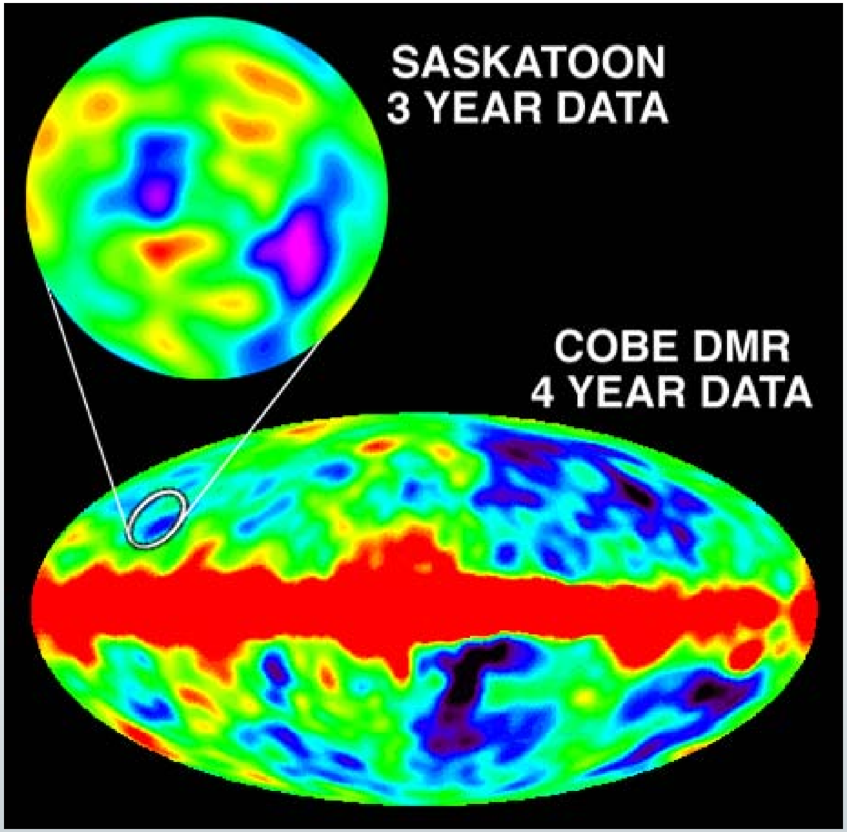

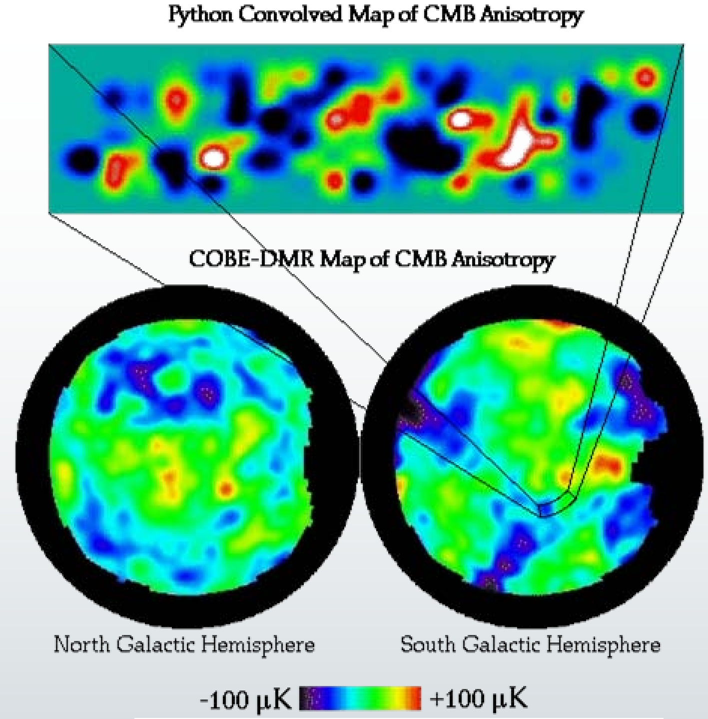

Cuvée RCF 1996

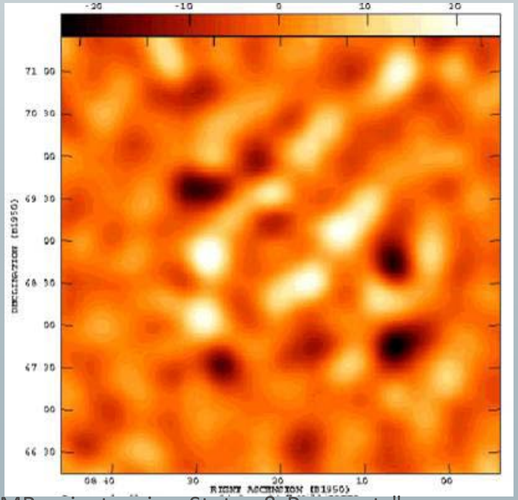

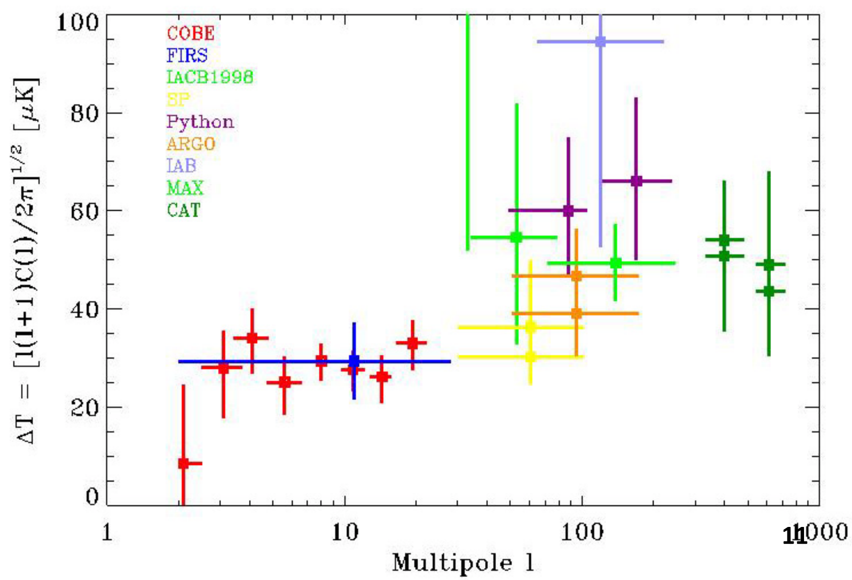

1999 vintage

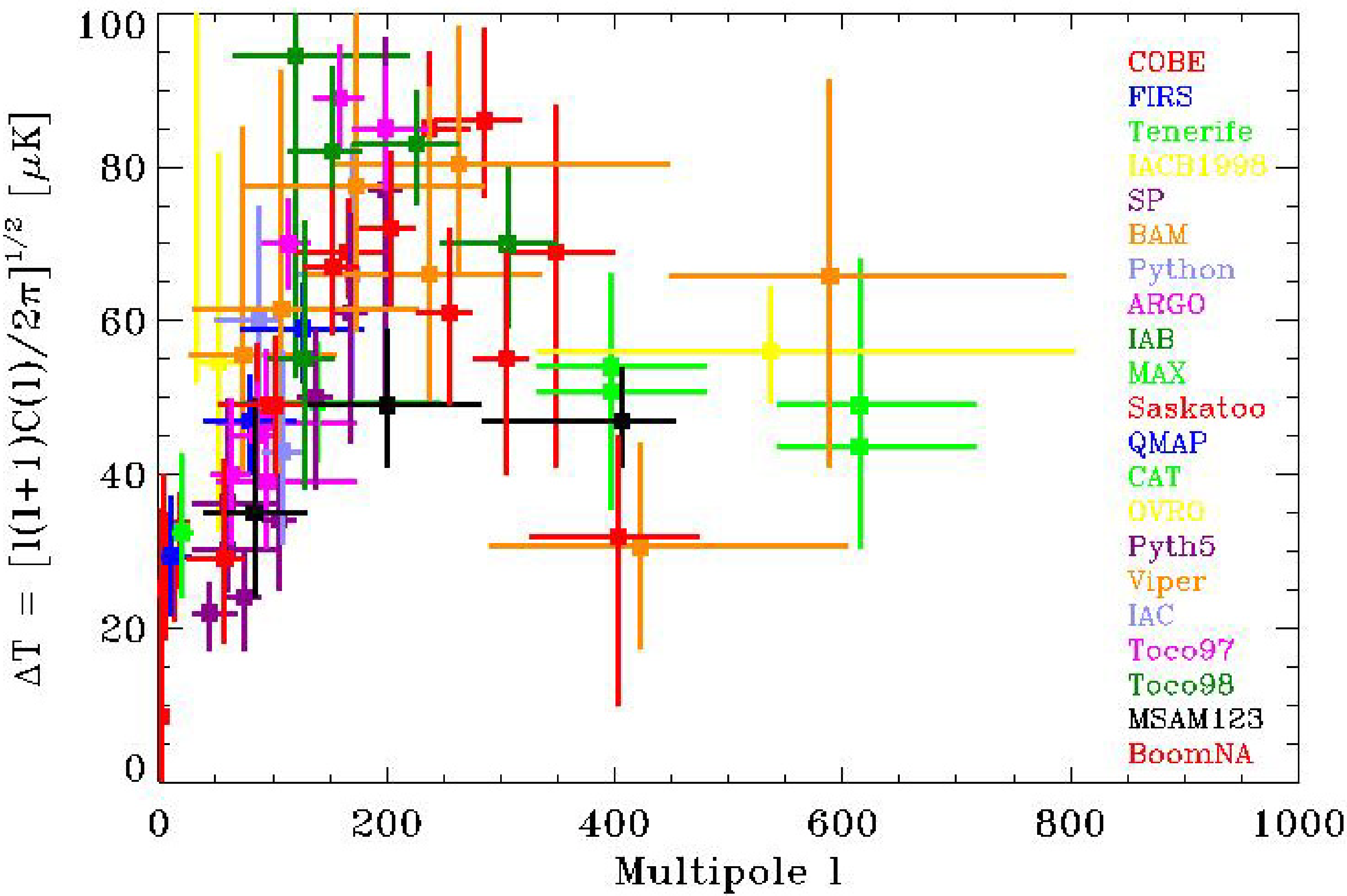

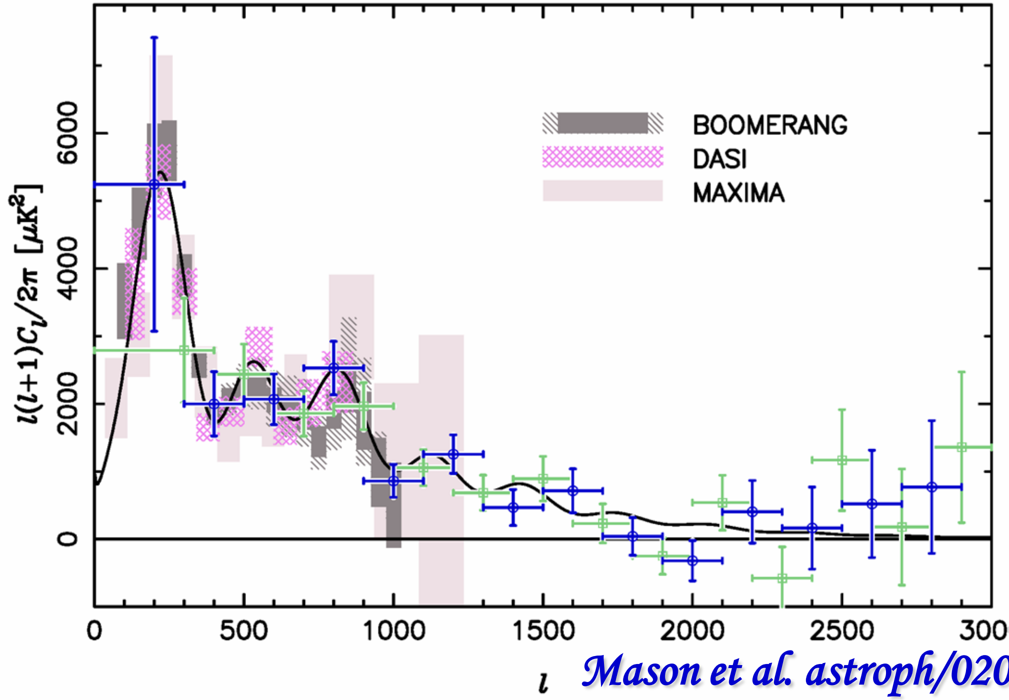

Mason et al. astroph/0205384

CBI…

(May 2002, as VSA)

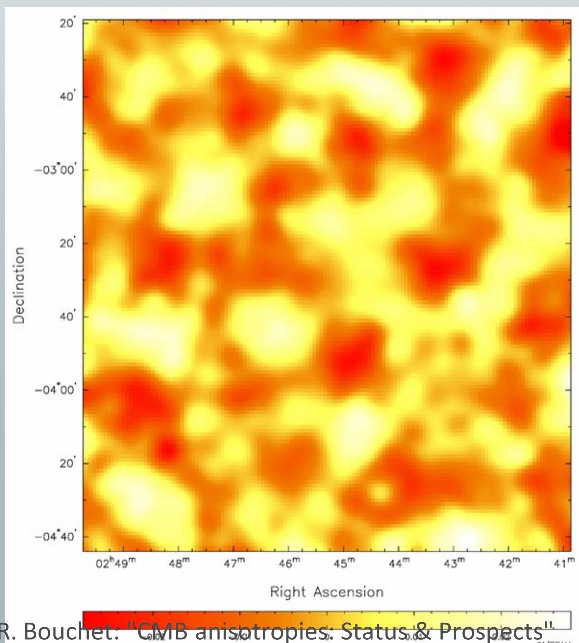

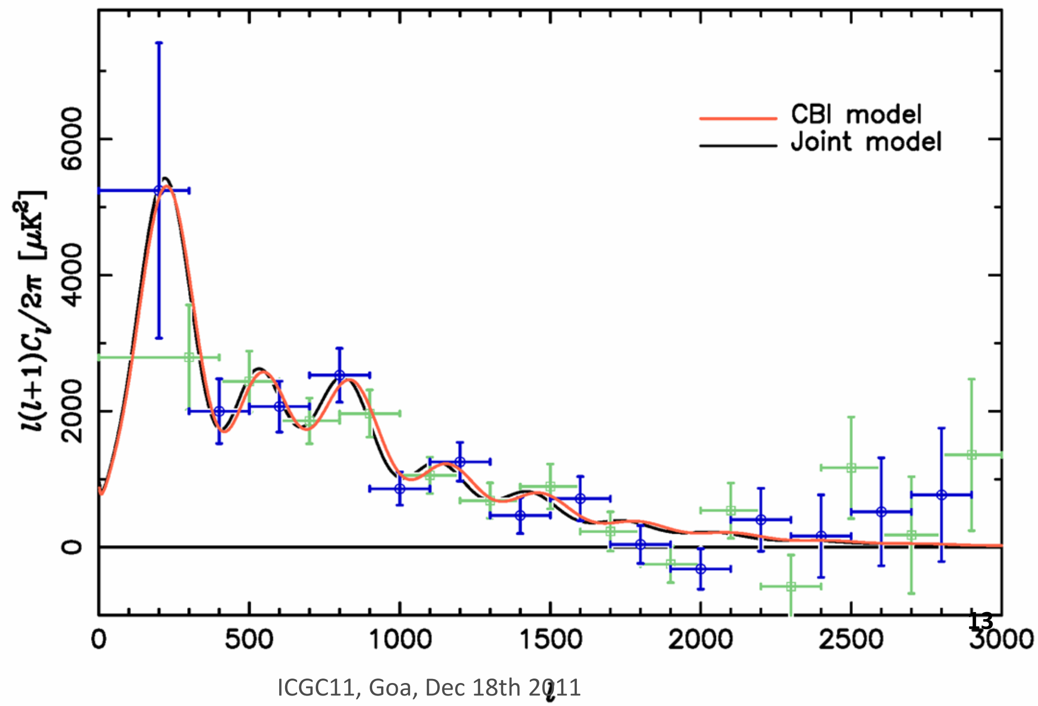

pre-wmap polarisation knowledge

(Figure from de Oliveira-Costa et al 2002)

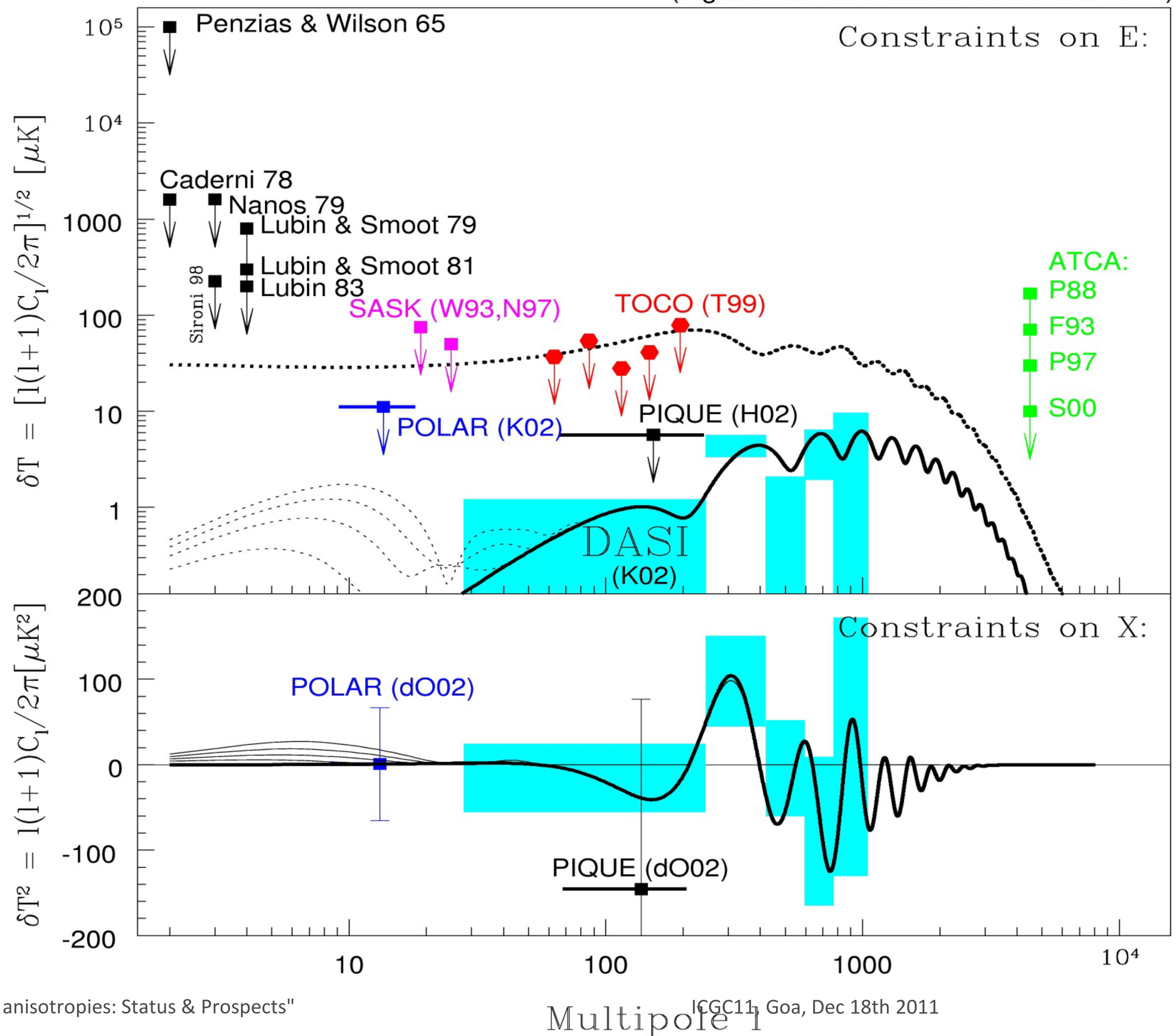

2005 vintage (october)

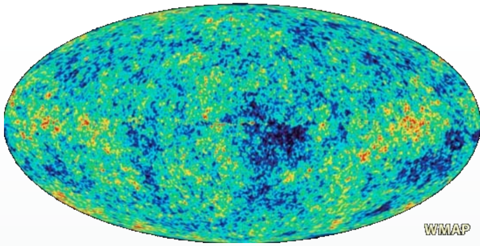

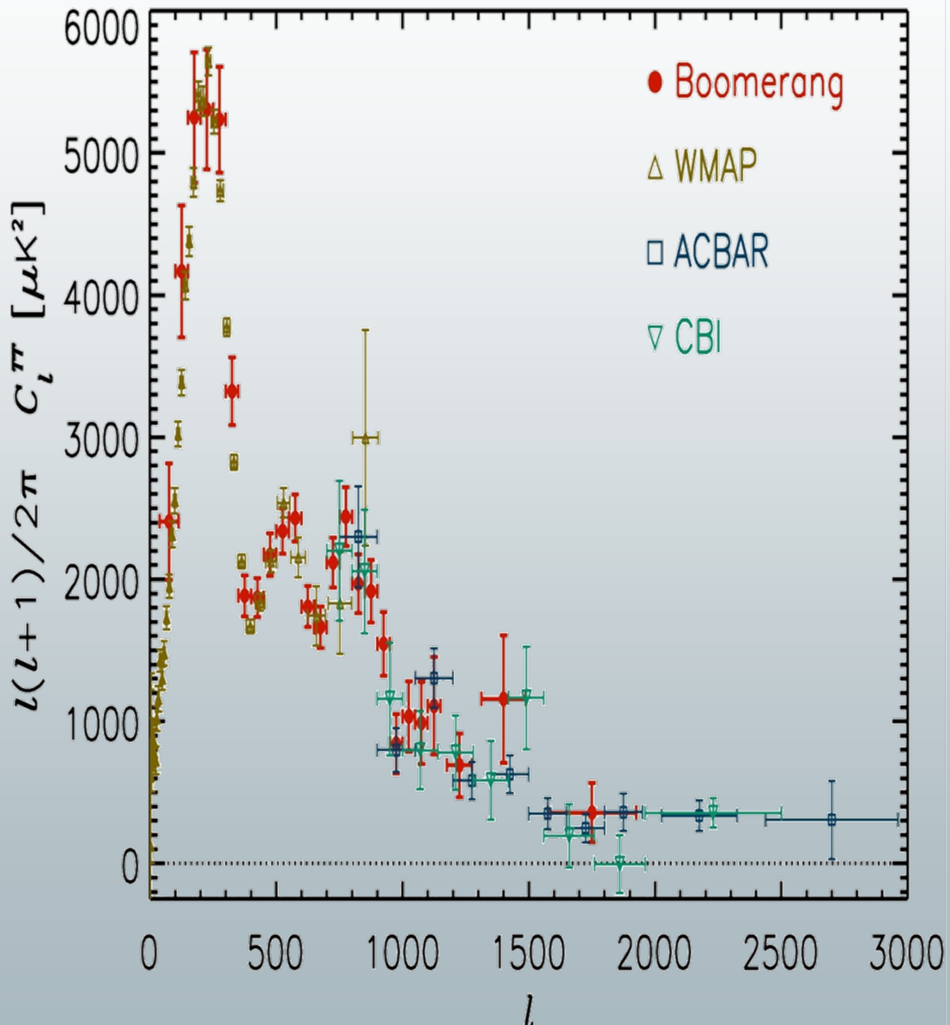

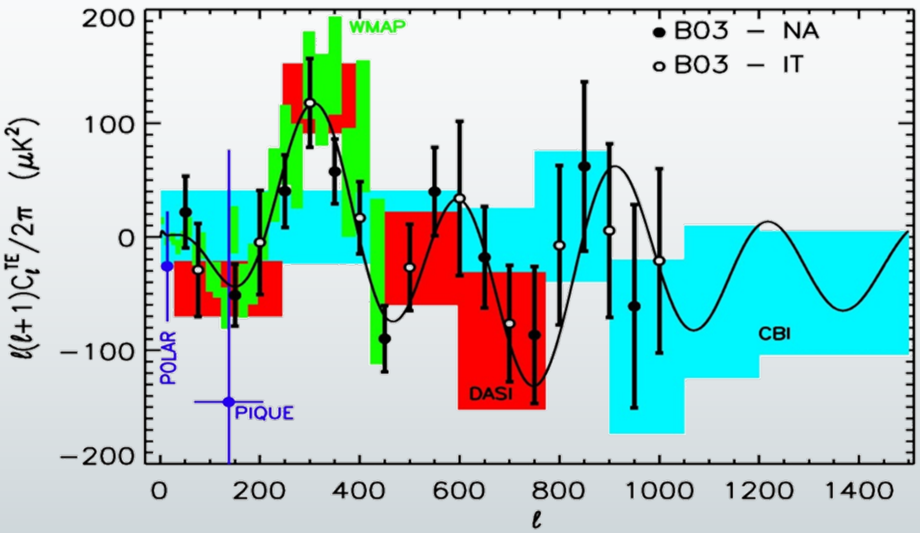

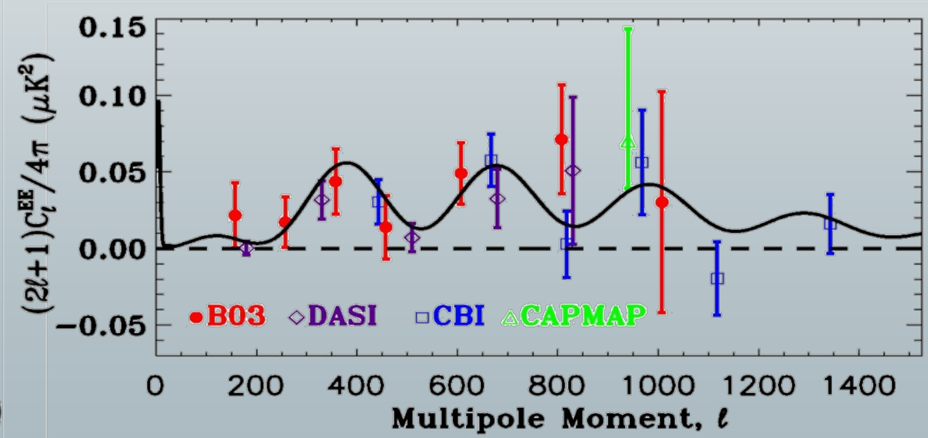

WMAP1, WMAP3, WMAP5, WMAP7

Nonparametric uncertainties on peak and dip locations and heights

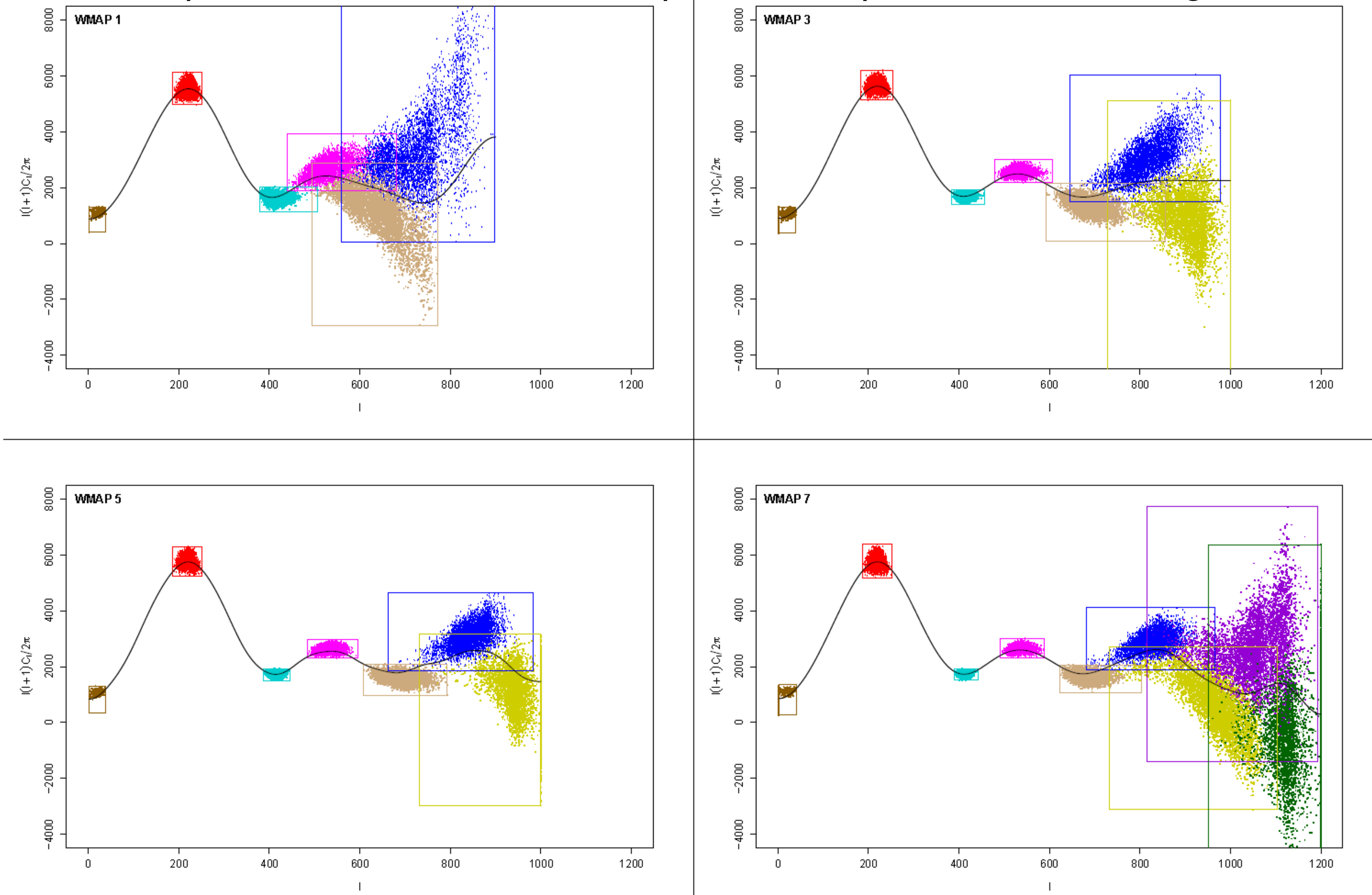

Aghamousa et al. arXiv:1107.0516v2

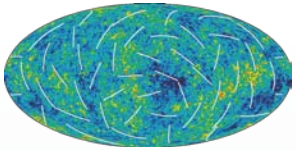

Current experimental status (12/2011)

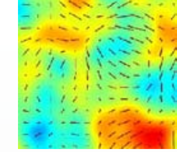

Temperature / Polarisation

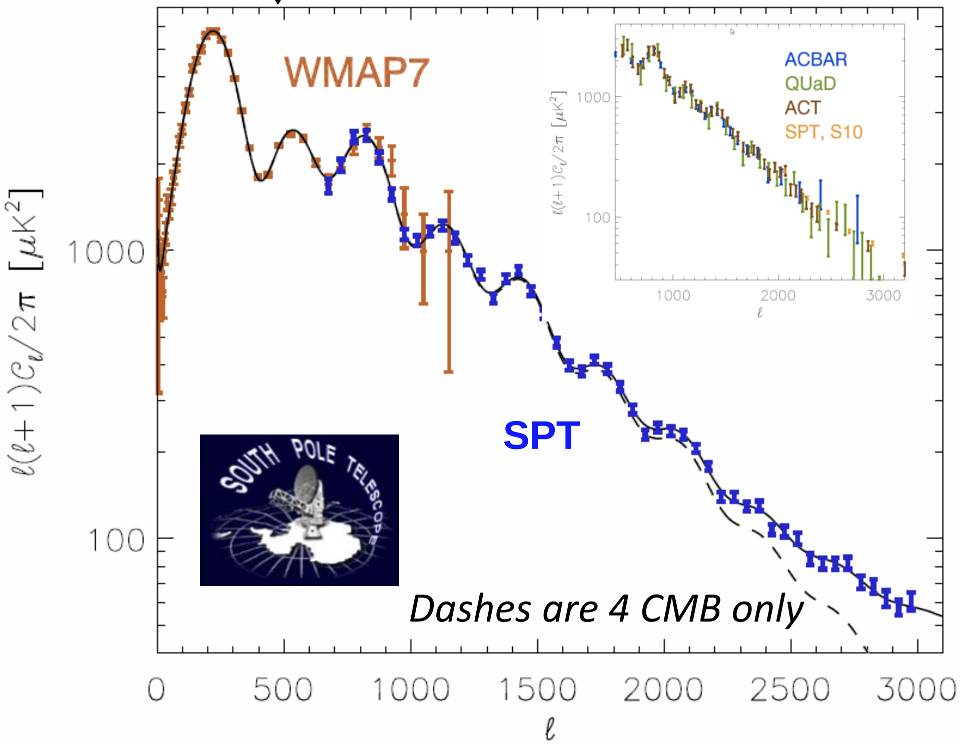

Keisler et al., arXiv:1105.3182

SPT bandpowers, WMAP bandpowers, and best-fit ΛCDM theory spectrum shown with dashed
(ds) lines. The bandpower errors do not include beam or calibration uncertainties.

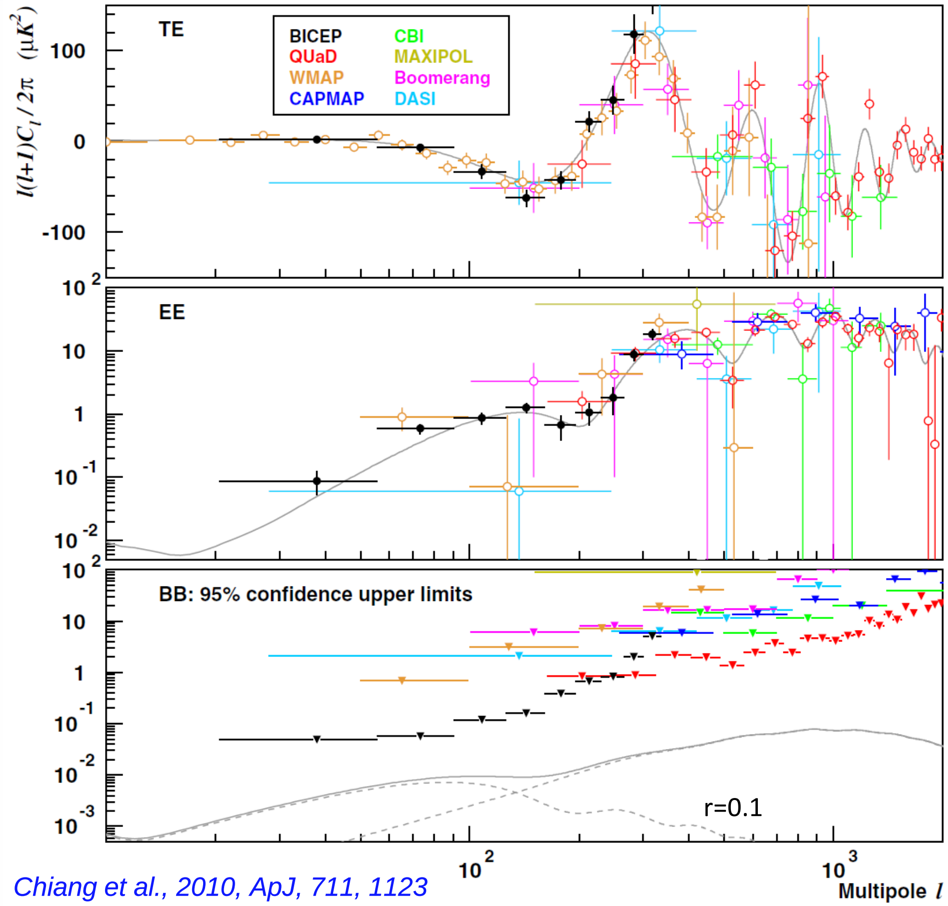

Chiang et al., 2010, ApJ, 711, 1123

The South Pole Telescope (SPT) data consist of 790 square degrees of sky observed at 150 GHz during 2008 & 2009.
(+ 95 & 220GHz data analysed in Nov11)

QUIET, ~1000 square degrees, observed at 43 & 95GHz, oct08 to dec10 2011ApJ...741..111Q
BICEP, ~2000 square degrees, observed at 100 & 150GHz, from 06 to 08, Apj2010.

The big picture: Basic ΛCDM still fits

- Fluctuations are, to a very good approximation:
  - *Isotropic*
  - *Gaussian*
  - *Adiabatic* *(fluctuations in pressure α to the density)*
  - *Coherent* *(fluctuations start @same time, harm. osc)*
  - *Scale invariant* *(no 4σ deviation from n_s =1)*
- With minimal cosmological content,
  - *Flat spatial geometry* *(is a good approximation)*
  - *Matter is mostly dark* *(cold)*
  - *"Dark energy" consistent with Λ* *(w=-1)*
  - *Small fraction of baryon, consistent with BBN*
- I.e. all consistent with inflationary *framework*
- Large scale ($5^o > \vartheta > 1^o$) TT versus TE anti-correlation:
  - *Signature of « super-horizon » fluctuations at decoupling and*
  - *Adiabaticity of primordial fluctuations (phases TT/TE)*
  - *An indication of apparently a-causal physics, calling for a period of accelerated expansion (Spergel & Zaldariaga 97)*

6 parameters LCDM "plain vanilla"

+ 3 foreground terms (Poisson + clustered sources+ SZ)

Keisler et al. (SPT), arXiv:1105.3182v2

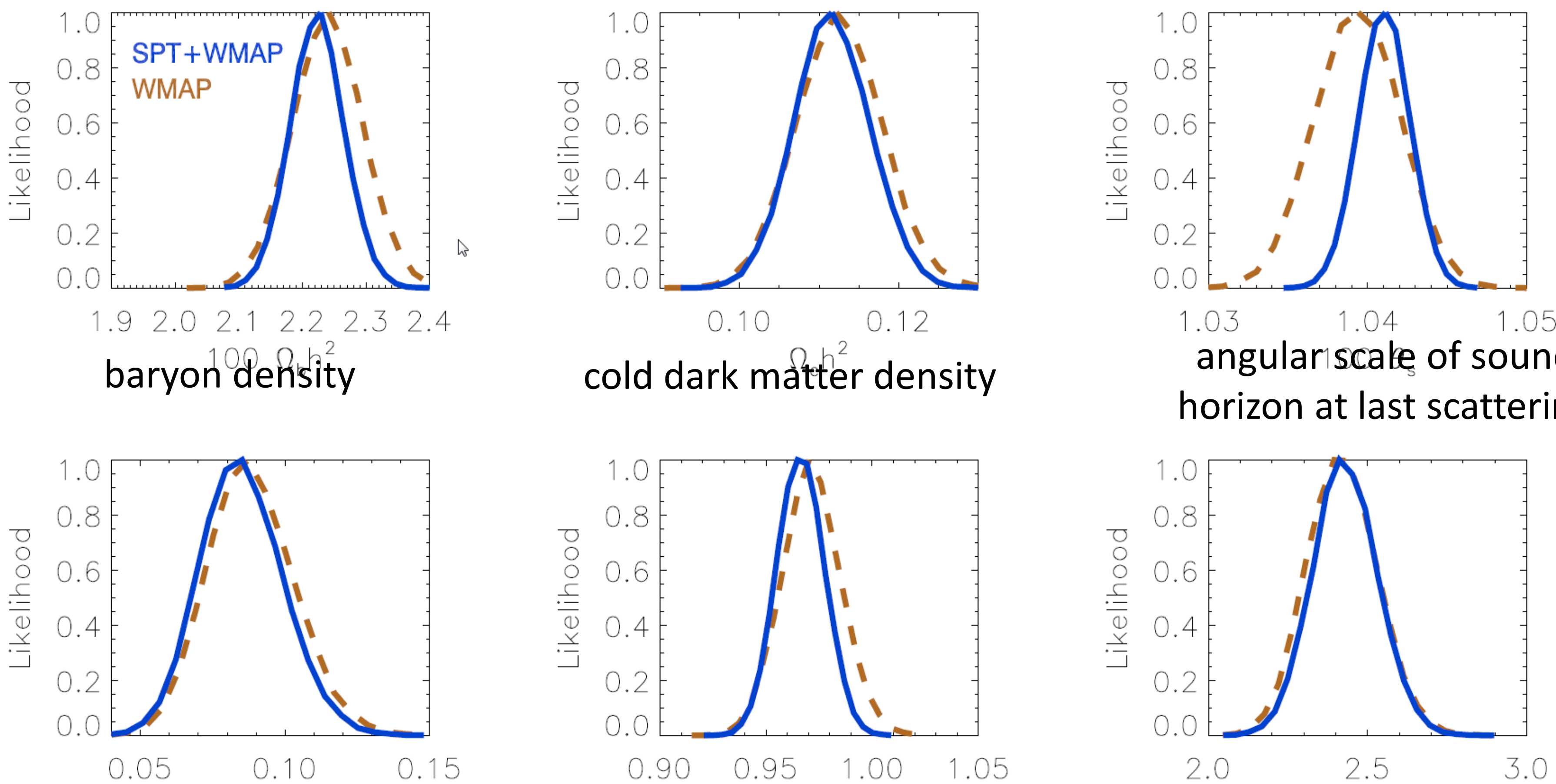

baryon density

cold dark matter density

angular scale of sound horizon at last scattering

optical depth of reionization

spectral index of scalar fluctuations

Amplitude of primordial scalar fluctuations.

→ All determined with 1-2 % accuracy

Primordial Power spectrum reconstruction

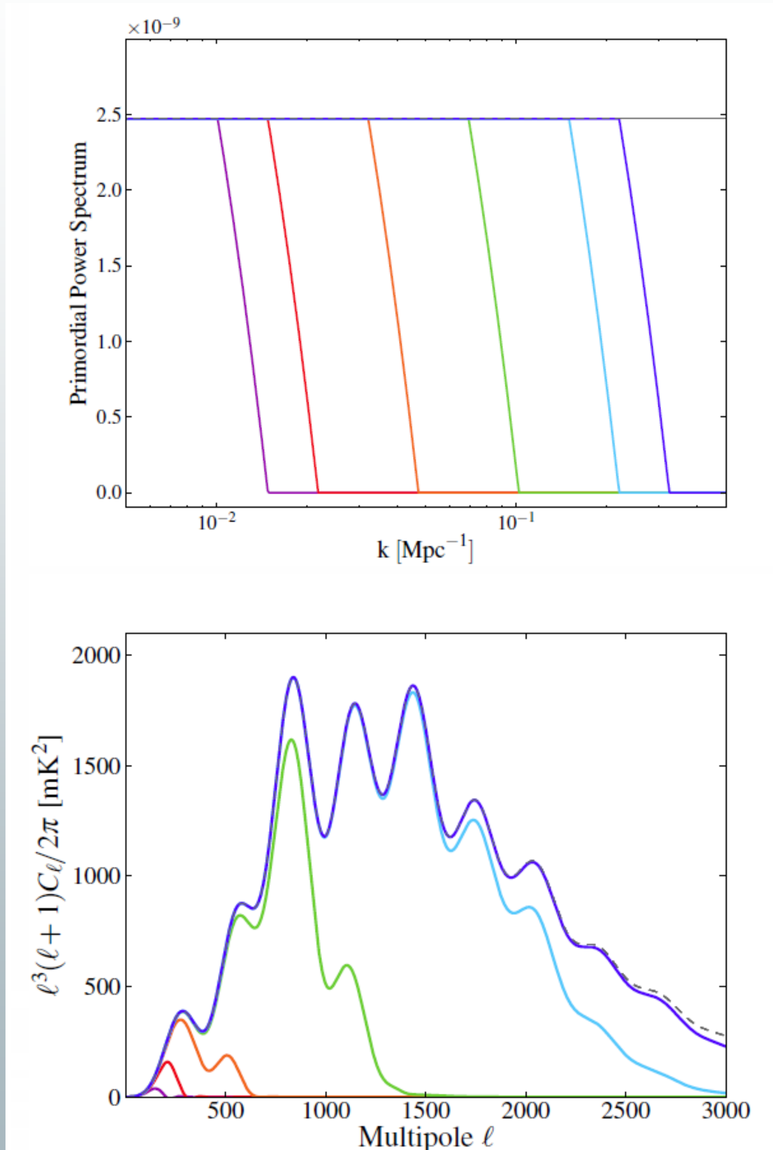

Obtained by simple change of parameterisation, i.e. 20 bins for P(k) (instead of As, ns) + 4 other standard model + 3 for foregrounds

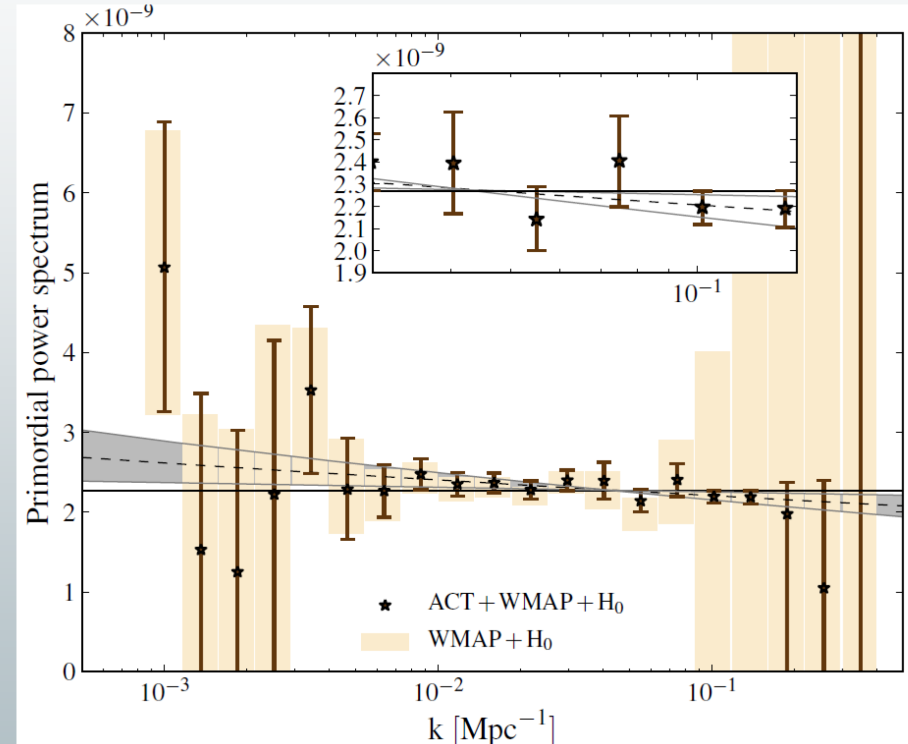

Now probing wave numbers up to k = 0.2 Mpc^{-1}

Dashes show n_s =0.962 (direct analysis ML)

Hlozek et al (ACT) arXiv:1105.4887v1

Primordial gravitational waves & B modes

- “Smoking gun” from inflation
  - *Amplitude given by Hubble parameter during inflation*
  - *Detectable in large-field models*
  - *Conversely, detection would rule out some other models*
    - Cyclic
    - Many string inspired ones

- Only upper limit so far
  - Define $r = A_T/A_s$ ($P_T=A_T.k^{n_T}$)
  - *T & E from WMAP7 → r < 0.36 (95%CL), degeneracies can be adressed with CMB at higher ell, or BAO+Ho: r < 0.22, see further.*
  - *B alone, from Bicep: r < 0.73 (Chiang et al. 2010, ApJ, 711, 1123)*
  - *NB: amplitude is related to the energy scale of inflation, $A_T \propto A_{IGW}^2 \propto E_{Inf}^4$ ($r = 0.1 \leftrightarrow E_{inf}=2 \times 10^{16}$ GeV).*
  - *and slope is related to amplitude for all slow roll models: $n_T = - r/8$*

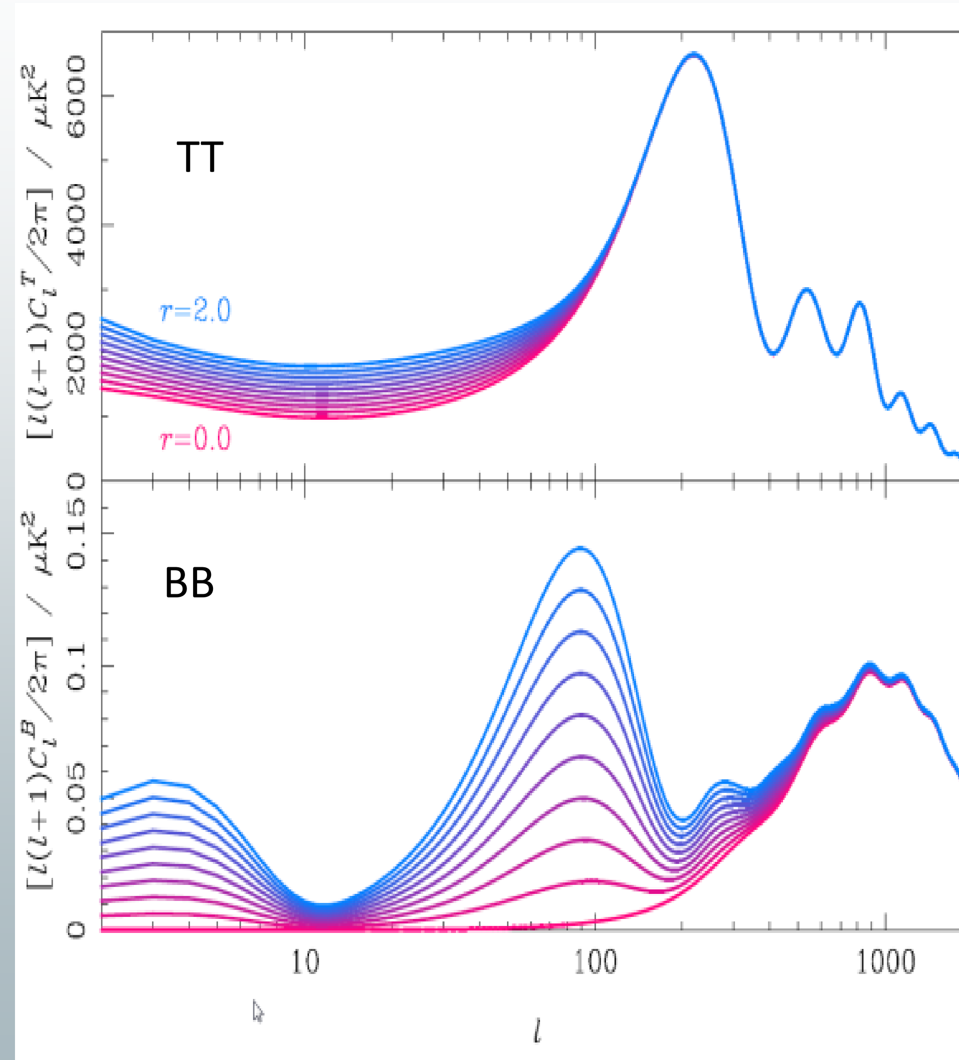

Model extensions signature/exclusion

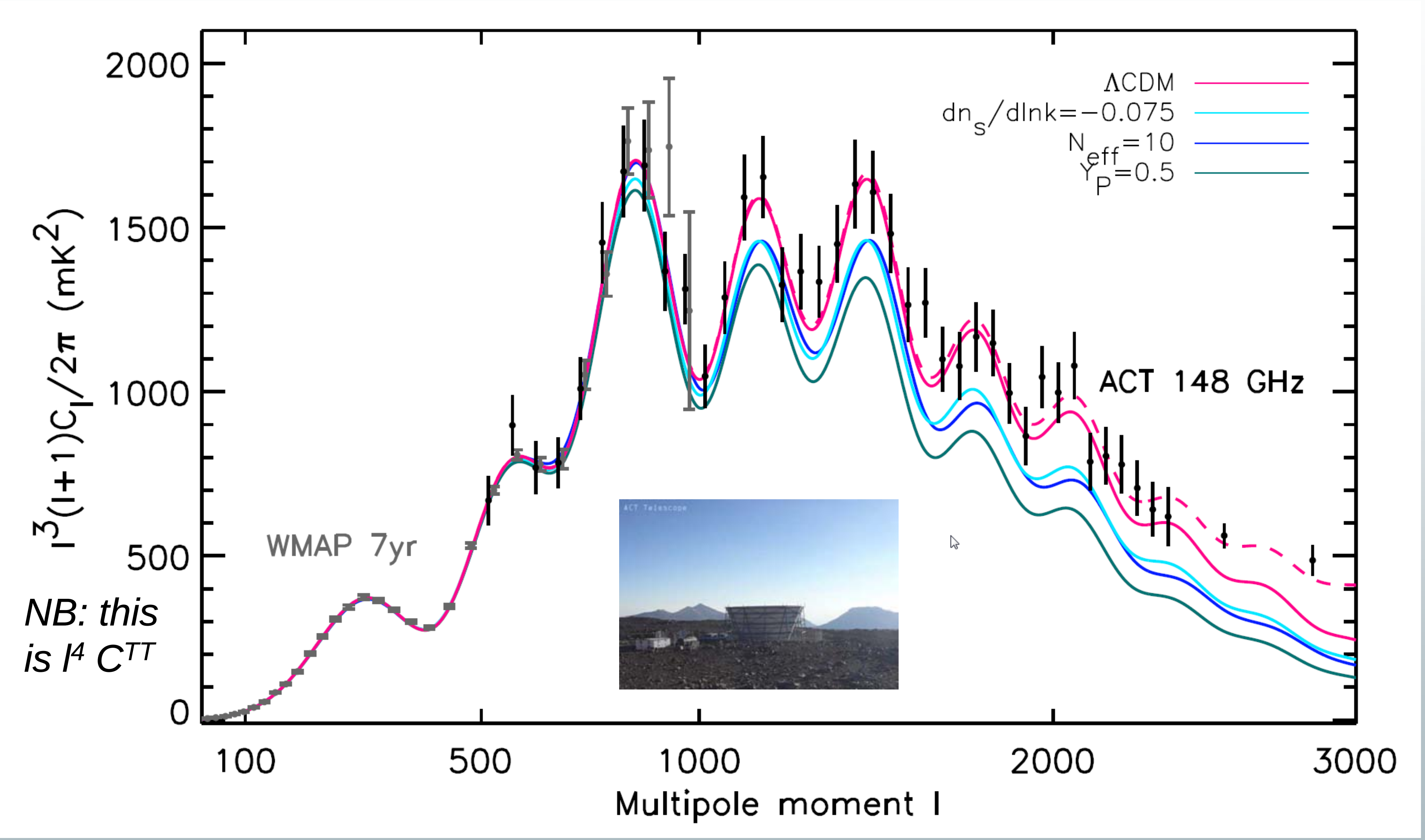

Dunkley et al, arXiv:1009.0866v1

Model Extensions, SPT versus ACT

tensor-to-scalar ratio r versus the scalar spectral index ns

1-ns ~0.03±0.01

r < 0.25 (95%CL) from SPT+WMAP

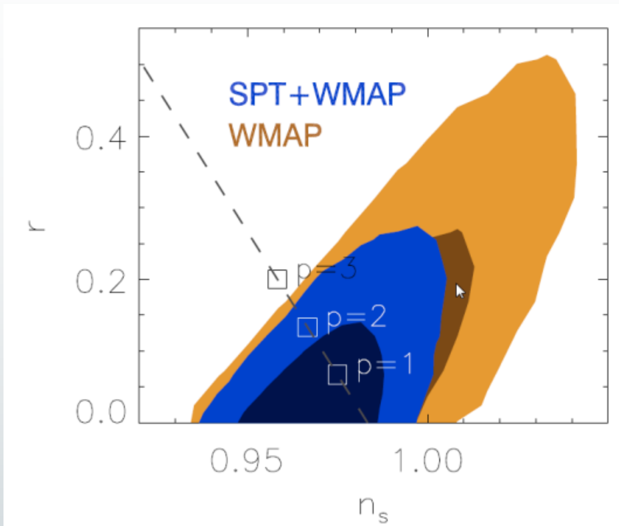

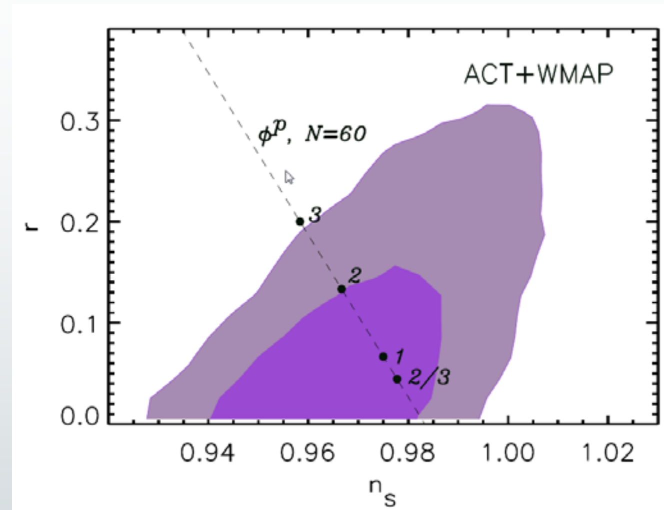

primordial helium abundance Y_p versus the effective number of relativistic species N_{eff}

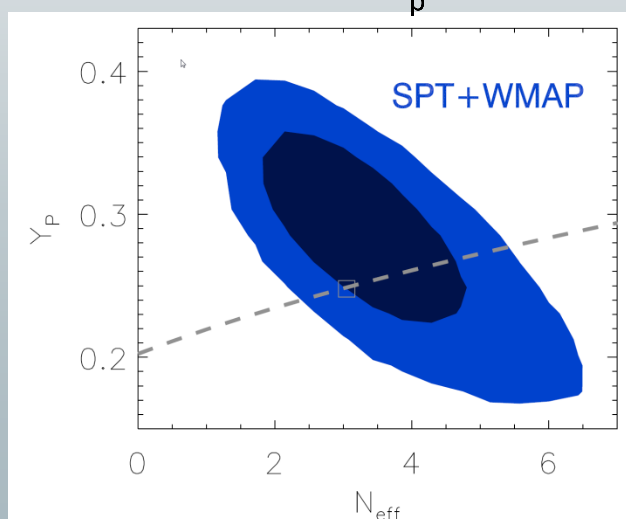

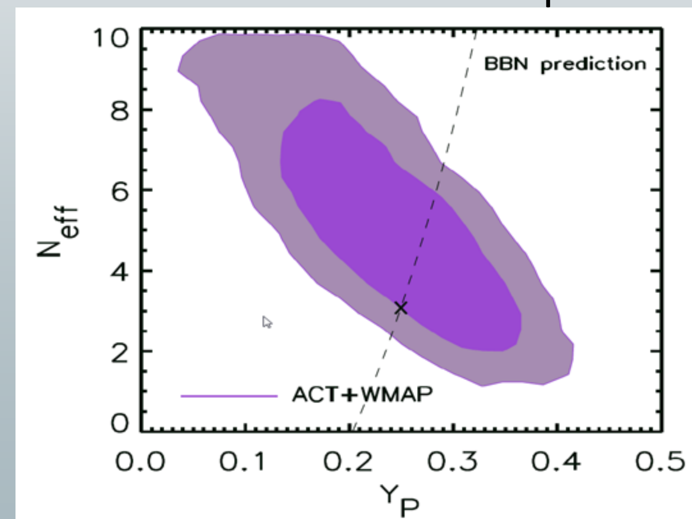

SPT, *Keisler et al, arXiv:1105.3182*

ACT, *Dunkley et al, 1009.0866v1*

➔ Very consistent view

Model Extensions summary

TABLE 5
CONSTRAINTS ON MODEL EXTENSIONS USING RECENT CMB DATASETS

	WMAP7	ACBAR+QUaD+WMAP7	ACT+WMAP7	SPT+WMAP7
r	< 0.7	< 0.33	< 0.25	< 0.21
$dn_s/d\ln k$	[-0.084, 0.020]	[-0.084, 0.003]	-0.034 ± 0.018	-0.024 ± 0.013
Y_p	< 0.51	0.326 ± 0.075	0.313 ± 0.044	0.296 ± 0.030
$N_{\rm eff}$	> 2.7	—	5.3 ± 1.3	3.85 ± 0.62

The constraints on cosmological parameters in certain model extensions using recent CMB datasets. We use WMAP7 (Larson et al. 2011; Komatsu et al. 2011), ACBAR (Reichardt et al. 2009), QUaD (Brown et al. 2009), ACT (Das et al. 2011a), and SPT (this work). All upper and lower limits and all two-sided limits (shown in brackets) are 95%.

SPT vs ACT in a 5 X 10 Deg^2 Field

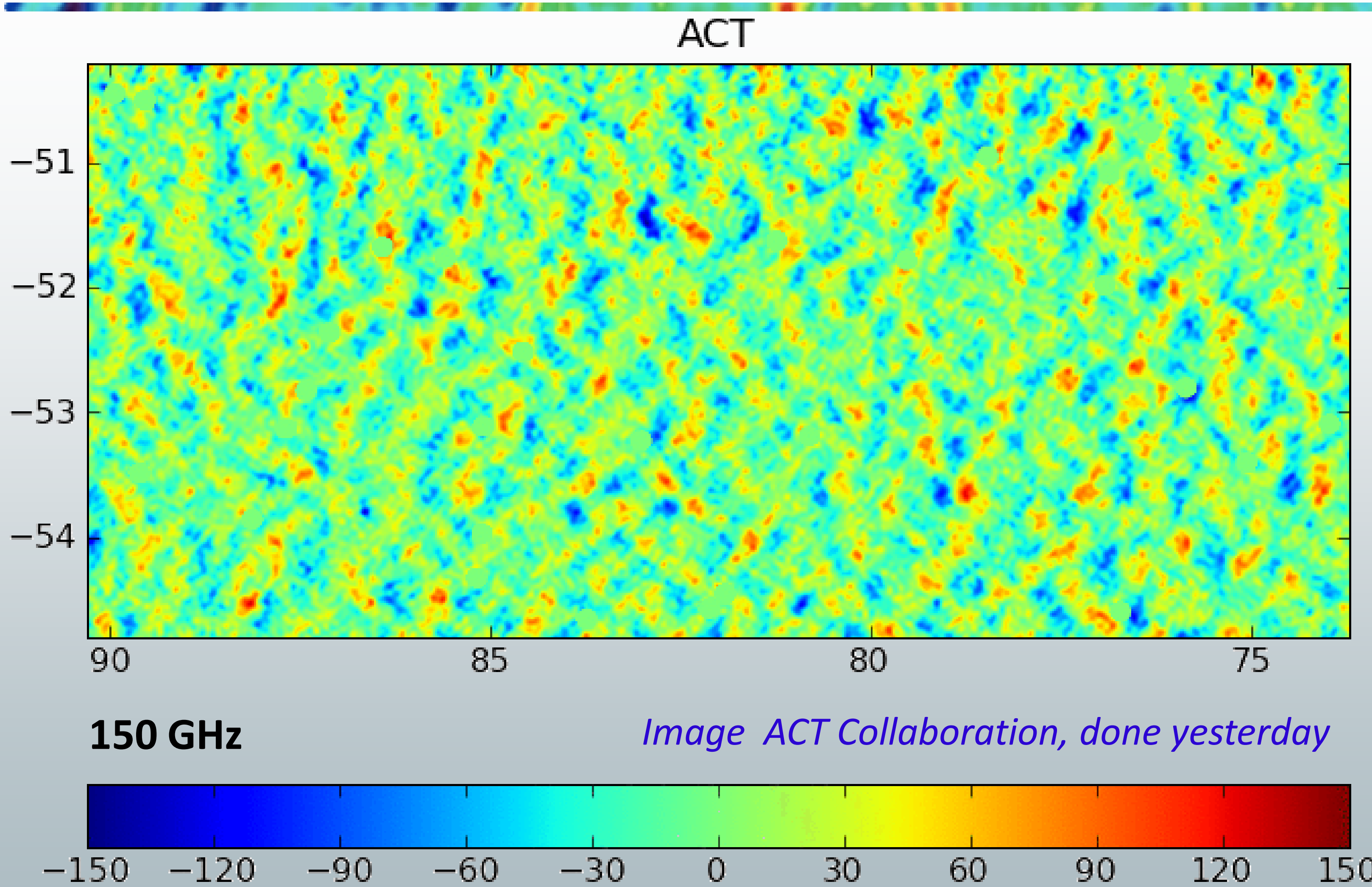

Recipe: apply SPT filter to ACT map and a low pass filter
so that either maps have information between 400~4500

ACT: Gμ < 1.6 × 10–7 (95% CL).

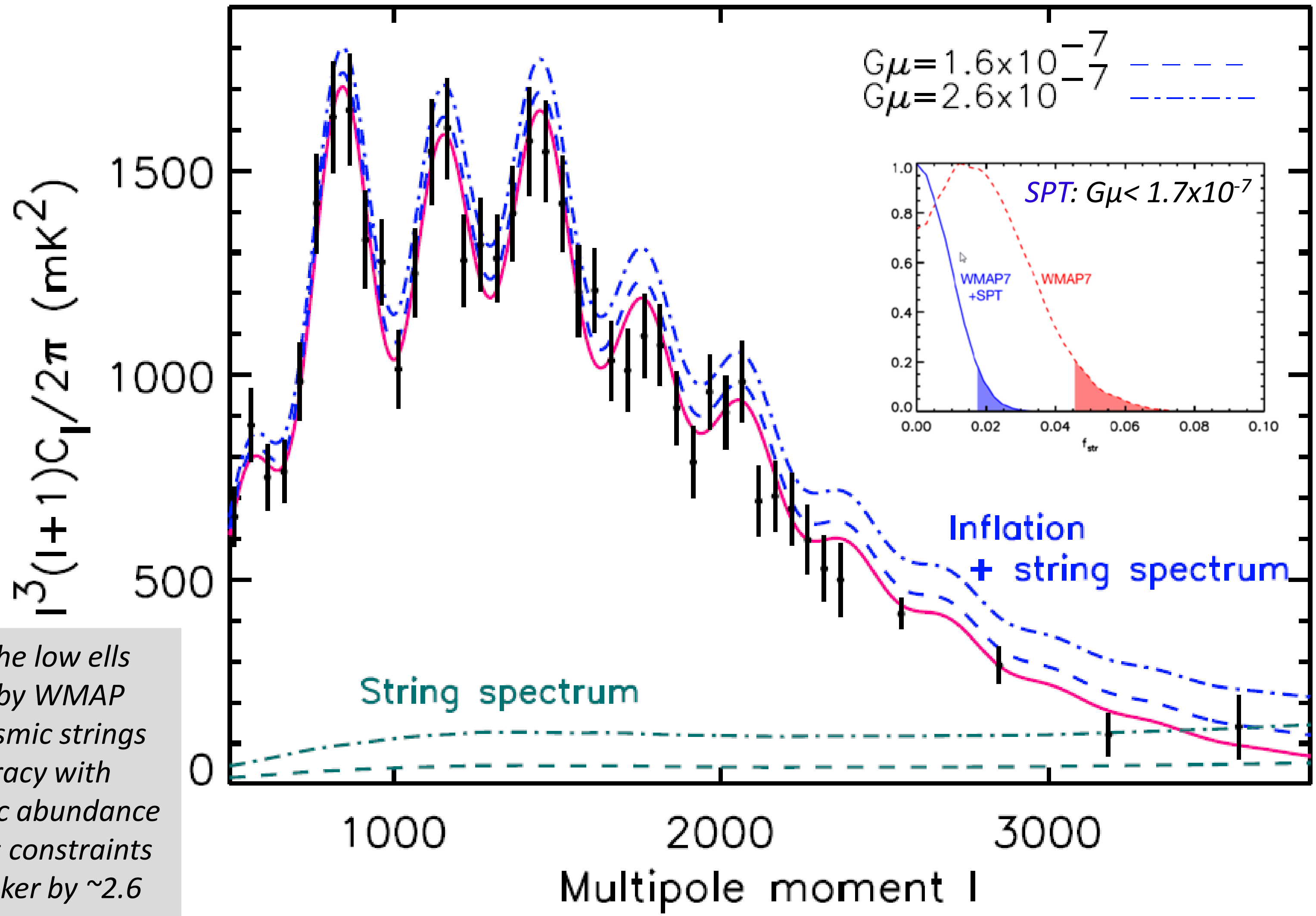

NB: at the low ells probed by WMAP only, cosmic strings degeneracy with Baryonic abundance explains constraints are weaker by ~2.6

The high-l frontier…is bordered by foregrounds

SPT, Reichardt et al. arXiv:1111.0932v1

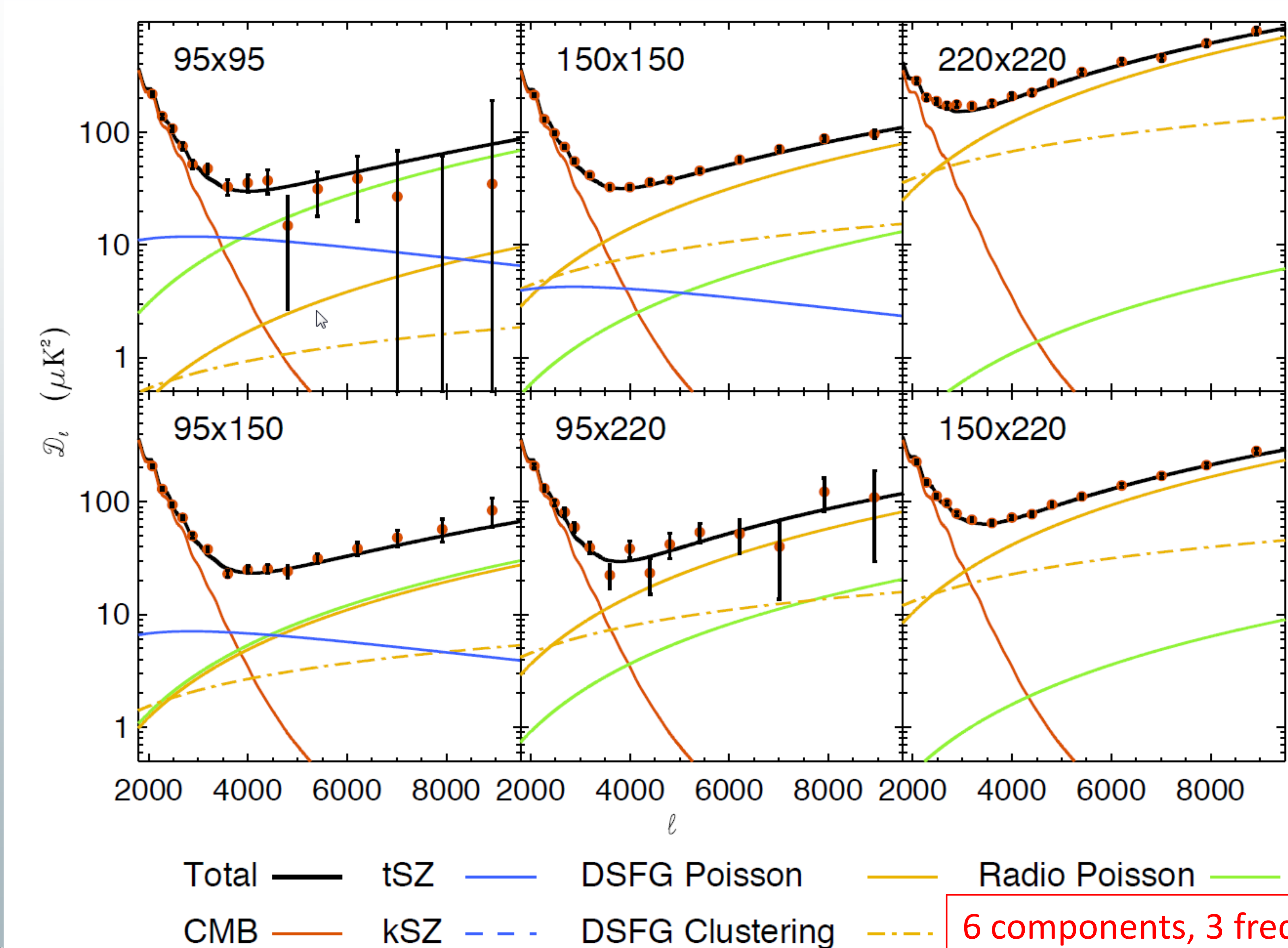

6 components, 3 frequencies

And pay-off: Neutrino masses constraints

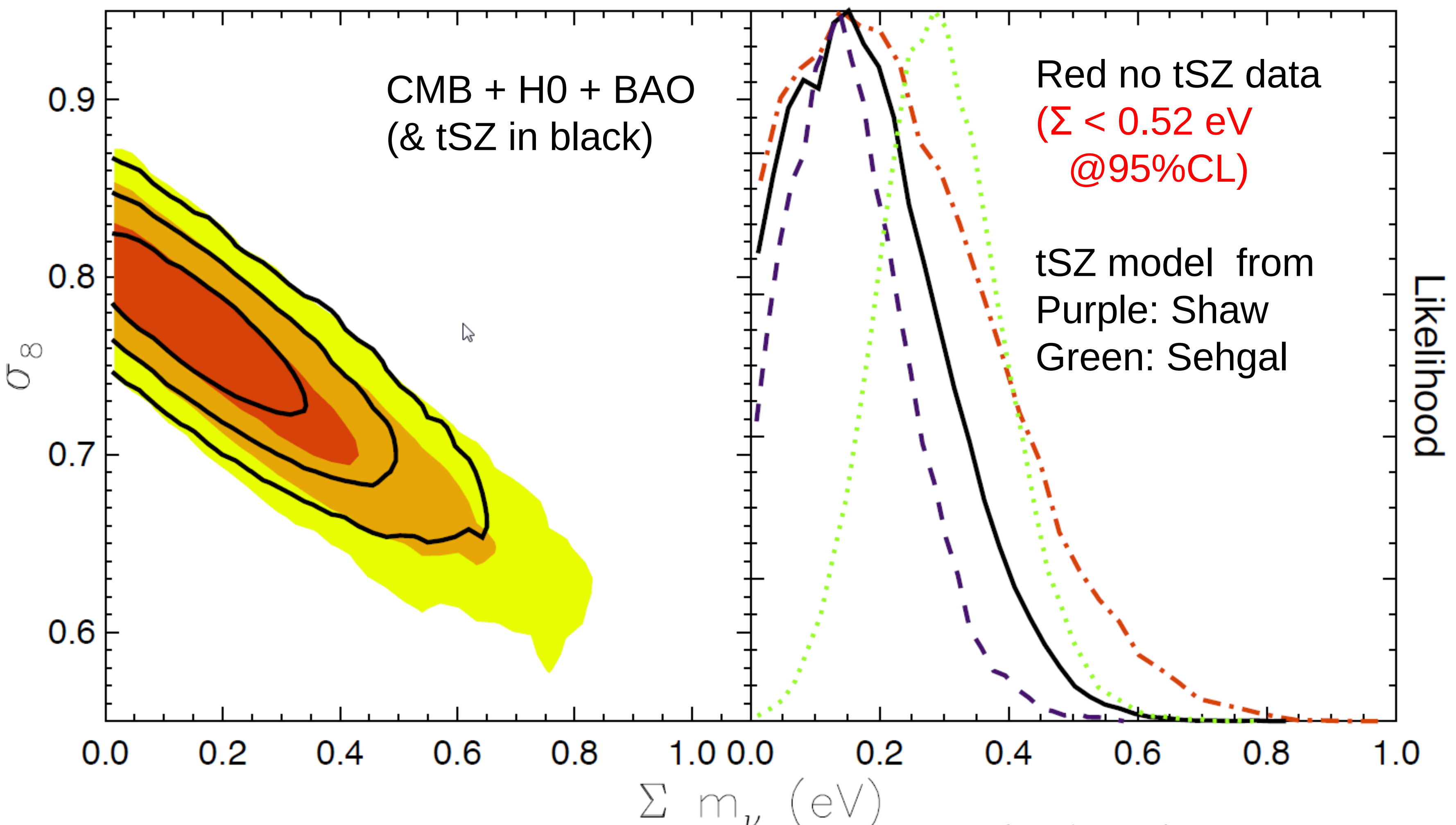

SPT, Reichardt et al. arXiv:1111.0932v1

And of course also knowledge of the "contaminants" (SZ, CIB)and related gastrophysics

Reionisation epoch

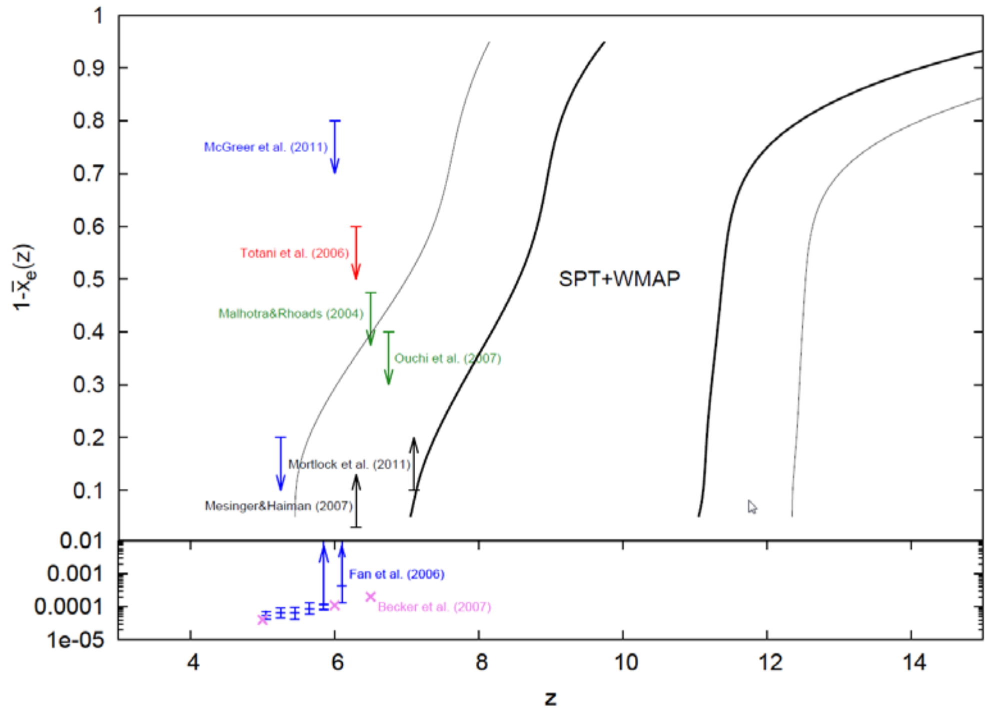

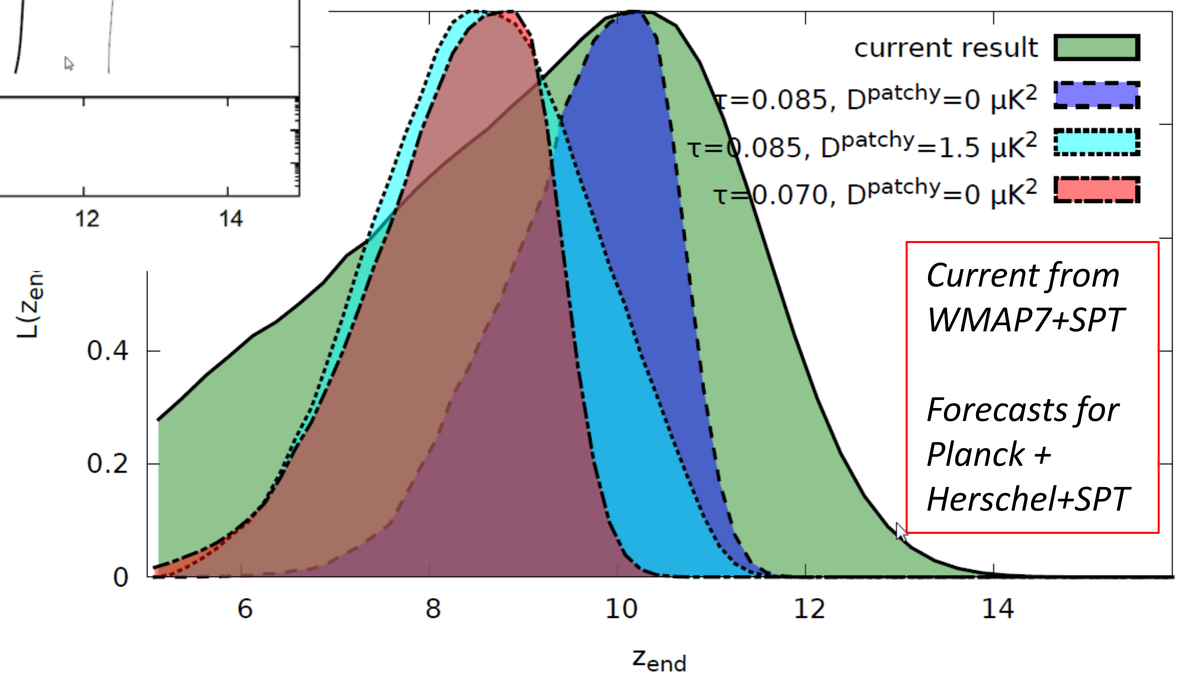

SPT, Zahn et al. arXiv:1111.6386v1

What's next?

- WMAP 7 years loses it (S/N <1) at ell ~900, and sensitive sub-orbital experiments explore only a small fraction of the sky (~2%) ➔ about ~90% of the primordial modes are not measured yet in temperature.
- It is *much* worse in polarization (large scales!).

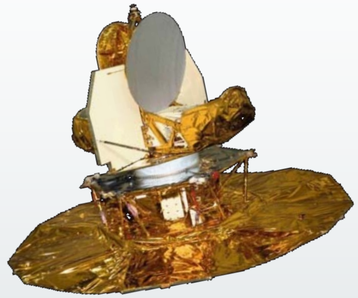

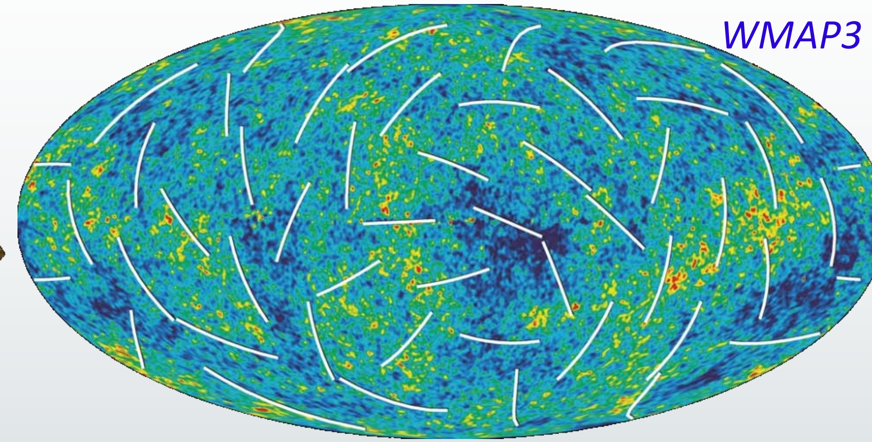

➔ *A lot* of information remains to extract, *in particular concerning the early Universe physics*

- A new generation of experiments is engaged, in particular
  - *BICEP2 → Keck,*
  - *ACT → ACTPOL,*
  - *SPT → SPTPOL,*
  - *SPIDER, EBEX, Polarbear…*
  - *For high -ells…*

and ESA's satellite Planck

The Planck concept

- to perform the "ultimate" measurement of the Cosmic Microwave Background (CMB) temperature anisotropies:
  - *full sky coverage & angular resolution / to survey all scales at which the CMB primary anisotropies contain information (~5')*
  - *sensitivity / essentially limited by ability to remove the astrophysical foregrounds*

  $\Rightarrow$ *enough sensitivity within large frequency range [30 GHz, 1 THz]*
  (~CMB photon noise limited for ~1yr in CMB primary window)

- get the best performances possible on the polarization with the technology available

$\Rightarrow$ ESA selection in 1996 (after ~ 3 year study)

NB: with the Ariane 501 failure delaying us by several years (03 → 07) and WMAP then flying well before us, polarization measurements became more and more a major goal

Planck performance goals

("Blue Book", twice better than requirements)

PLANCK	LFI			HFI					
Center Freq (GHz)	30	44	70	100	143	217	353	545	857
Angular resolution (FWHM arcmin)	33	24	14	10	7.1	5.0	5.0	5	5
Sensitivity in I [μK.deg] [$\sigma_{pix}\ \Omega_{pix}^{1/2}$]	3.0	3.0	3.0	1.1	0,7	1.1	3.3	33	3.0

The leap forward w.r.t. WMAP

WMAP Center Freq.	23	33	41	61	94
Angular resolution (FWHM arcmin)	49	37	29	20	12,6
Sensitivity in I [μK.deg], 1 yr (8 yr)	12.6 (4.5)	12.9 (4.6)	13.3 (4.7)	15.6 (5.5)	15.0 (5.3)

The aggregated sensitivity of Planck core CMB channels is ~0.5μK.deg in T (nominal mission - 14months)

NB: Anticipated survey duration is now ~30 months, so final sensitivity ~0.33 μK.deg in T
(approx 1000 years of WMAP 60+90GHz aggregated sensitivity of 10.8 μK.deg in1yr)

E current data versus Planck Forecast

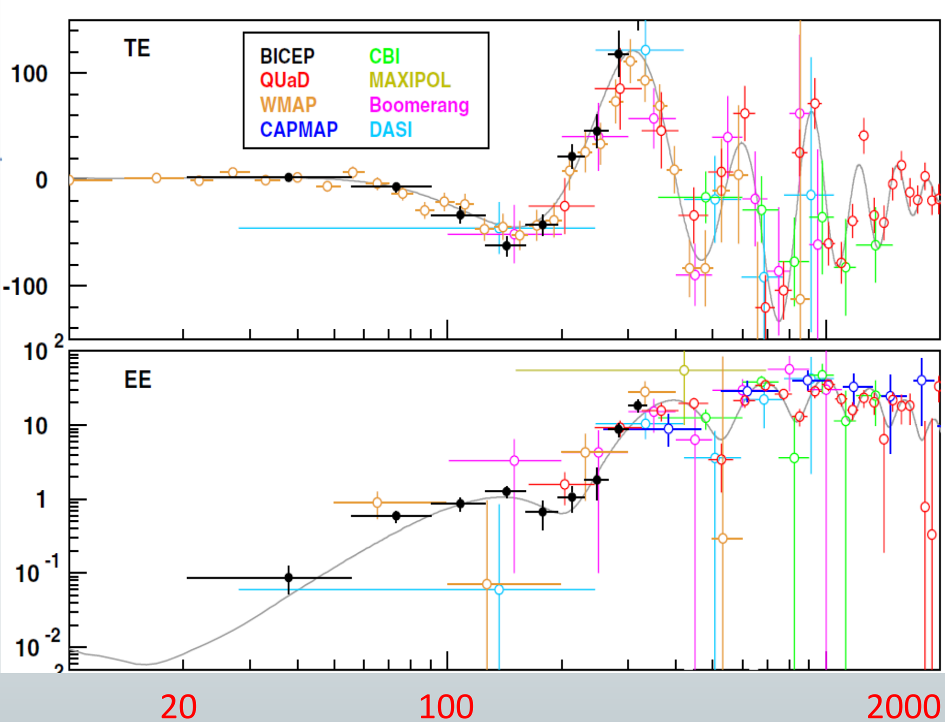

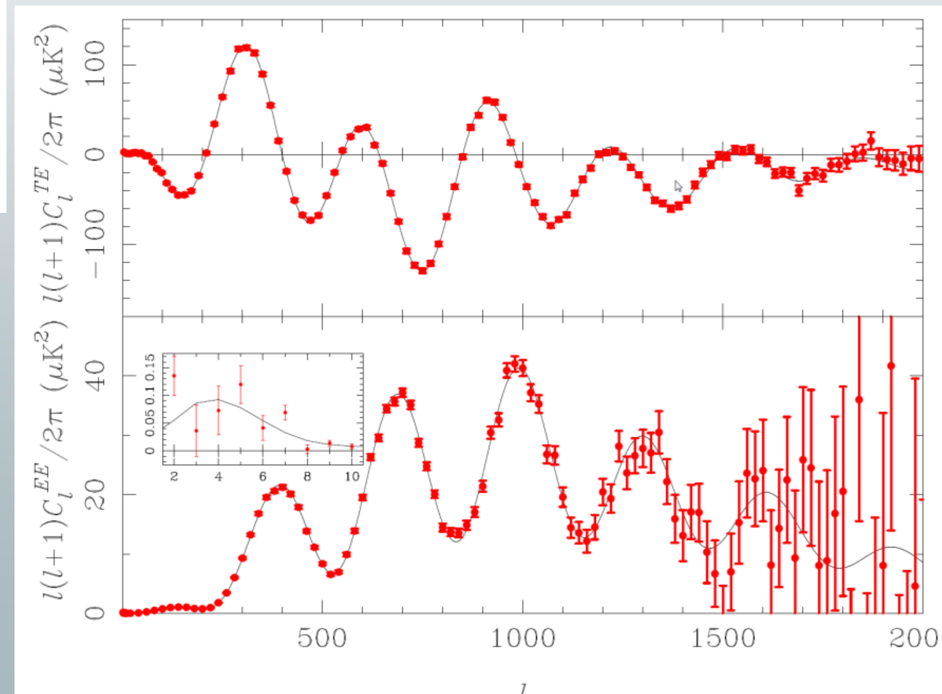

Planck needed breakthroughs

- The performance goals of Planck require several technological performances never achieved in space before
  - *Sensitive & fast bolometers with*
    - NEP< 2 10^{-17} W/$Hz^{1/2}$ & time constants typically < 5 msec

    (thus cooling them to 100 mK, very low heat capacity & charged particles sensitivity)
  - *total power read out electronics with very low noise*
    - < 6nV/$Hz^{1/2}$ from 10 mHz to 100 Hz
  - *Excellent temperature stability, from 10 mHz (1 rpm) to 100 Hz (cf. Lamarre et al. 04)*
    - < 10 µK/$Hz^{1/2}$ for 4K box (30% emissivity)
    - < 30 µK/$Hz^{1/2}$ on 1.6K filter plate (20% emissivity)
    - < 20 nK/$Hz^{1/2}$ for detector plate (~5000 damping factor needed)
  - *low noise HEMT amplifiers ($\Rightarrow$ cooled to 20K) & very stable cold reference loads (4K)*
- Additionally:
  - *low emissivity, very low side lobes, telescope (strongly under-illuminated)*
  - *no windows, minimum warm surfaces between detectors and telescope*
  - *Complex cryogenic cooling chain: 50K (passive)+20K+4K+0.1K active coolers*
    - 20K for LFI with large cooling power K (0.7W)
    - 4K, 1.6K and 100mK for HFI
    - Thermal architecture optimised to damp thermal fluctuations (active+passive)
  - *NB: 100mK cooling by dilution cooler does not tolerate micro-vibrations at sub-mg level or 7.10^{10} He atoms accumulated on dilution heat exchanger (typically He pressure 1.10^{-10} mb)*

$\Rightarrow$ ***Integration of 3 intertwined complex chains - optical, electronic, cryogenic***

HFI cut-away

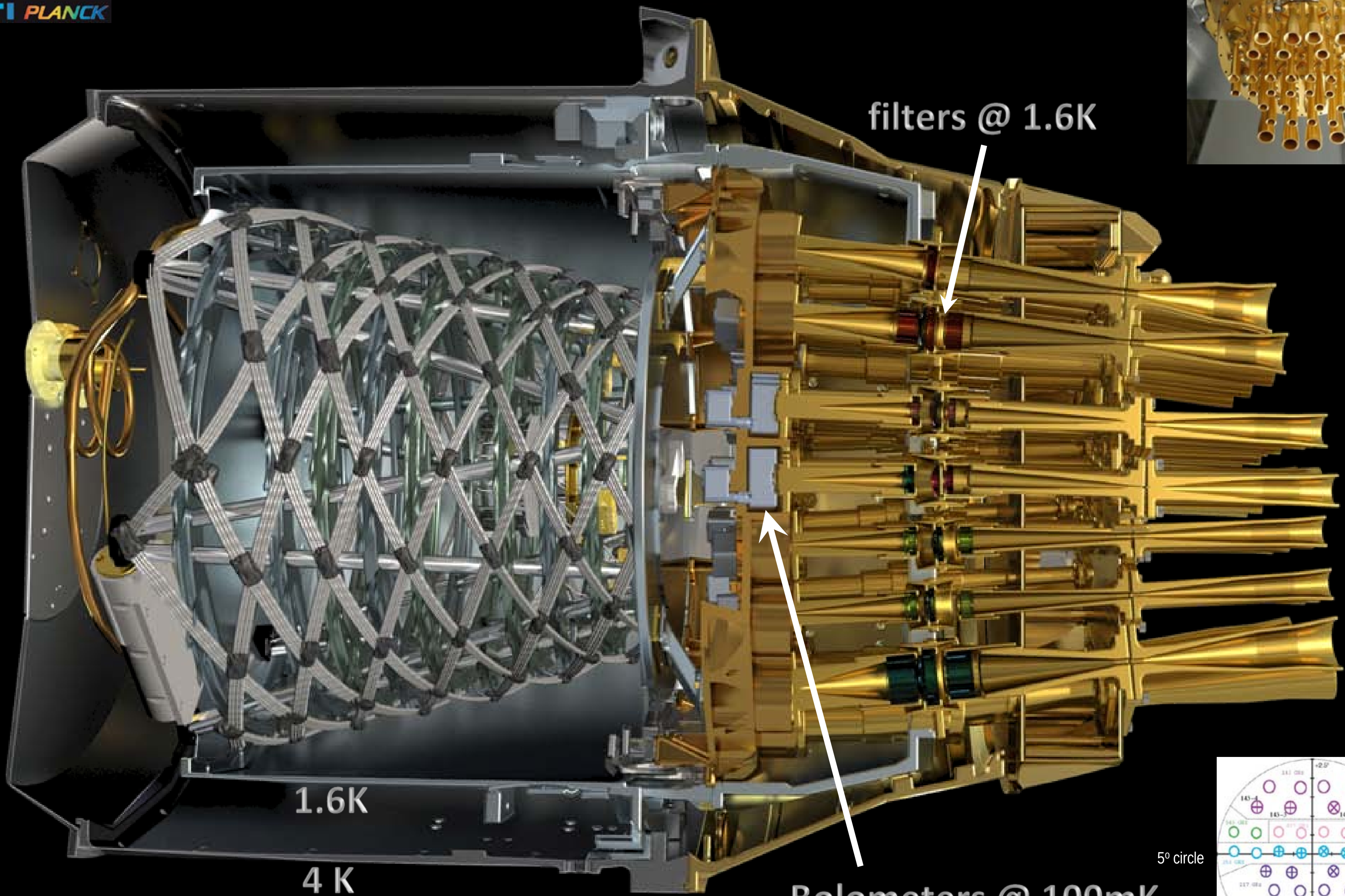

5° circle

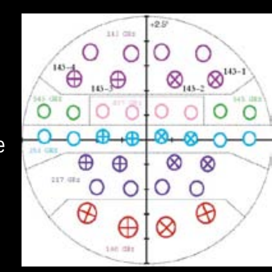

The Low Frequency Instrument LFI

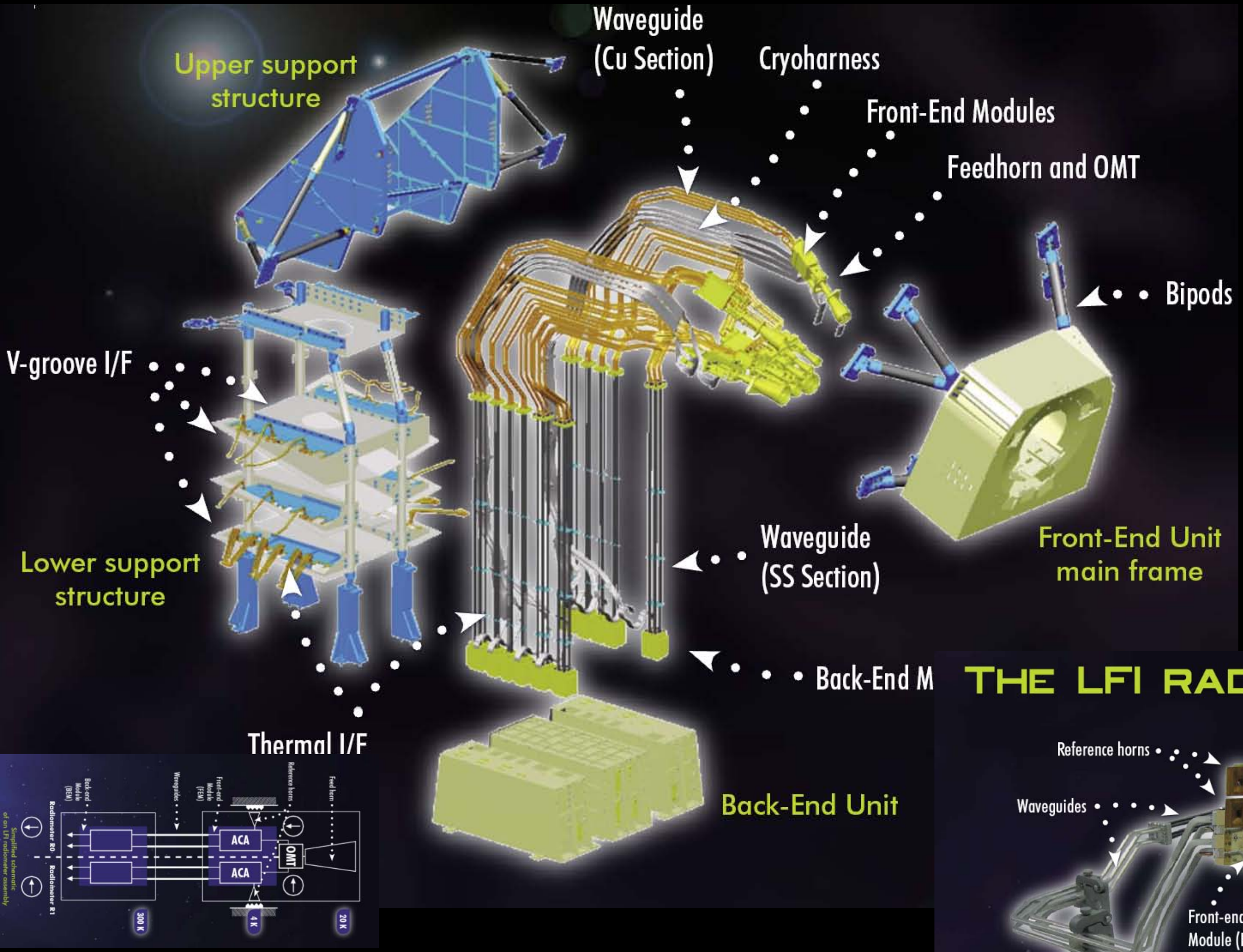

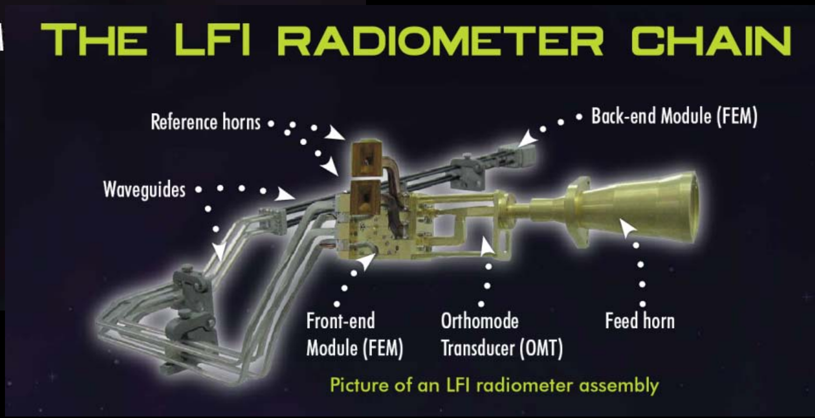

Birth of the Cool


…STING IT OFF…
AFTER 16 YEARS
OF HOPES & WORK
CSG
CSG

Ariane 5 ECA Launch • HERSCHEL – PLANCK - May 14, 2009

Planck is in L2 orbit since July 2009

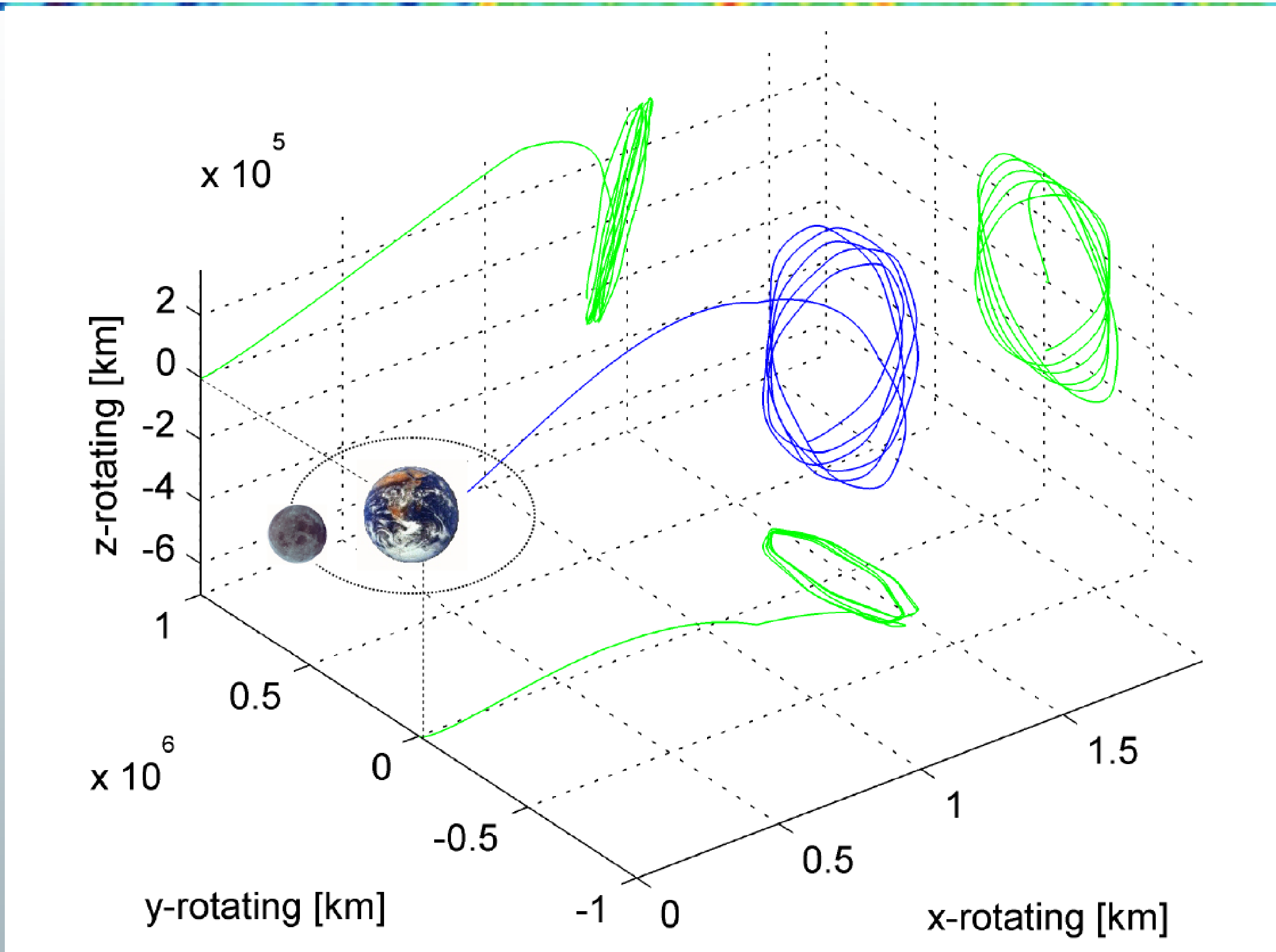

Status & Schedule

- Instruments are very stable, continuously mapping the sky, with essentially no hiccups from the beginning of survey, on August 13th 2009, till now.
- Expectations on sensitivities confirmed in flight: HFI reaches or exceeds its goals
- It is not to say that data analysis is easy, but the data potential is here.

- First complete coverage of the sky by all detectors was obtained in June 2010 with the first nearly ***10 months*** of survey data. ERCSC release & batch of 25 papers on "Planck early results: xxx", submission **in Jan 2011**(now printed in A&A Volume 536, Dec 2011); some highlights are presented next.

- Nominal mission was completed on November 27th 2010, having collected about ***15.5 months*** of survey data insuring that all the sky at been seen at least twice by each detector; expect:
  - *more CMB foregrounds results, **starting early 2012** (foregrounds conf in Bologna in february).*
  - *first cosmological analyses and public delivery of T data **in early 2013**.*

- While I speak, HFI is performing EOL activities (spin-up, etc) and will go warm January 15th 2012. We have collected ~5 surveys, ~ twice the nominal duration. This, together with some additional LFI data, will be the basis of our final data delivery (DD2) in **early 2014.** (will contain clean TOIs, frequency and component maps (T Q U), a likelihood code+ ancillary data

Yesterday's msg from Spacecraft Operations

FYI

Dear all,

The concluding activities for the spin-up campaign were successfully executed today (Friday 16 December) from 12:00z-15:40z.

After (OCM) slewing to anti-sun pointing, the spin-down from 1.4rpm to 1.0rpm was executed in 2 stages between 13:08z-13:45z.
The spacecraft was then aligned with the start attitude of the first pointing set in the return to the nominal scanning law.

The first scanning law pointing commences after an initial scanning law slew at 18:35z.

This concludes an extremely successful test campaign. The relatively flawless execution is testament to the preparatory work done by many people, and their commitment and assiduousness is both recognised and appreciated.

Many regards
Steve
____
Planck Deputy Spacecraft Operations Manager
Planck Instrument Engineer
European Space Operations Centre

4th Press Release (05/07/2010)

The Planck "one-year" all-sky survey

esa

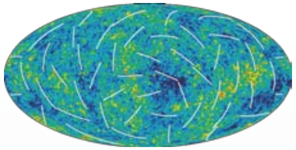

Foregrounds !!!

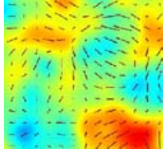

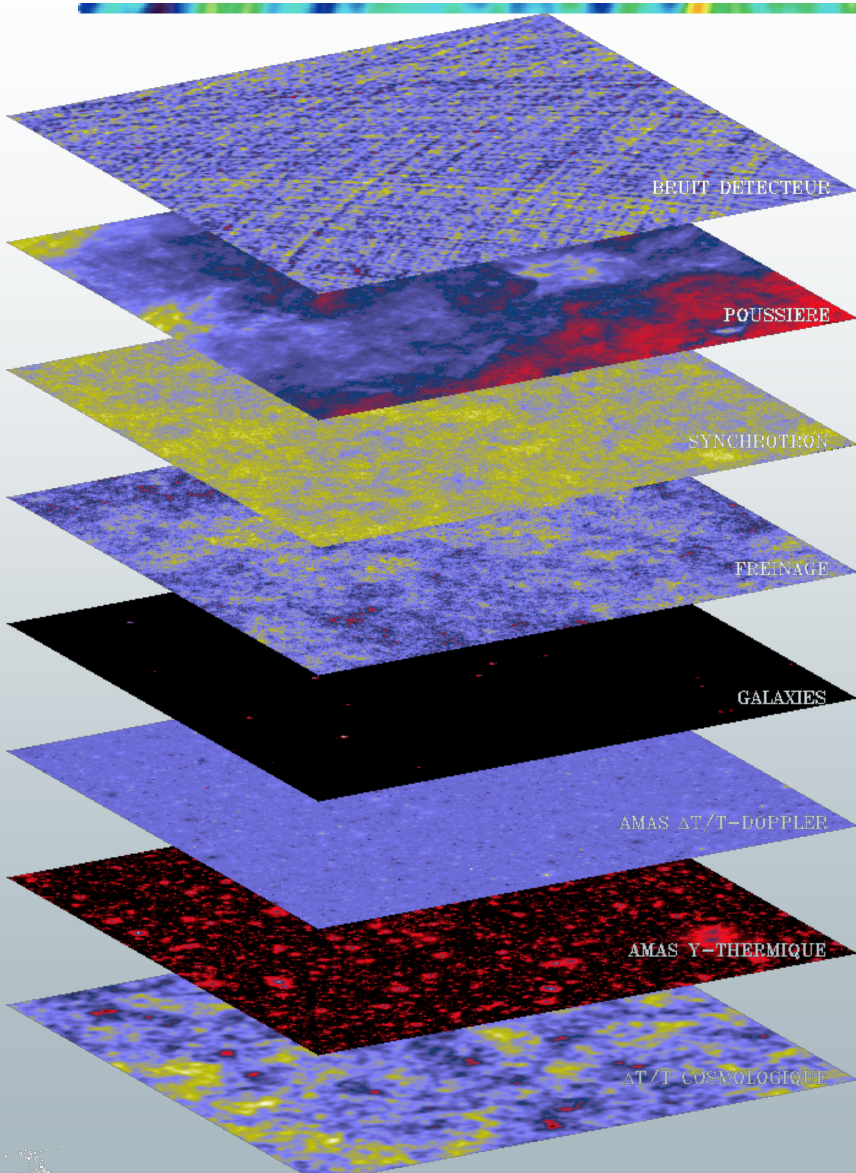

F.R. BOUCHET & R. GISPERT 1996

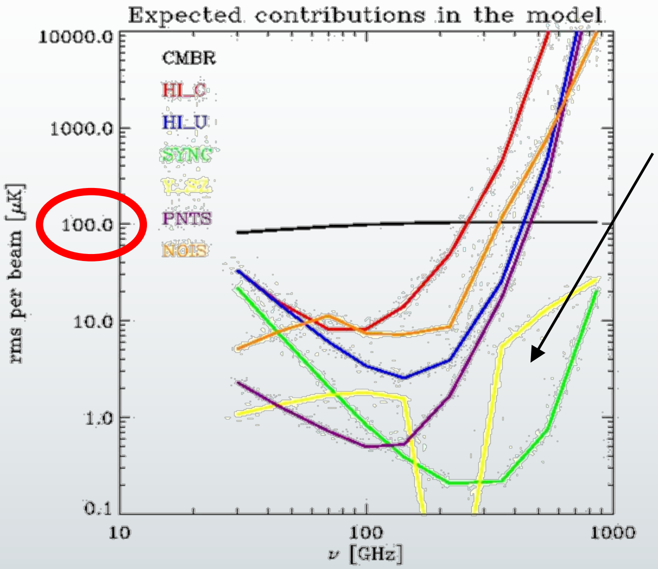

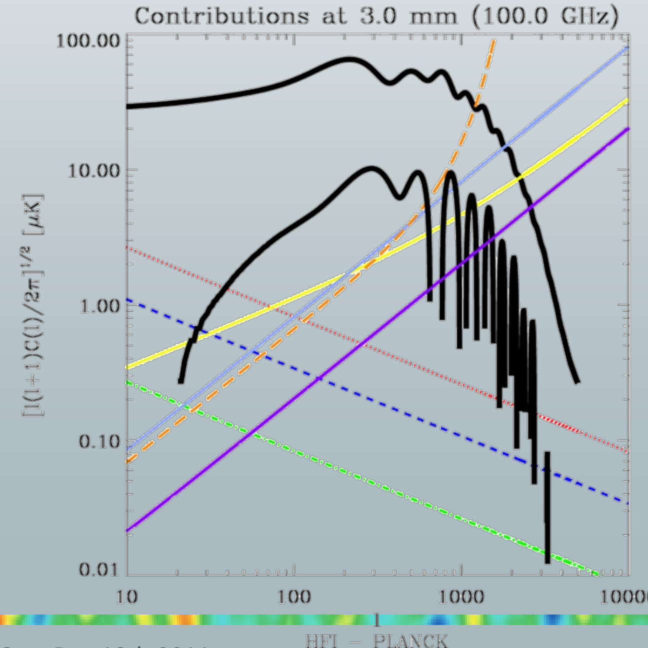

ΔH_0
=2%

The Planck Foregrounds sky

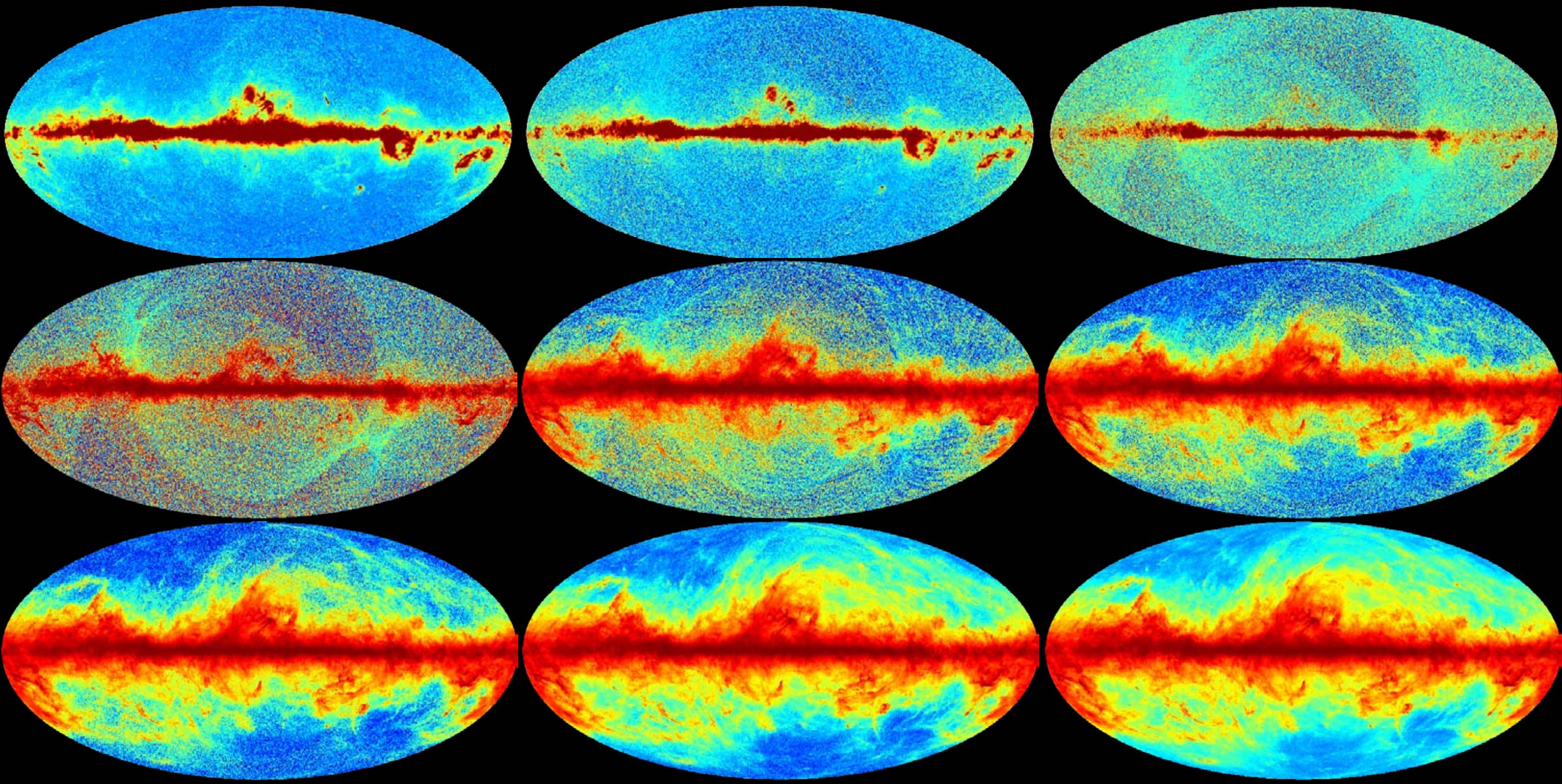

© ESA, HFI & LFI, Jan 2011

The Planck Foregrounds sky

Planck Early Release Compact Source Catalogue

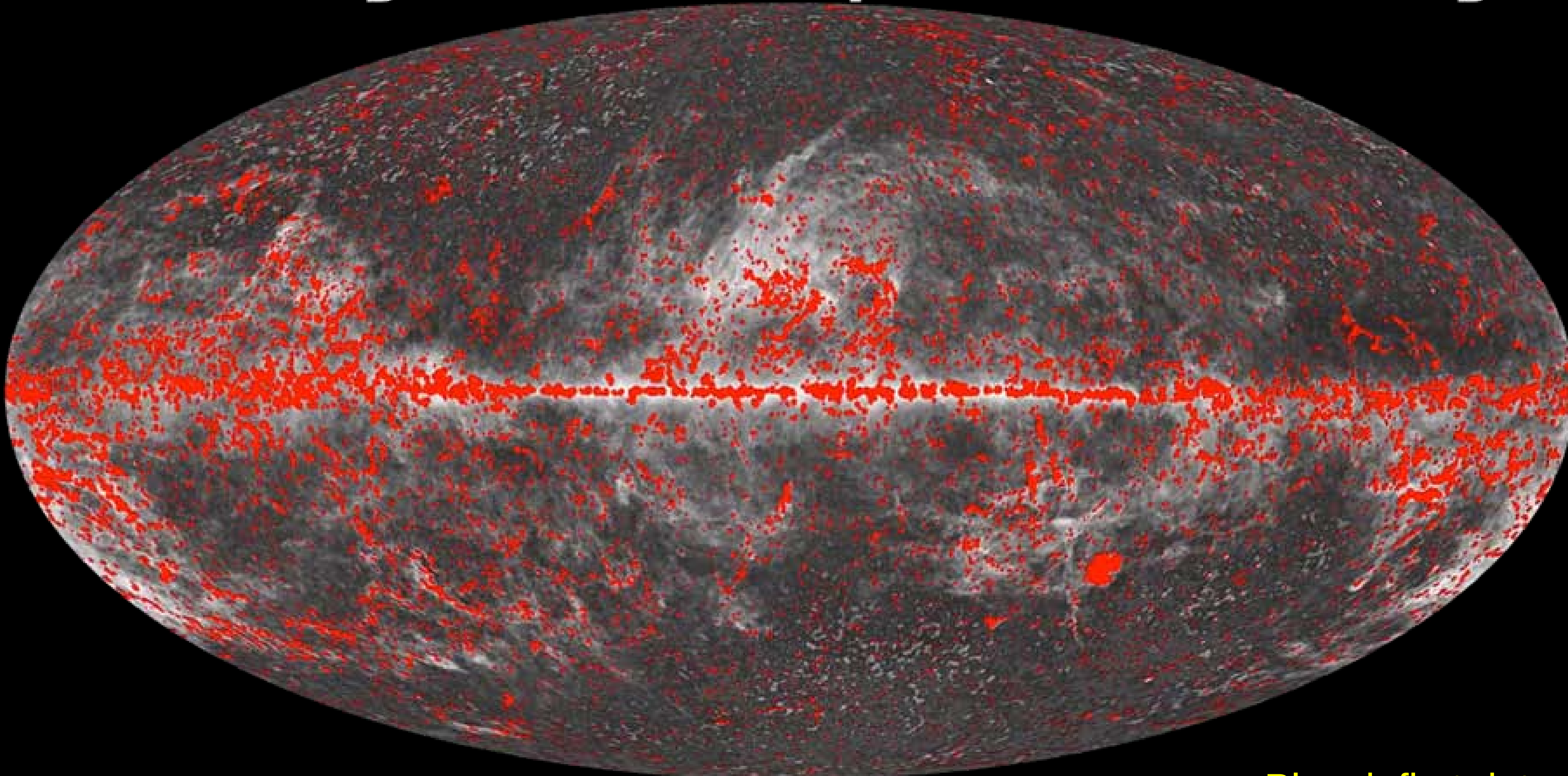

All compact sources

Planck first data delivery, on time

The Planck SZ sky

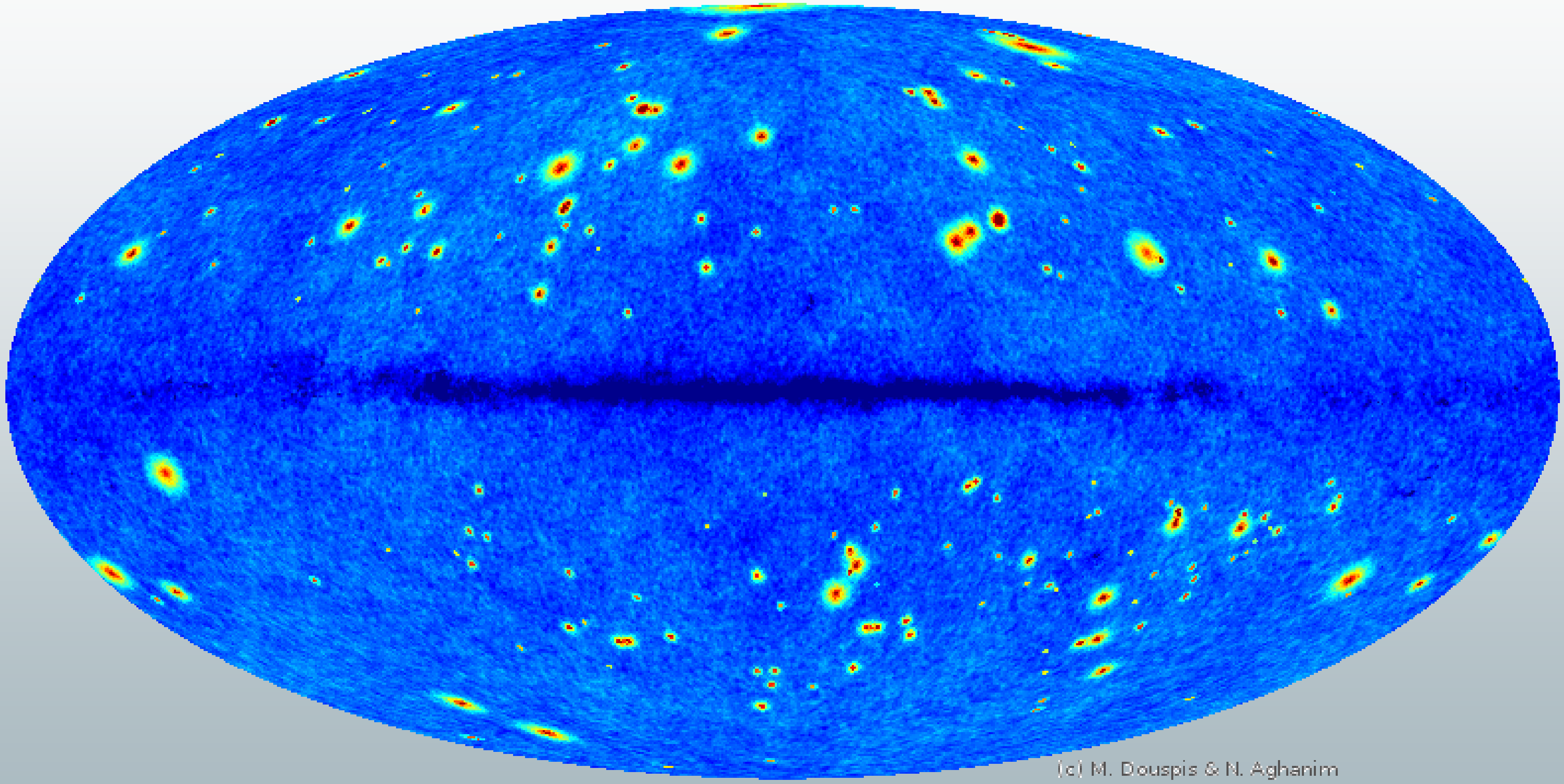

Planck clusters versus other samples

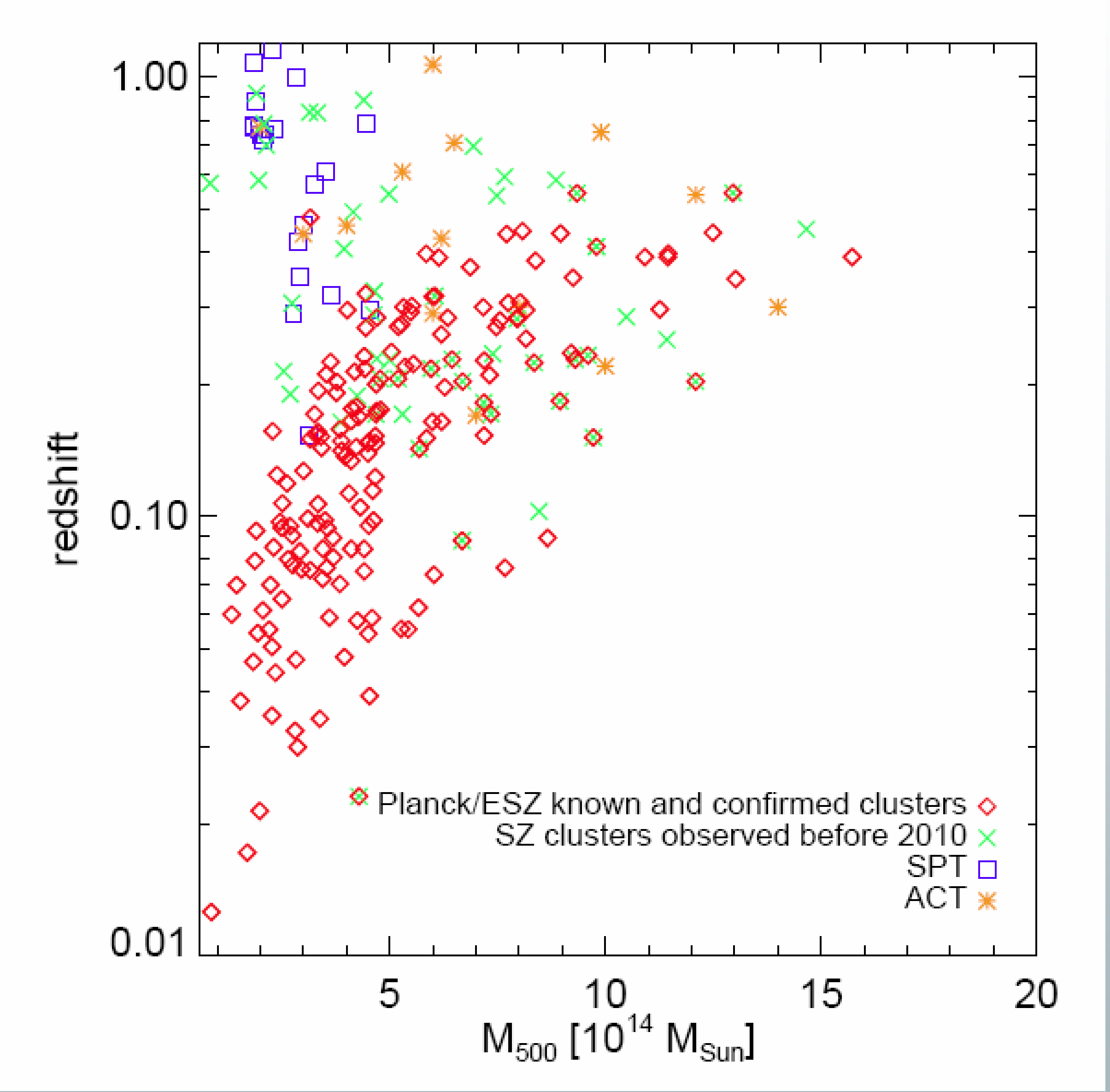

Planck indeed detects the rarest and most massive clusters in our local universe

CIB appearance versus frequency

1. As we move towards lower frequencies we see structures in the universe at higher z, closer and closer to the bulk of IR galaxy formation
2. The same structures are seen in successive bands illustrating the high signal to noise
3. we expect the lowest Planck frequency CIB maps (217 Ghz) shows structures formed less than 2 billion years after the big bang

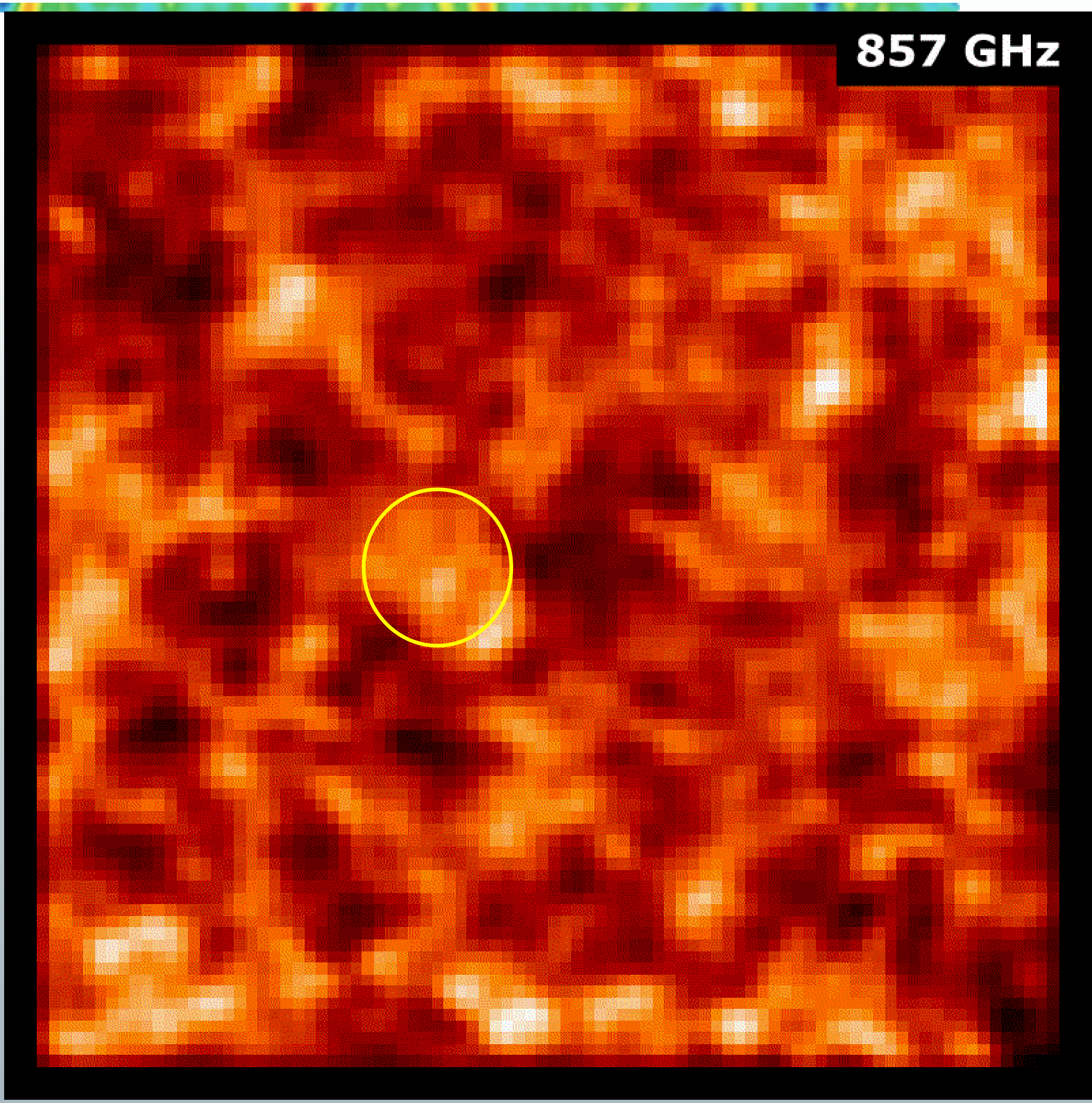

BLAST & SPT versus HFI

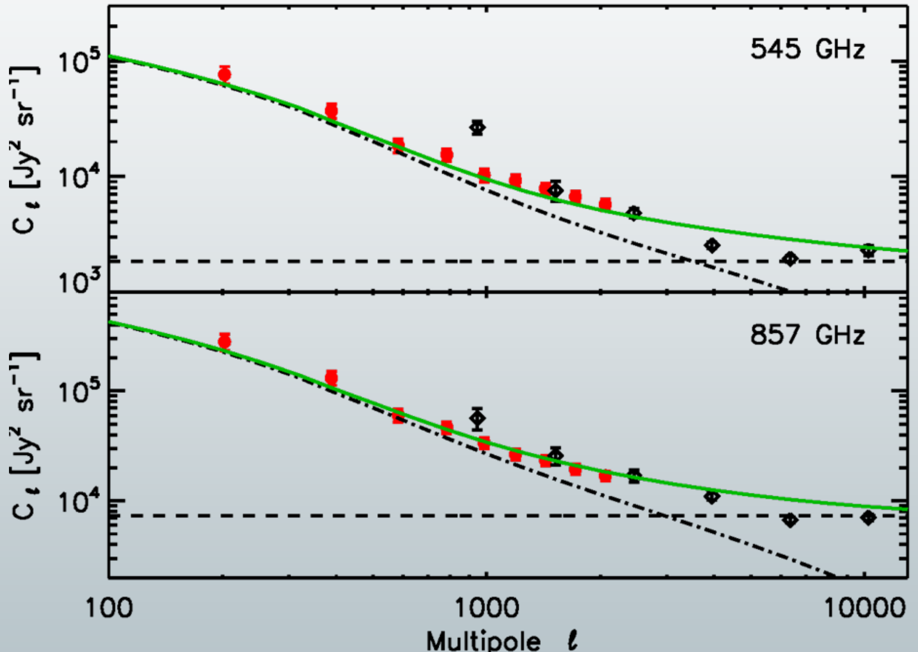

NB: BLAST values are color-corrected using the CIB mean spectrum (1.05 @ 857 & 0.7 @ 545 GHz)

HFI+SPT: (Reichardt 2011, arXiv:1111.0932v1)
Clustered component scale dependance $\propto l^{-0.8}$

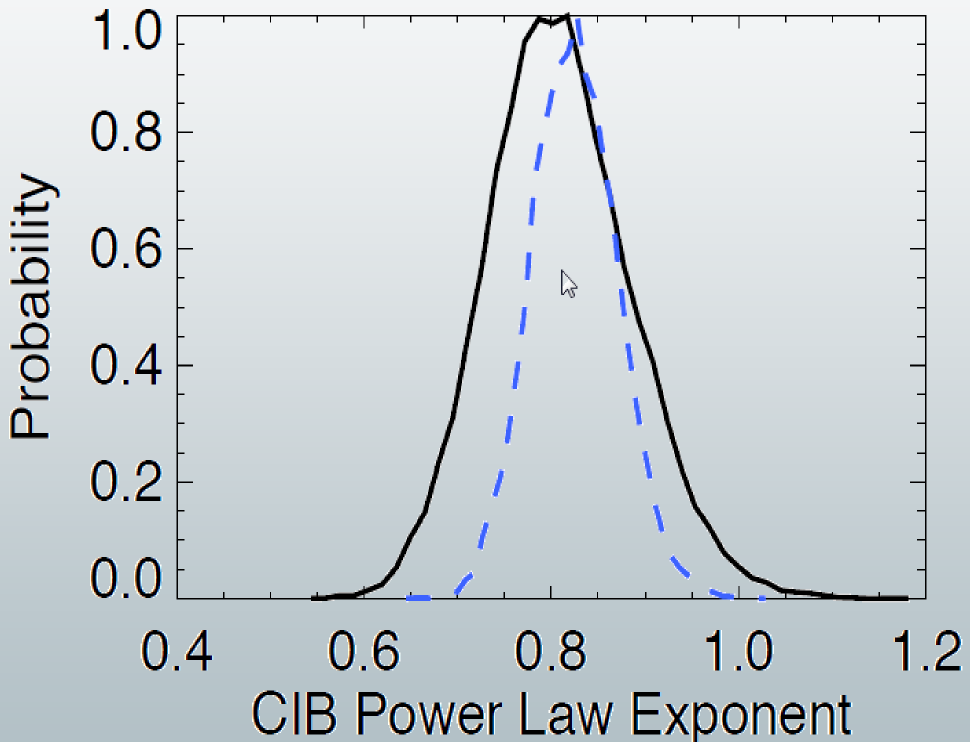

Blue dashes when HFI 353 GHz CIB bandpower constraint is included

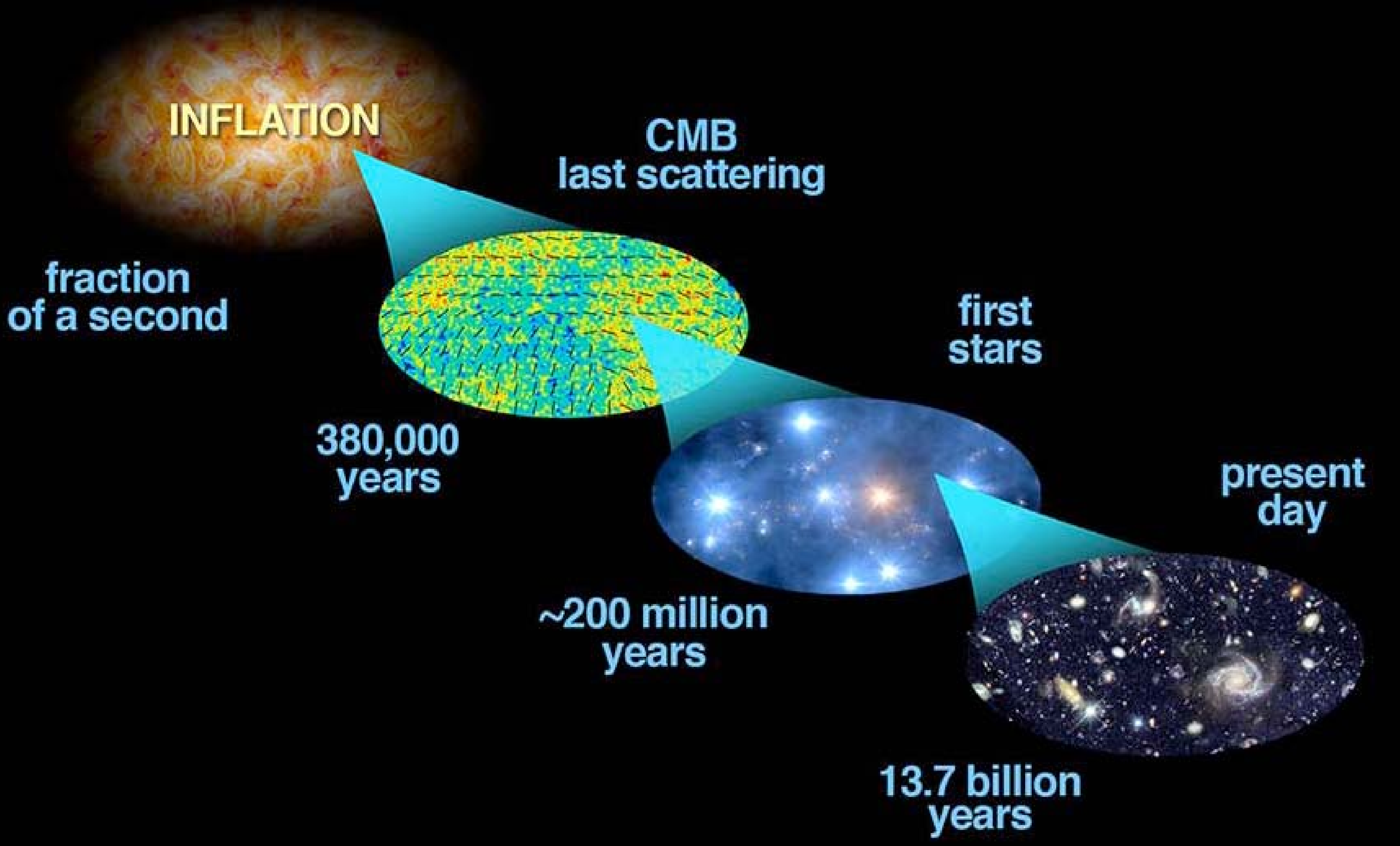
INFLATION
CMB
last scattering
fraction
of a second
first
stars
380,000
years
present
day
~200 million
years
13.7 billion
years

Inflation has many variants...

- assisted brane inflation
- anomaly-induced inflation
- assisted inflation
- assisted chaotic inflation
- B-inflation
- boundary inflation
- brane inflation
- brane-assisted inflation
- brane gas inflation
- brane-antibrane inflation
- braneworld inflation
- Brans-Dicke chaotic inflation
- Brans-Dicke inflation
- bulky brane inflation
- chaotic inflation
- chaotic hybrid inflation
- chaotic new inflation
- D-brane inflation
- D-term inflation
- dilaton-driven inflation
- dilaton-driven brane inflation
- double inflation
- double D-term inflation
- dual inflation
- dynamical inflation
- dynamical SUSY inflation
- S-dimensional assisted inflation
- eternal inflation
- extended inflation
- extended open inflation
- extended warm inflation
- extra dimensional inflation
- F-term inflation

- F-term hybrid inflation
- false-vacuum inflation
- false-vacuum chaotic inflation
- fast-roll inflation
- first-order inflation
- gauged inflation
- Ghost inflation
- Hagedorn inflation

- higher-curvature inflation
- hybrid inflation
- Hyper-extended inflation
- induced gravity inflation
- intermediate inflation
- inverted hybrid inflation
- Power-law inflation
- K-inflation
- Super symmetric inflation
- Roulette inflation

- Quintessential inflation
- curvature inflation
- Natural inflation
- Warm natural inflation
- Super inflation
- Super natural inflation
- Thermal inflation
- Discrete inflation
- Polarcap inflation
- Open inflation
- Topological inflation
- Multiple inflation
- Warm inflation
- Stochastic inflation
- Generalised assisted inflation
- Self-sustained inflation
- Graduated inflation
- Local inflation
- Singular inflation
- Slinky inflation
- Locked inflation
- Elastic inflation
- Mixed inflation
- Phantom inflation
- Non-commutative inflation
- Tachyonic inflation
- Tsunami inflation
- Lambda inflation
- Steep inflation
- Oscillating inflation
- Mutated hybrid inflation
- Inhomogeneous inflation

Where is the machete for the inflationary jungle?

- We now have a couple of percent accuracy on the 6 parameter of the minimal model, which still fits all the data, with no sign yet than anything else is needed.
- In particular, regarding early Universe physics, no need besides *single field canonical inflation*: not even strong evidence for any of (n_s-1, dn_s/dlnk, r) to be non-zero.
- And indeed lack of detection of any extension/anomalies
- (And cyclic/LQC universes are OK too)

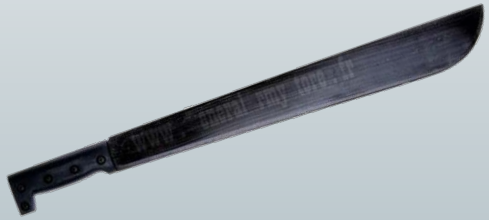

- Planck will help clearing the ground by
  - *tightening the constraints on the trio above, or making detections!*
  - *Look additionally at the signatures of specific models: existence of Isocurvature modes,*
  - *specific Non-Gaussianities: an additional quatuor: (f_{NL}-local, f_{NL}-equilateral, f_{NL}-orthogonal, g_{NL})*
- Alone first, and in conjunction (Planck-EXT) with SS CMB, LSS

Plain vanilla accuracy forecast

WMAP 4 years (94 GHz)
Planck 1 year (143 GHz)

Qualitative Advance in Precision

Bond et al.astroph/0406195

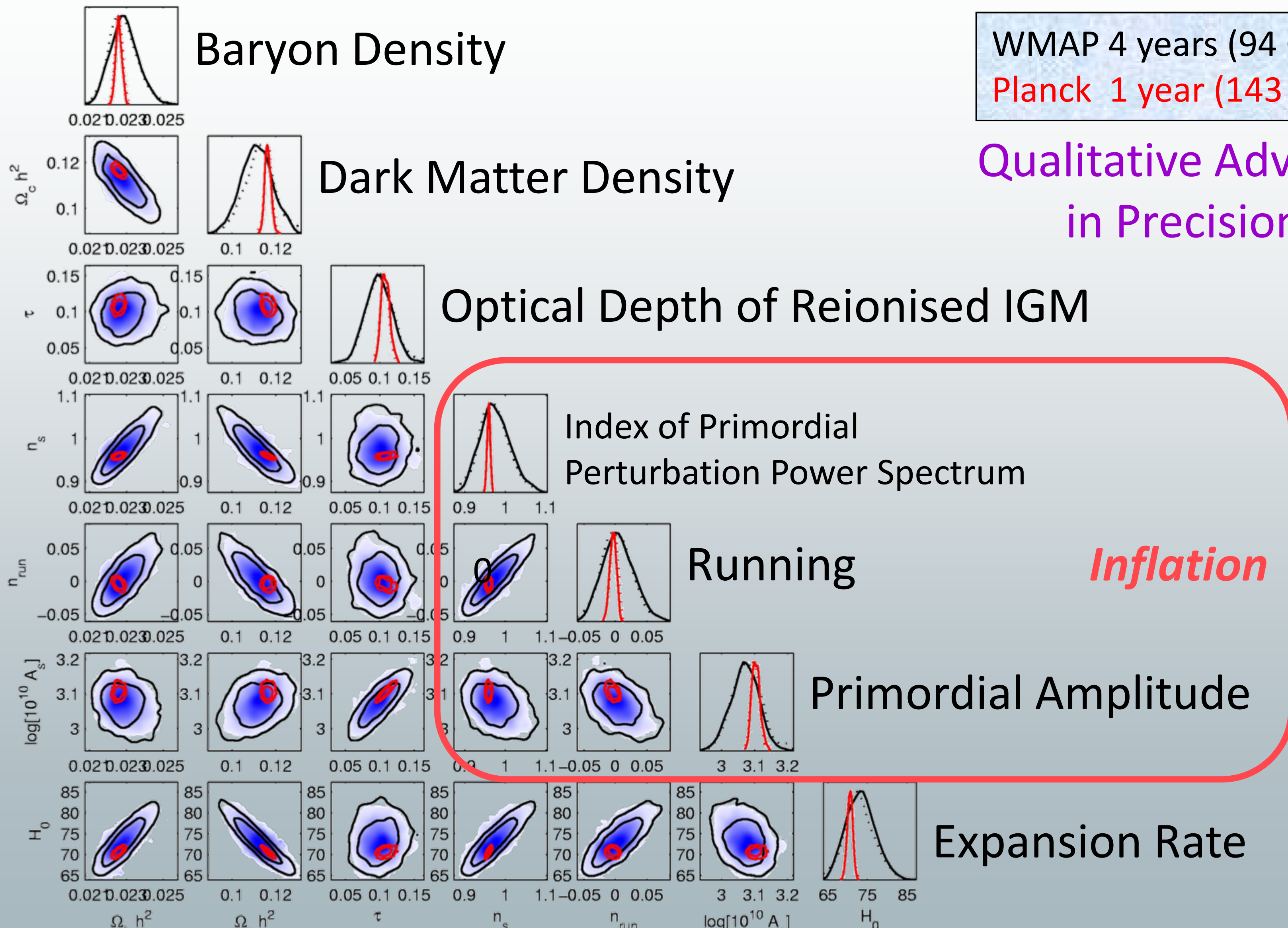

Planck vs Ideal (including polarisation)

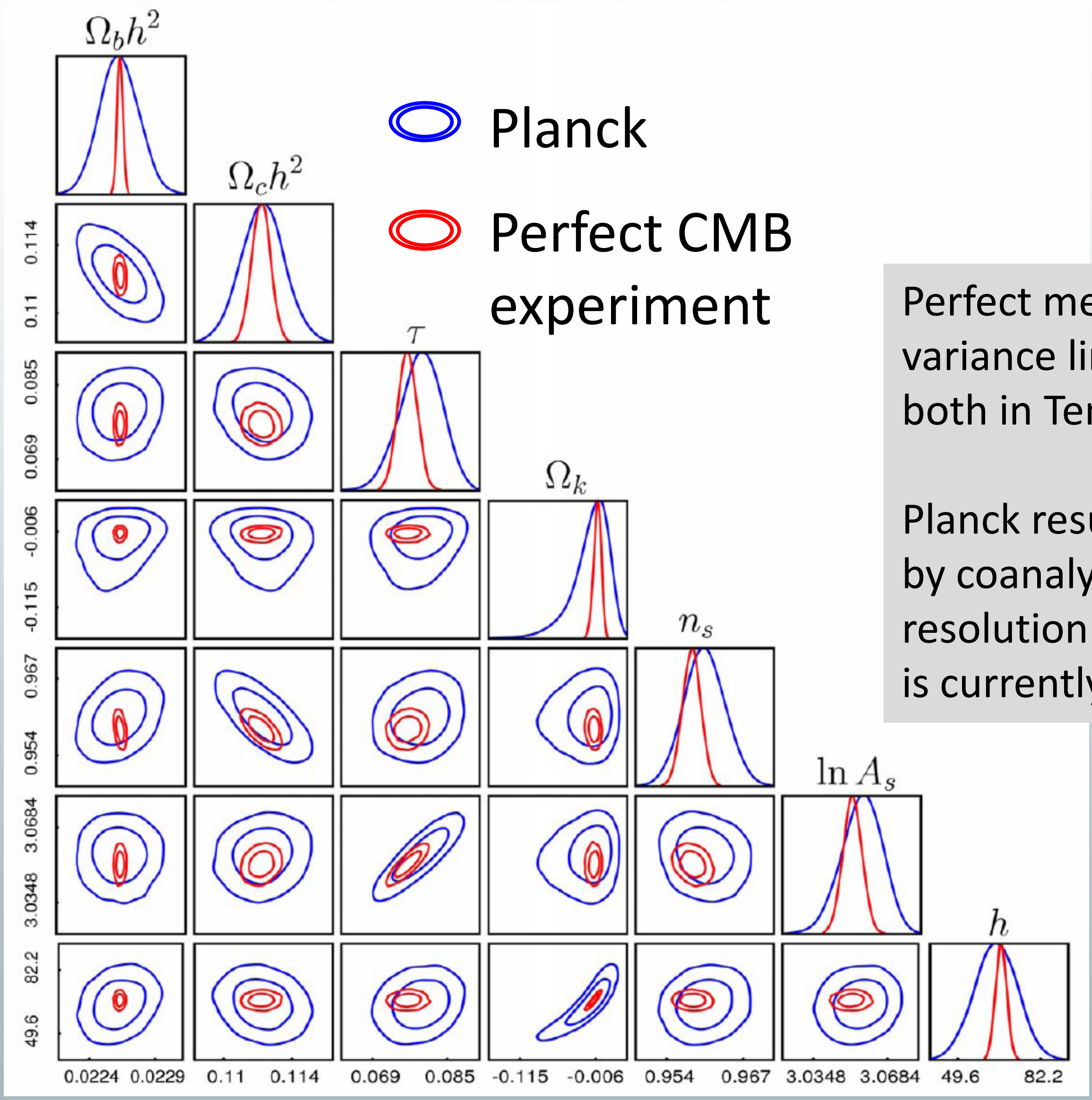

Fendt & Wandelt

Perfect means zero-noise (i.e. Cosmic variance limited) for all ell <~3000, both in Temperature and polarization.

Planck results will be further improved by coanalysing Planck with higher resolution experiments (PlanckEXT), as is currently done with WMAP.

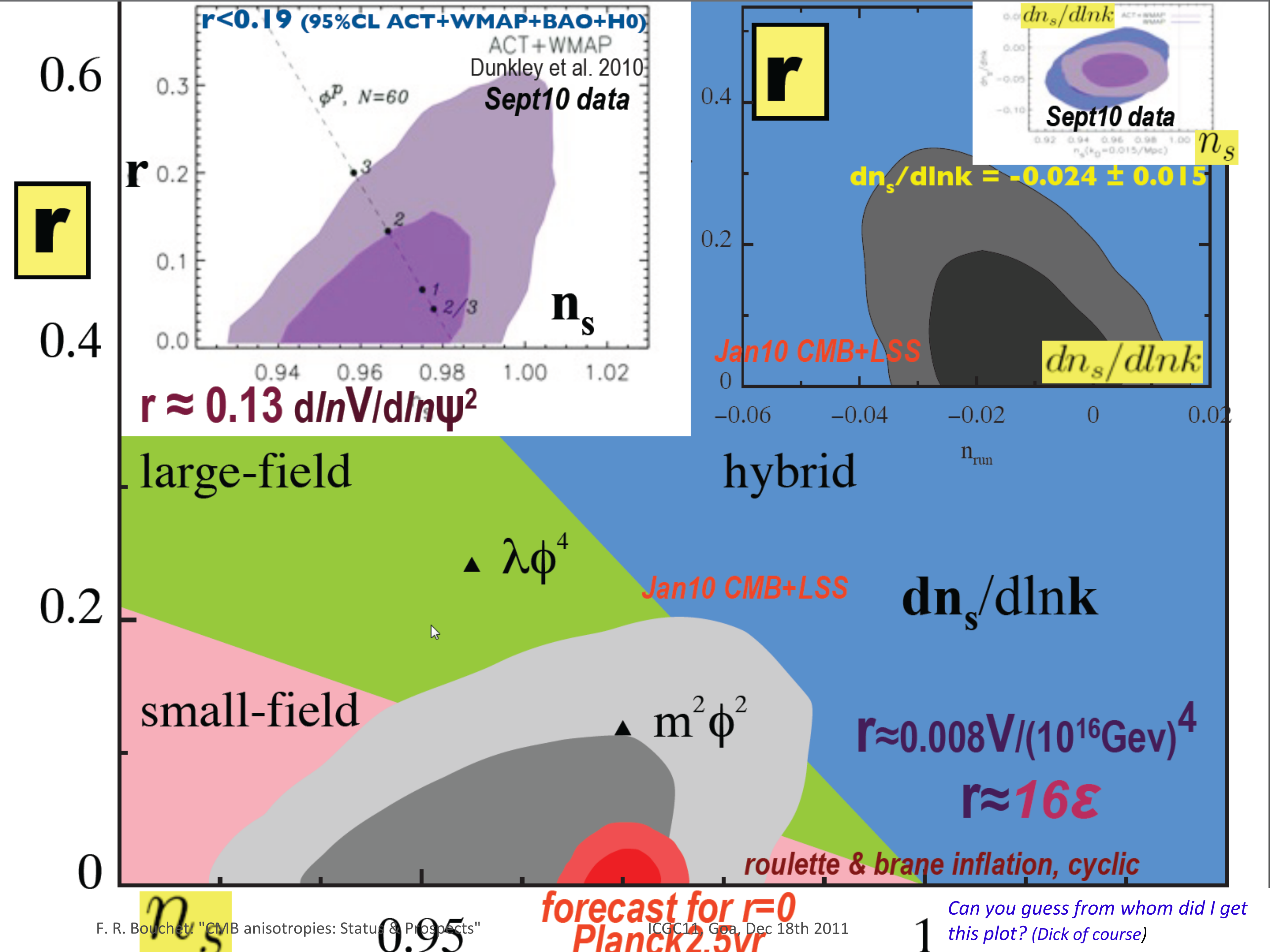

Can you guess from whom did I get this plot? (Dick of course)

Planck vs LSS forecasts for ΛMDM

Hamann et al., JCAP 2010/07

Current status

Model	Data set	$\sum m_\nu/\mathrm{eV}$	N_{eff}	w
vanilla+f_ν+N_{eff}+w	CMB+HST	< 2.58	$4.68^{+3.72}_{-3.48}$	$-1.33^{+0.77}_{-0.87}$
	CMB+HST+BAO	< 1.47	$3.68^{+1.90}_{-1.84}$	$-1.42^{+0.60}_{-0.65}$
	CMB+HST+HPS	< 1.16	$4.79^{+2.02}_{-2.02}$	$-1.02^{+0.39}_{-0.44}$

NB: Mean & limits of the 95% credible intervals

Planck & LSS forecast w.r.t. current status

	Planck	P+BAO	P+HPS	P+HST	P+HST+BAO	P+HST+HPS
ω_{dm}	0.22	0.24	0.20	0.21	0.21	0.19
N_{eff}	0.21	0.21	0.22	0.21	0.21	0.22
$\sum m_\nu$	0.68	0.81	0.44	0.67	0.73	0.44
w	2.14	1.16	0.72	0.74	0.76	0.55
n_S	0.46	0.48	0.49	0.46	0.48	0.48

Table 3. Projected sensitivity of Planck data (P) combined with LSS data to selected parame of the vanilla+f_ν+N_{eff}+w model. Given are the standard deviations of the marginalised posteri normalised to the values obtained with current CMB+HST+HPS data. Note that just like for curr

Planck *alone* should do better by a factor 2-4 than the current CMB+LSS data: i.e less reliance on external datasets. Main (large) improvement is for w

HPS: halo power spectrum constructed from the luminous red galaxy sample of the 7th data release of the Sloan Digital Sky Survey (SDSSDR7).

ISOCURVATURE MODES

$\prod = 8.10^{-11}$ $\prod = 7.10^{-24}$

	MAP T adia only	MAP TP adia only	MAP T all modes	MAP TP all modes	PLANCK T adia only	PLANCK TP adia only	PLANCK T all modes	PLANCK T+P all modes	PLANCK TP all modes
$\delta h/h$	12.37	7.42	175.84	20.40	9.93	3.69	40.13	7.31	4.36
$\delta\Omega_b/\Omega_b$	27.76	13.34	325.38	28.57	19.37	7.26	68.85	14.42	8.61
$\delta\Omega_k$	9.79	2.72	75.32	4.55	4.92	1.83	20.56	3.59	2.18
$\delta\Omega_\Lambda/\Omega_\Lambda$	12.92	5.02	123.63	18.53	2.74	1.21	5.93	2.45	1.49
$\delta n_s/n_s$	7.02	1.62	89.89	6.53	0.73	0.37	3.92	0.90	0.70
τ_{reion}	37.39	1.81	104.81	2.23	8.25	0.41	35.35	0.74	0.56
$\langle NIV, NIV \rangle$	..	..	114.34	11.47	..	..	43.45	1.36	1.14
$\langle BI, BI \rangle$	..	..	573.46	29.71	..	..	53.29	6.16	4.23
$\langle NID, NID \rangle$	..	..	351.79	29.87	..	..	19.18	4.77	2.37
$\langle NIV, AD \rangle$	..	..	434.70	44.06	..	..	121.59	8.21	4.69
$\langle BI, AD \rangle$	..	..	1035.02	59.25	..	..	58.75	15.03	8.97
$\langle NID, AD \rangle$	..	..	1287.60	67.49	..	..	114.39	13.87	5.77
$\langle NIV, BI \rangle$	..	..	601.70	32.29	..	..	46.91	7.72	3.67
$\langle NIV, NID \rangle$	..	..	744.00	46.46	..	..	80.01	7.55	2.97
$\langle BI, NID \rangle$	..	..	534.32	39.11	..	..	100.97	7.56	4.60

TABLE I. This table indicates the one sigma percentage errors on cosmological parameters and isocurvature mode amplitudes anticipated for the MAP and PLANCK satellite experiments. In the column headers, T denotes constraints inferred from temperature measurements alone, TP those from the complete temperature and polarisation measurements, and T+P those inferred if temperature and polarisation information is used separately without including the cross-correlation.

Bucher, Moodley, Turok, astroph/0012141 (see also Trotta & Durrer)

NB: Still assuming simple scale-invariant (initial) P(k)…

NB2: Can add LSS, or HST+SN1A to improve Ω_k, cf. Dunkley et al. astroph/0507473, but reliance on external data)

➔ *Much less reliance on theoretical priors*

LSS deviate background light

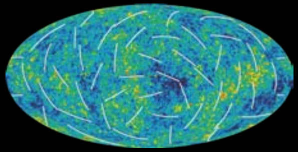

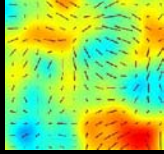

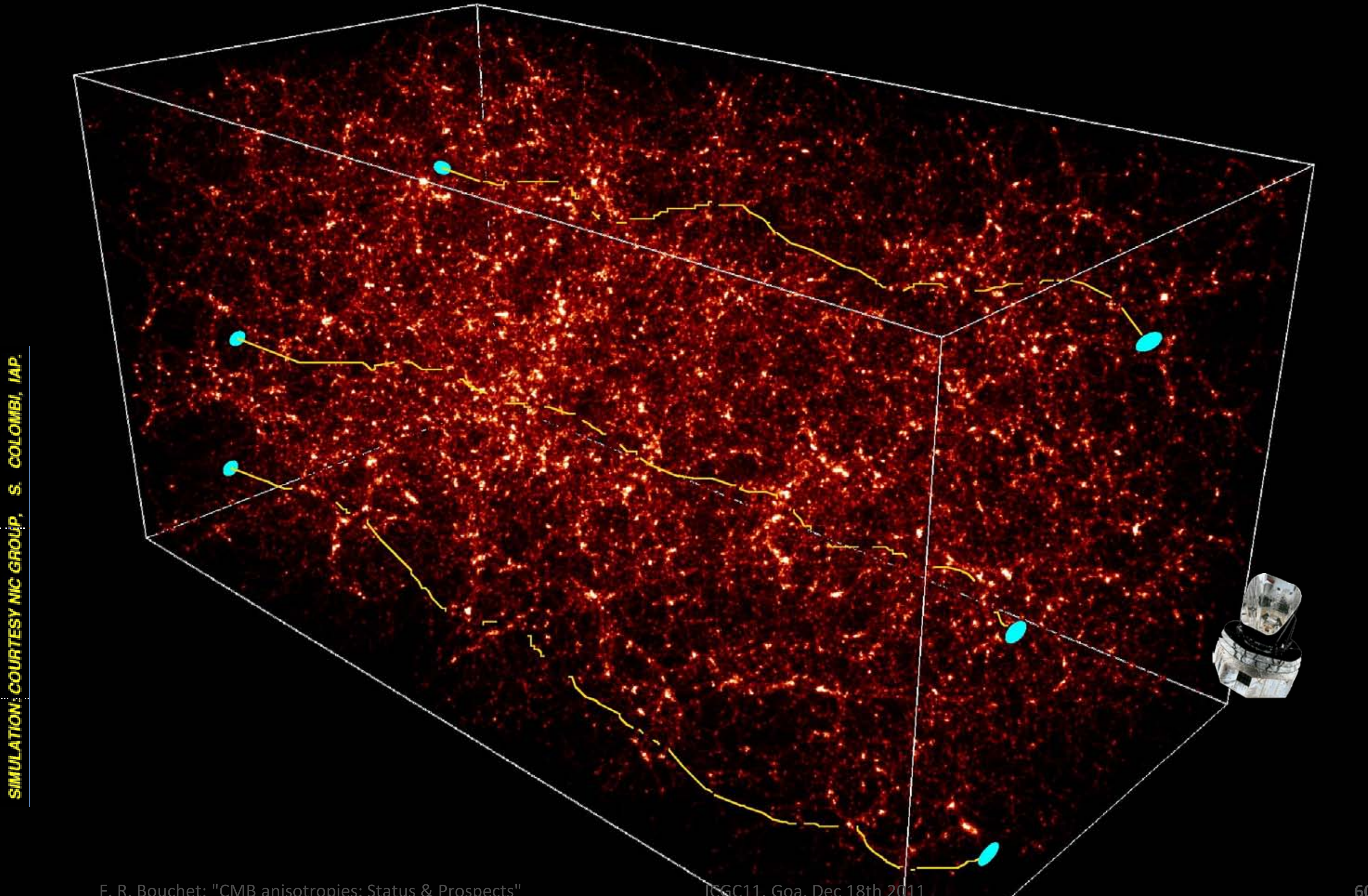

Unlensed CMB

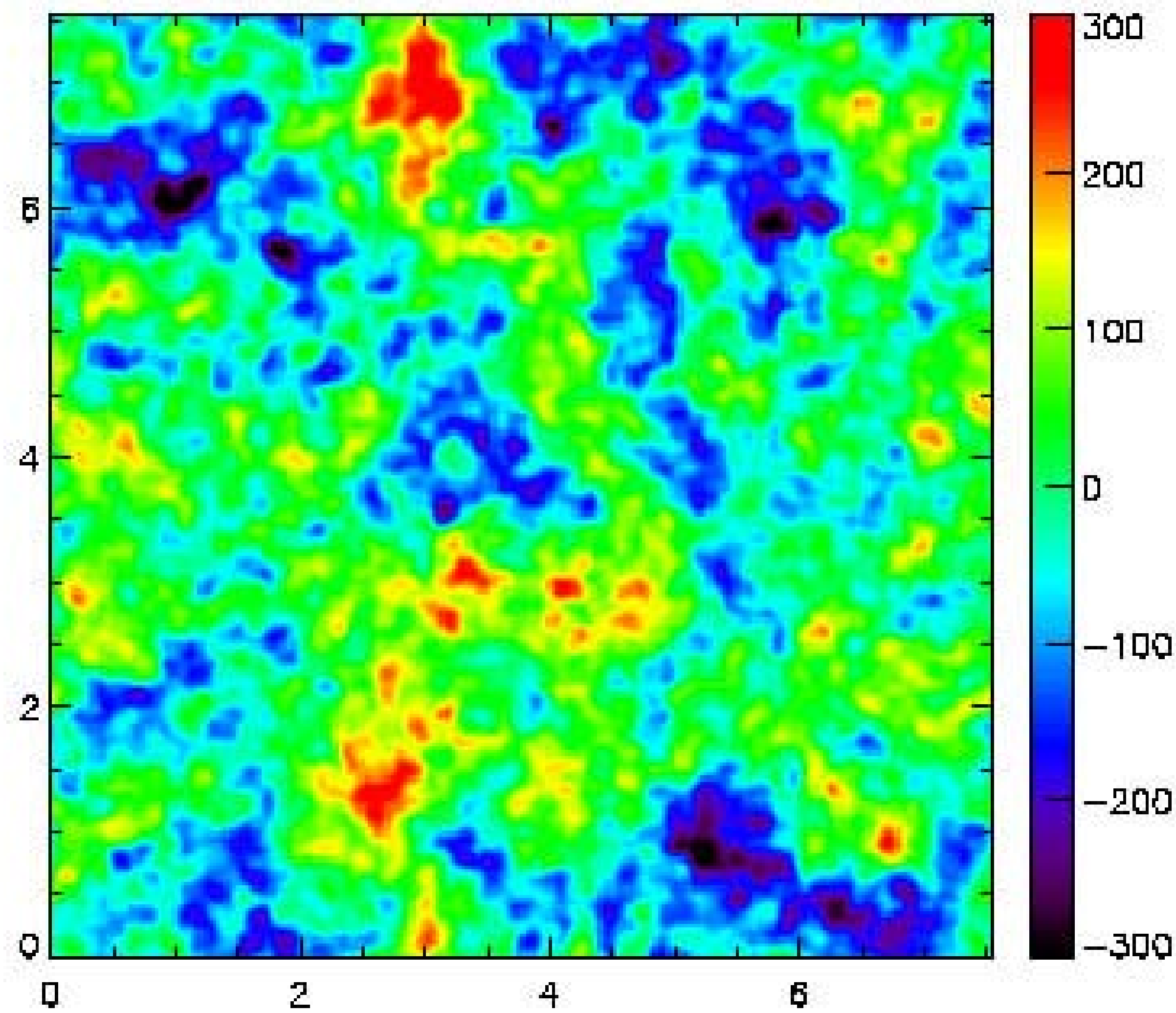

Image from Basak et al 2009

Lensed CMB

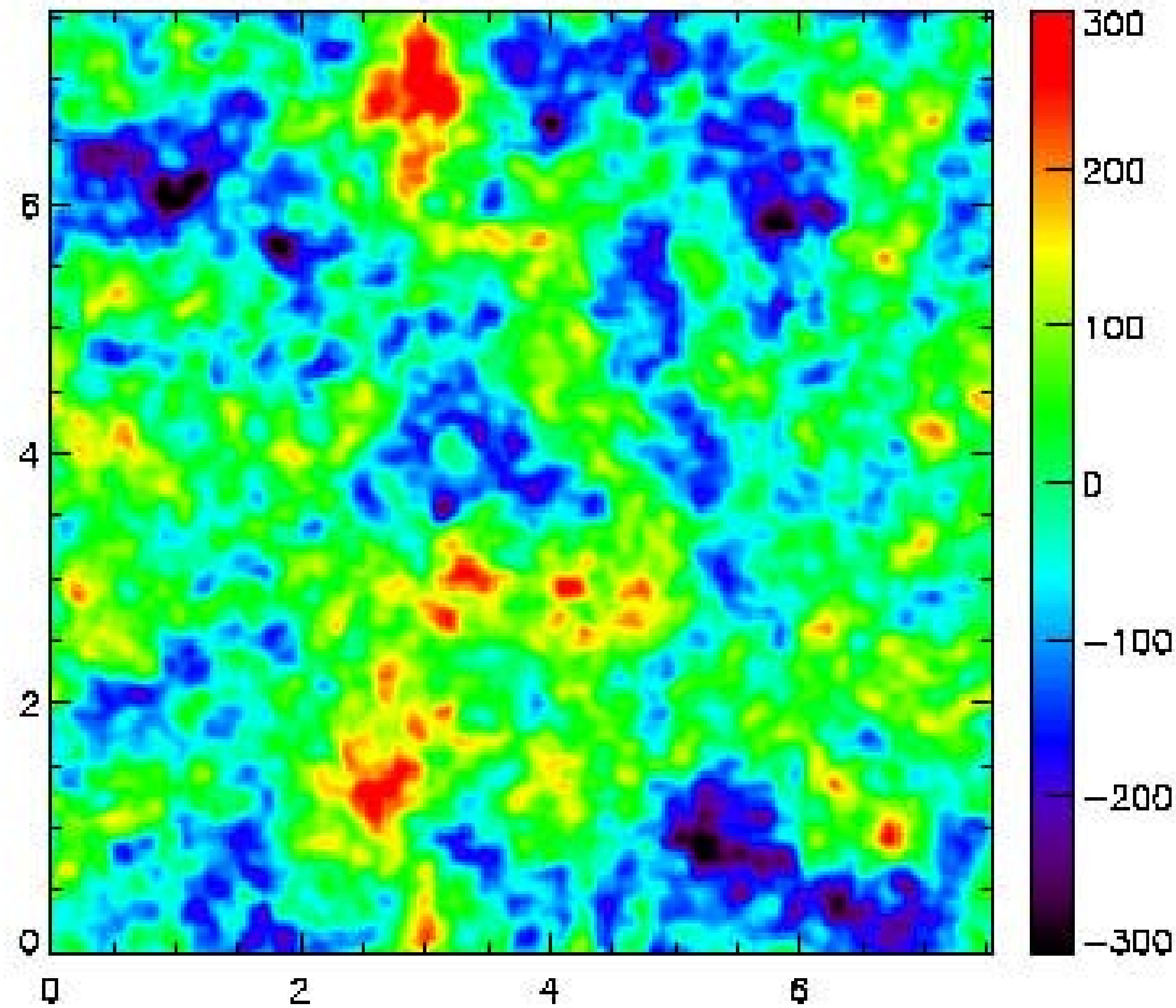

Deflection are ~2' , but coherent over degrees

Image from Basak et al 2009

Deflections smooth the spectra

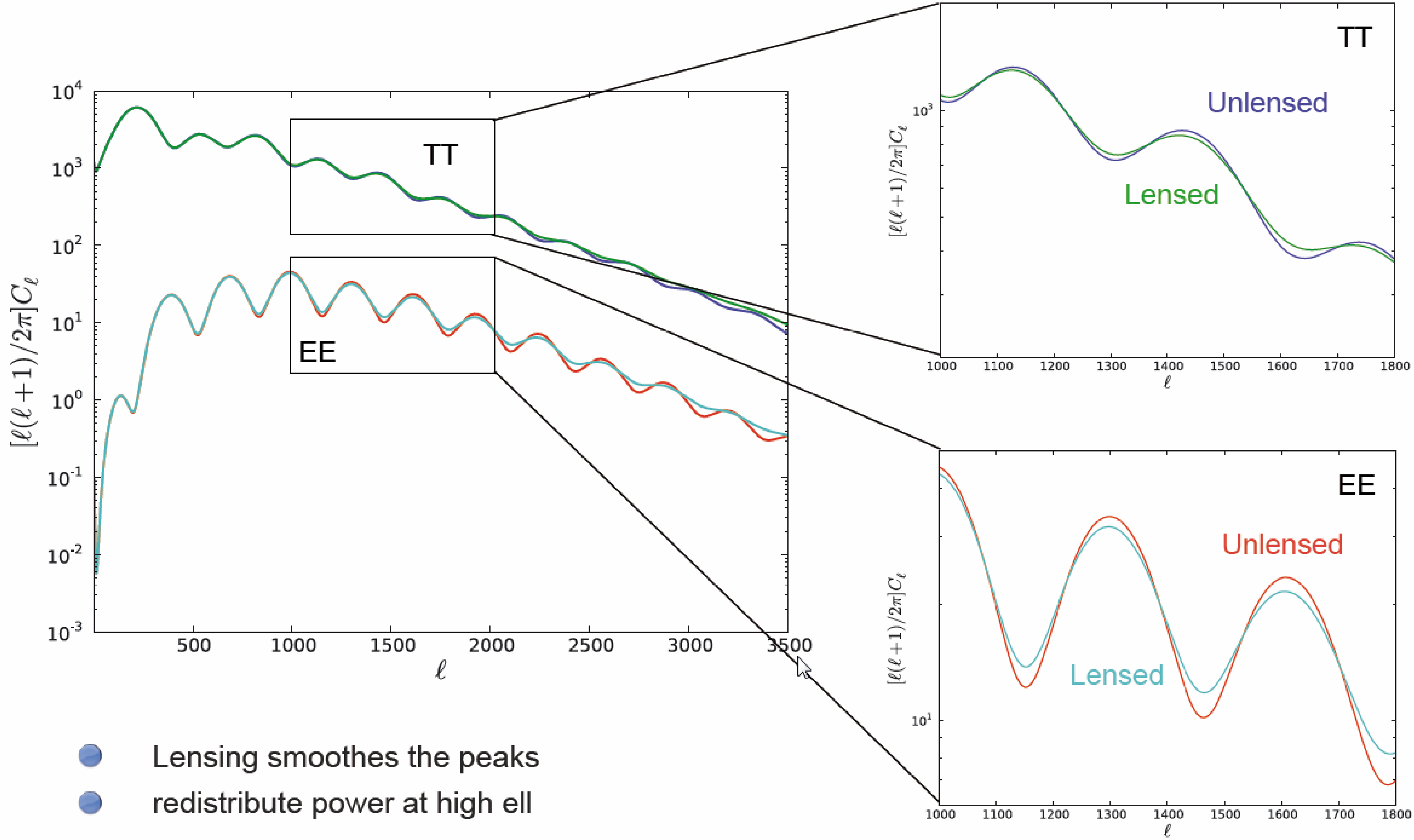

- Lensing smoothes the peaks
- redistribute power at high ell

(And create specific non-Gaussianities which can be exploited...)

And generates weak B modes

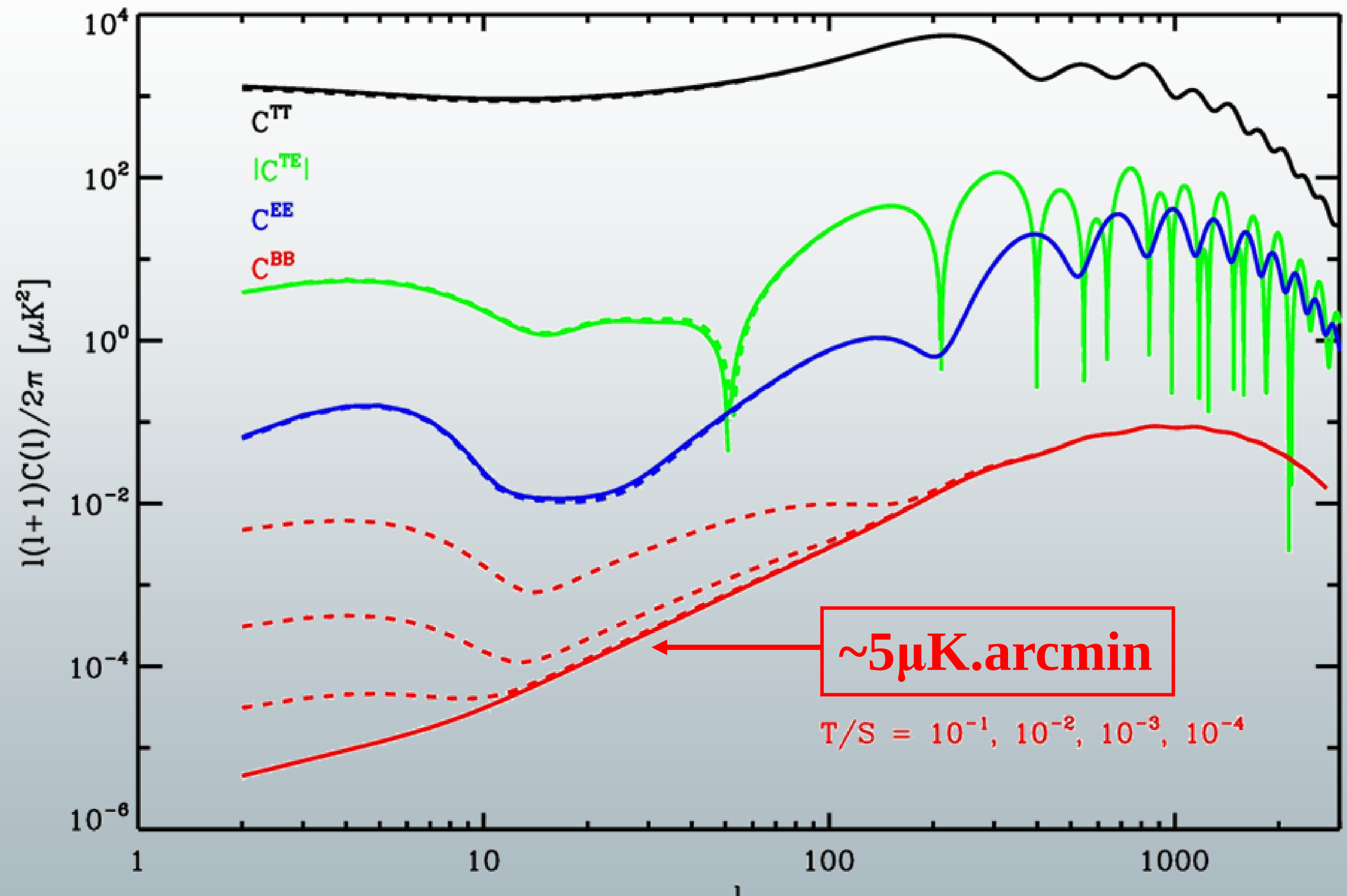

A white noise level of 5μK.arcmin implies fluctuation with an rms of 5/θ μK in a pixel of size θ
i.e. typically 100 nK in a 50 arcmin pixel (~B_{GW} signal for T/S ~ 10^{-2})
(NB: $\sigma_{Temperature}$ ~ 100 μK)

Detection – measurements status

- First detection by cross-correlation
  - *Smith et al., 2007 : WMAP + NVSS: 3.4 σ*
  - *Hirata et al., 2008 : WMAP + NVSS + SDSS + : 2.5 σ*
- Internal detection (via spectrum smoothing)
  - *Das et al. 2010 (ACT),* $C_l^{\Phi\Phi} = A_L C_{l,\,fid}^{\Phi\Phi}$, $A_L = 1.3^{+0.5(+1.2)}_{-0.5(-1.0)}$

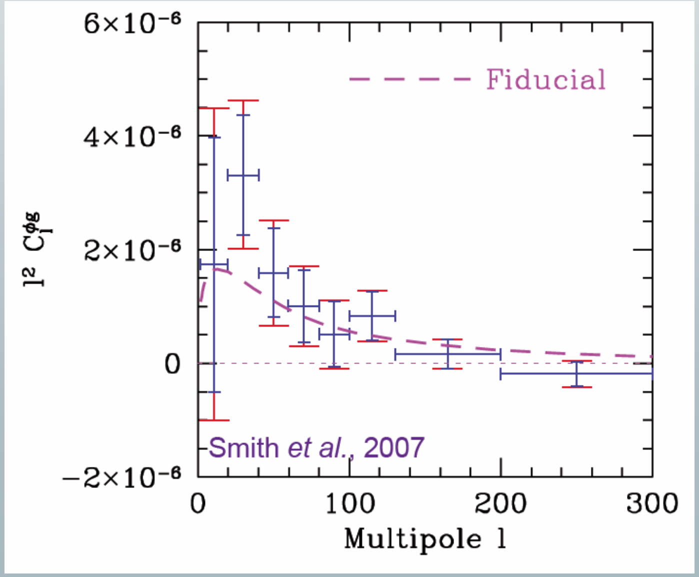

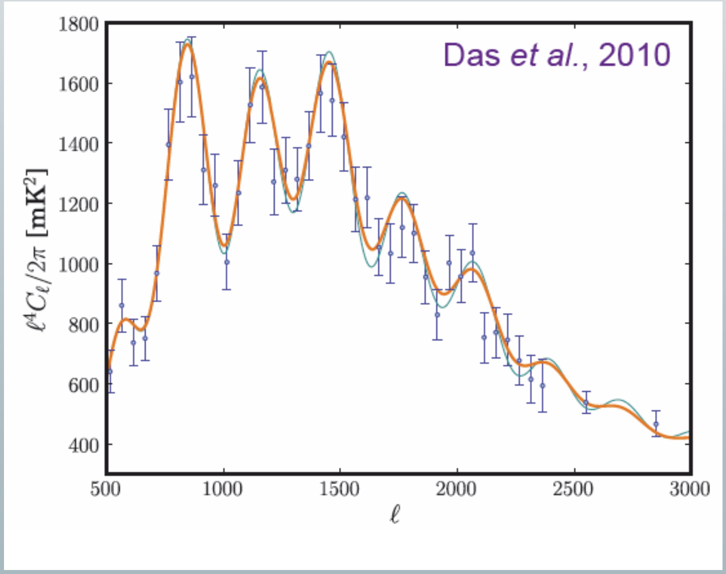

Lensing potential reconstruction

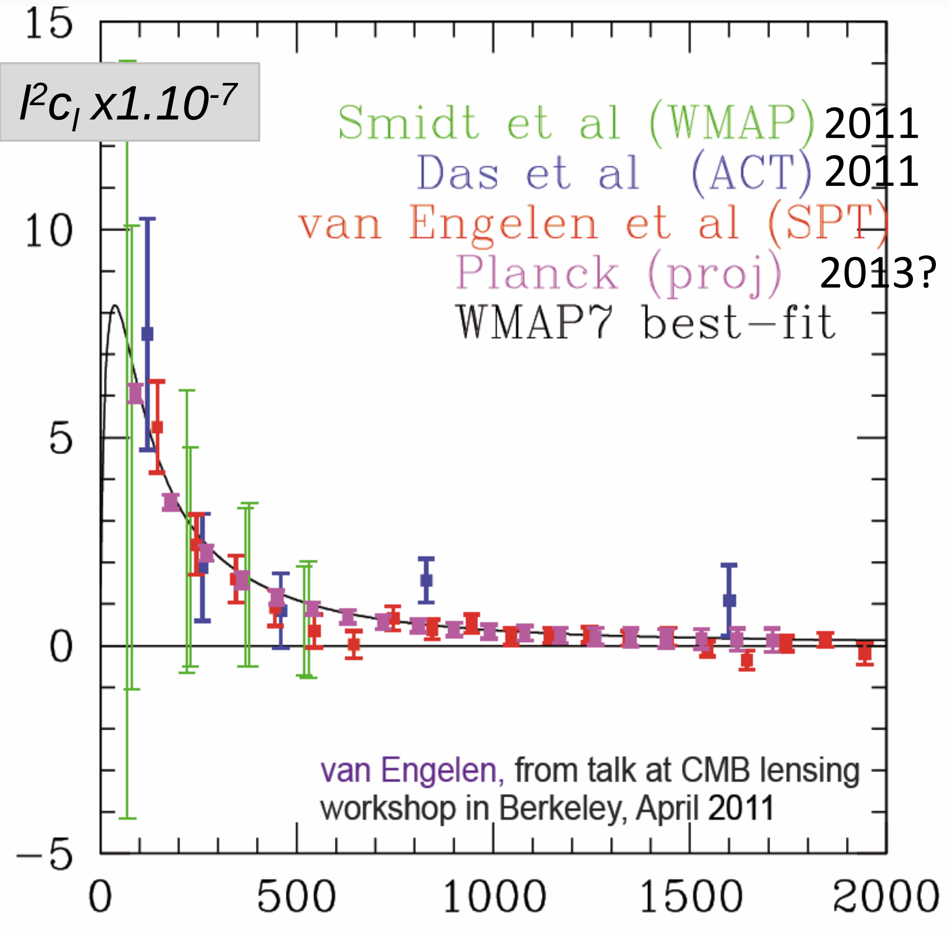

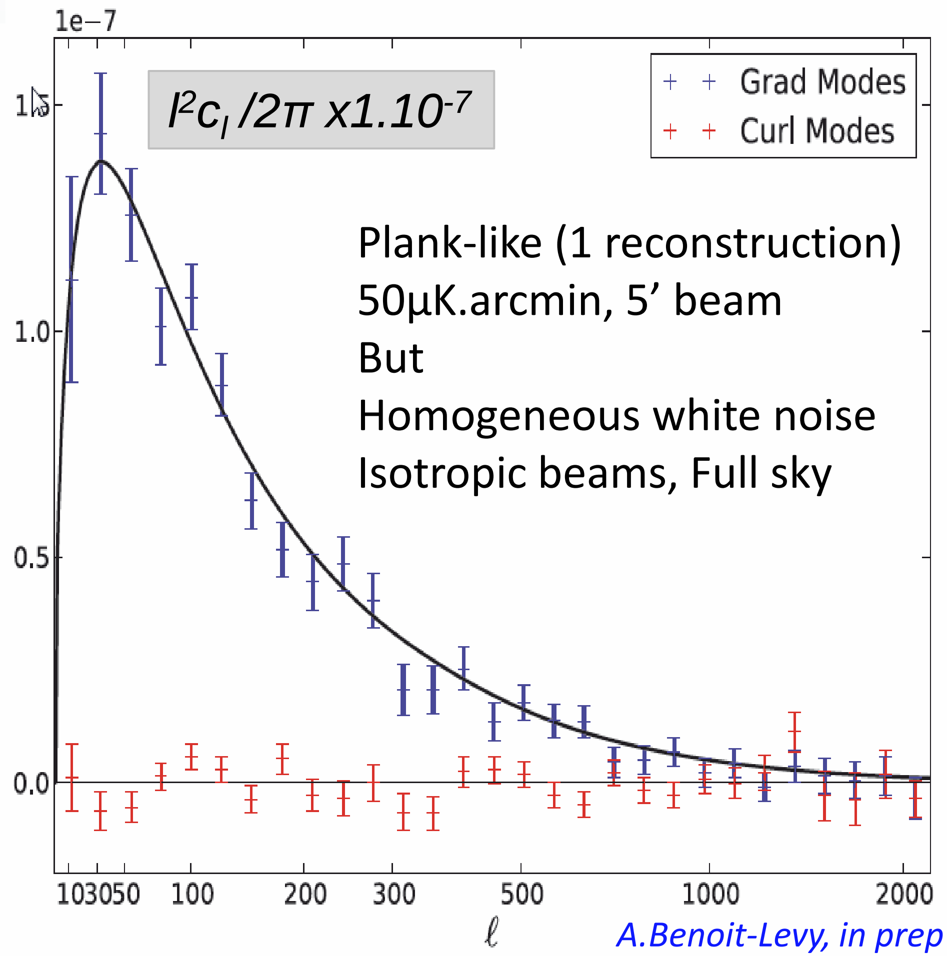

A.Benoit-Levy, in prep

→ Spectrum is sensitive to geometry & matter power spectrum in 0.5 < z < 6.5 range

→ Low z constraints on curvature, m_ν, dark energy…

Planck alone forecast for ΛMDM

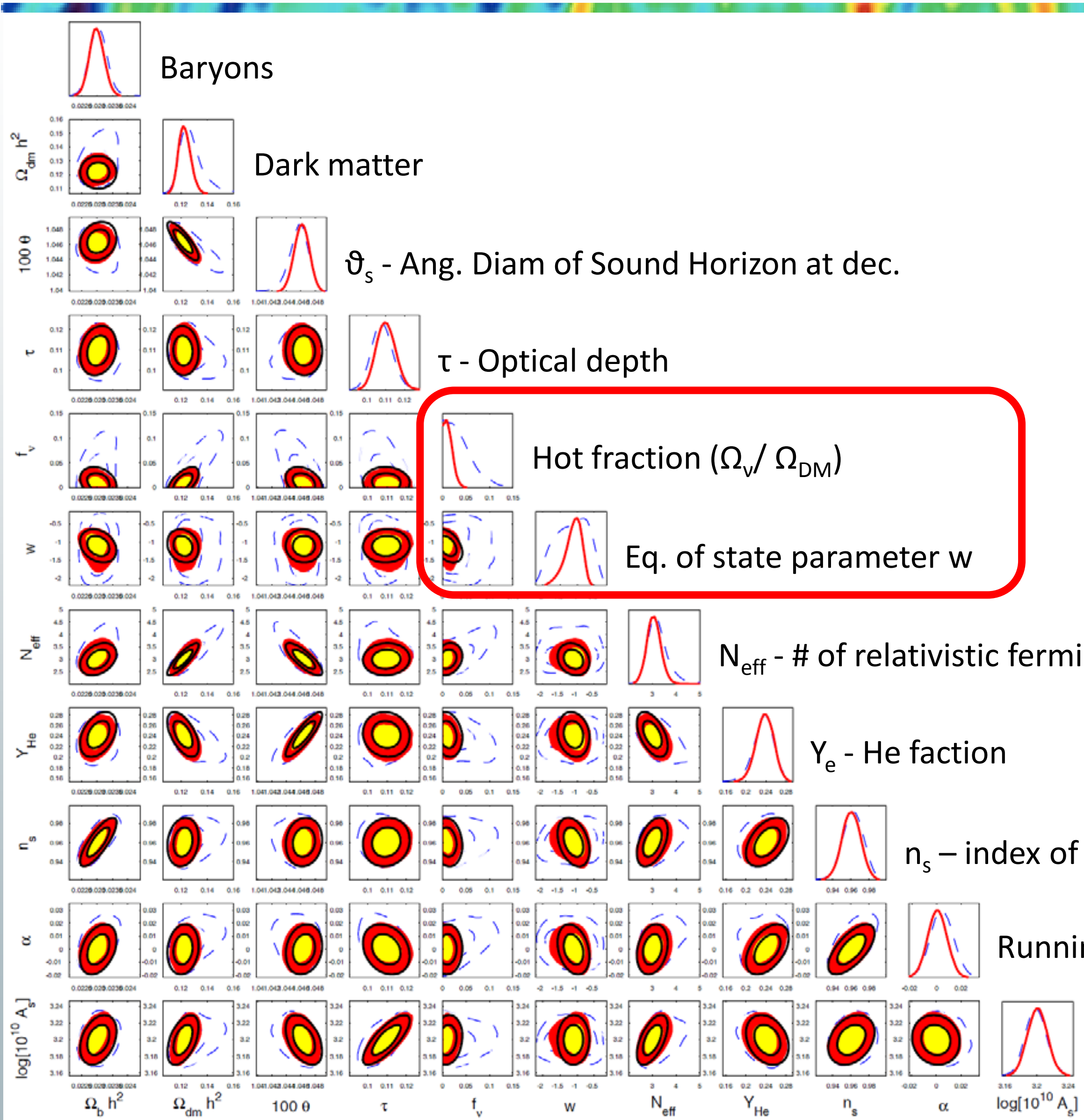

The blue dashed lines indicate the degradation incurred without lensing information extraction

Largest improvements indeed concern the Hot fraction (& DM) & eq. of state parameter, ie low-z

Perotto et al., JCAP 2006

Planck alone forecast for ΛMDM

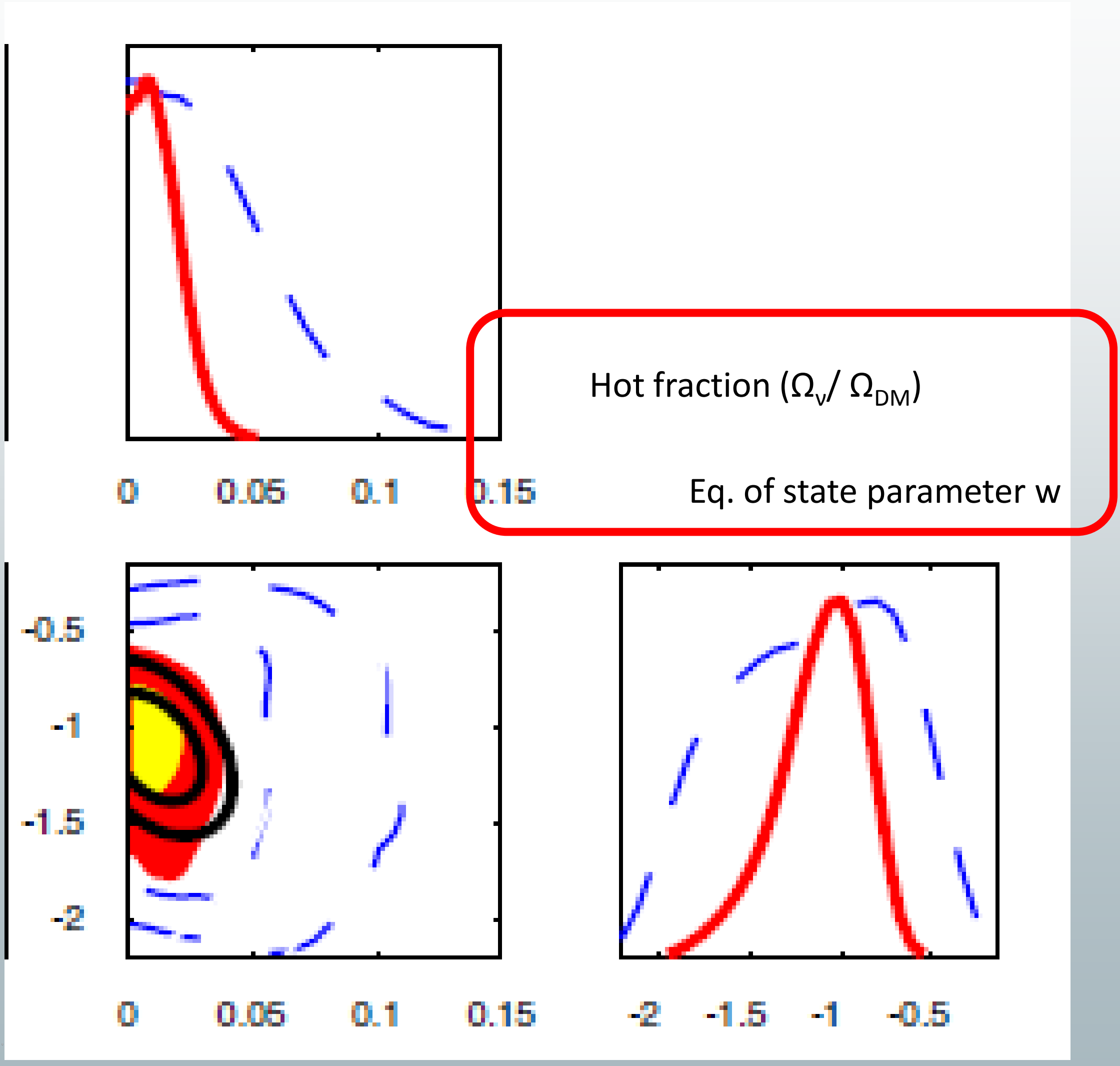

Perotto et al., JCAP 2006

The blue dashed lines indicate the degradation incurred without lensing information extraction

Largest improvements indeed concern the Hot fraction (& DM) & eq. of state parameter, ie low-z

Expectations for Planck

- ~30 σ detection using temperature only
  - *CMB x Lensing likelihood for cosmology*
- ~15 σ detection using TT X TE
  - *Low correlation with the TT x TT estimate*
- ~5 σ detection using TE X TE

- ~5 σ detection using ISW x Lensing
- Higher significance (10 to 20 σ) with other LSS probes (VSS, SDSS…)
- ~30 σ detection of CIB x Lensing
- They will instruct on how these tracers relate to underlying grav. potential

- Assuming we shall tame:
  - *Mask & weighting issues*
  - *Beams*
  - *Inhomogeneous noise*
  - *Diffuse foregrounds residuals*
  - *Compact source residuals*
  - *Pointing & pixel substructures…*

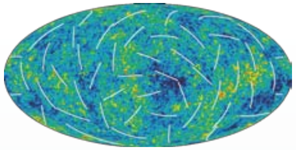

There are more things in heaven and earth, than 2 points…

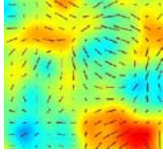

Harmonic coefficients of a map $a_{lm} = T^{-1} \int d^2\hat{\mathbf{n}} \Delta T(\hat{\mathbf{n}}) Y^*_{\ell m}$

Are directly related to curvature perturbations (p =T, E, B)

$$a^p_{\ell m} = b_\ell\, 4\pi (-i)^\ell \int \frac{d^3k}{(2\pi)^3} \Phi(\mathbf{k})\, g^p_\ell(k) Y^*_{\ell m}(\hat{\mathbf{k}}) + n_{\ell m}$$

Therefore their distribution :

$$P(a) = \frac{1}{(2\pi)^{N_{\rm harm}/2} |C|^{1/2}} \exp\left[-\frac{1}{2}\sum_{lm}\sum_{l'm'} a^*_{lm} (C^{-1})_{lm,l'm'} a_{l'm'}\right]$$

$$\times \left\{1 + \frac{1}{6} \sum_{\text{all } l_i m_j} \langle a_{l_1 m_1} a_{l_2 m_2} a_{l_3 m_3} \rangle \left[(C^{-1}a)_{l_1 m_1} (C^{-1}a)_{l_2 m_2} (C^{-1}a)_{l_3 m_3} \right.\right.$$

$$\left.\left. -3 (C^{-1})_{l_1 m_1, l_2 m_2} (C^{-1}a)_{l_3 m_3}\right]\right\}.$$

Can be used to infer properties of the transfer Function (content) and on "initial conditions" and in particular the curvature perturbation (Φ) spectrum & bispectrum

$$C_\ell = 4\pi \int_0^\infty \frac{dk}{k} \Delta^2_\Phi(k) g^2_{\mathrm{T}\ell}(k)$$

$$\langle \Phi(\boldsymbol{k}_1)\Phi(\boldsymbol{k}_2)\Phi(\boldsymbol{k}_3)\rangle = (2\pi)^3 \delta^D(\boldsymbol{k}_1 + \boldsymbol{k}_2 + \boldsymbol{k}_3) F(k_1, k_2, k_3)$$

There are many ways to arrange 3 pts!

And they are produced by different underlying physics

- squeezed triangle (k1~k2>> k3), the dominating shape from multi-field, curvaton, inhomogeneous reheating and Ekpyrotic models.
- equilateral triangle (k1 = k2 = k3), produced by non-canonical kinetic energy with higher derivative interactions and non-trivial speeds of sound.
- folded triangle (k1 = 2k2 = 2k3), produced by non-adiabatic-vacuum models.

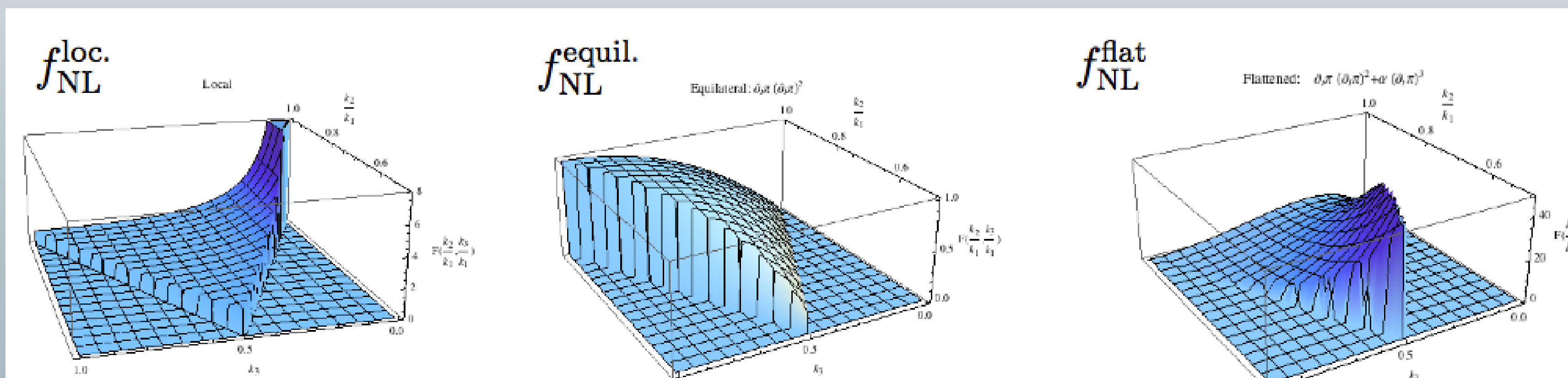

Remarks

- Assuming $\Phi=\Phi_L+f_{NL}\Phi_L^2$ as in *Salopek & Bond 1990, (Komatsu & Spergel 2001)*
  - *Φ_L~10^{-5} is a Gaussian, linear curvature perturbation in the matter era*
  - *Therefore, $f_{NL\text{-}local}$<100 means that the distribution of Φ is consistent with a Gaussian distribution to ~100 ×$(10^{-5})^2/(10^{-5})$=**0.1% accuracy** at 95% CL.*
- A lot of work already to assess f_{NL} for various scenarii
  - *f_{NL} ~ 0.05 canonical inflation (single field, couple of derivatives)*
  - *(Maldacena 2003, Acquaviva etal 2003)*
  - *f_{NL} ~ 0.1--100 → higher order derivatives*
    - ~100: DBI inflation (Alishahiha, Silverstein and Tong 2004)
    - ~0.1 : UV cutoff (Creminelli and Cosmol, 2003)
  - *f_{NL} >10 curvaton models (Lyth, Ungarelli and Wands, 2003)*
  - *f_{NL} ~100 ghost inflation (Arkani-Hamed et al., Cosmol, 2004)*
  - *...*
- NB: a detection of primordial NG in the squeezed limit (when k1~k2>>k3) would rule out ALL single-field inflation models, because these obey B(k1, k2, k3→0) = $(1-n_s)$P(k1)P(k2), and $1-n_s$ is measured to be ~< 0.05)
- Nice reviews of recent NG work & CMB in Komatsu 2010, 1003.6097v2 and Yadav & Wandelt 2010

$f_{NL} = 100$

Positive f_{NL} = More Cold Spots

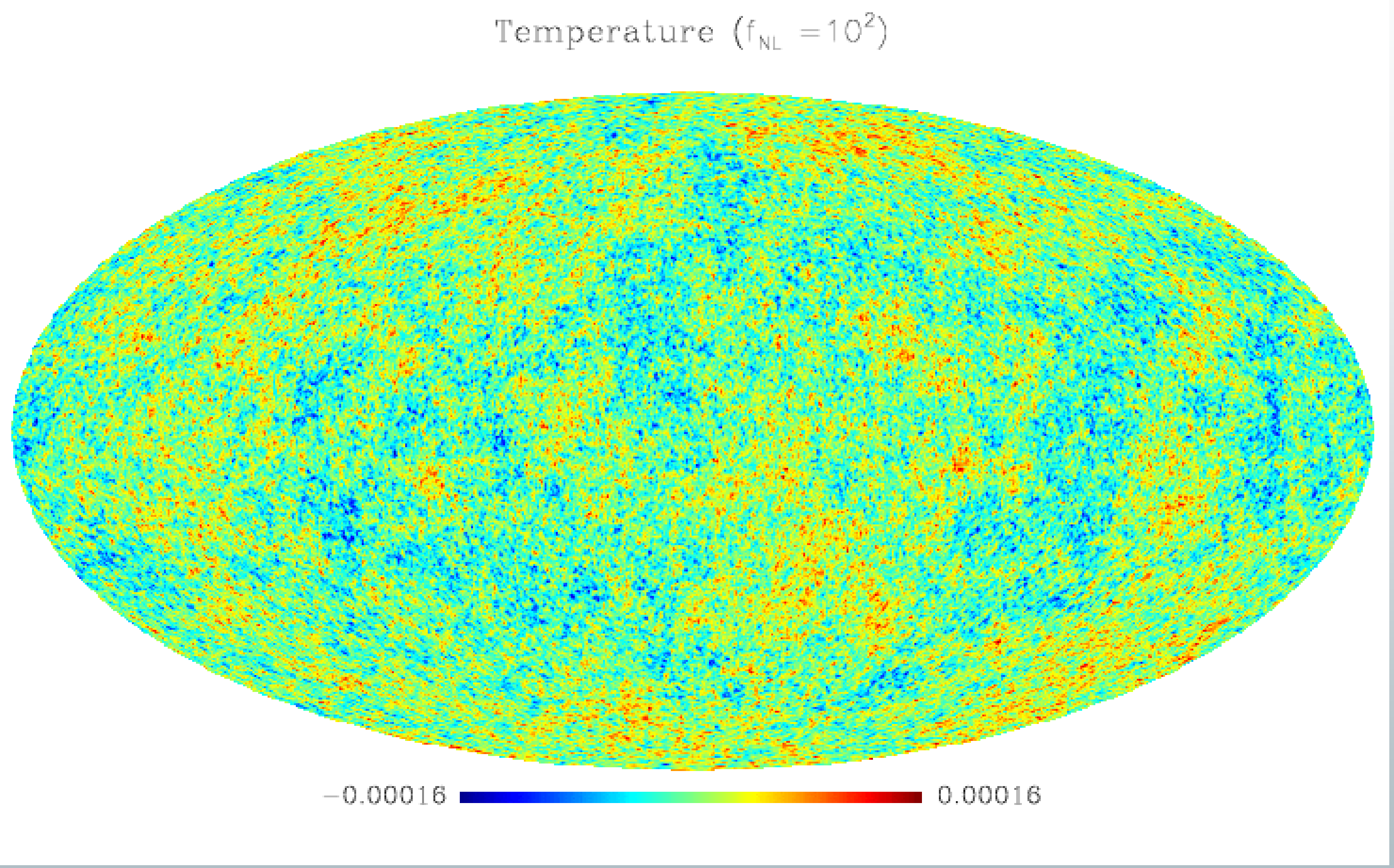

"The frightening power of statistics"

Liguori, Yadav, Hansen, Komatsu, Matarrese, Wandelt 2007

$f_{NL} = 0$

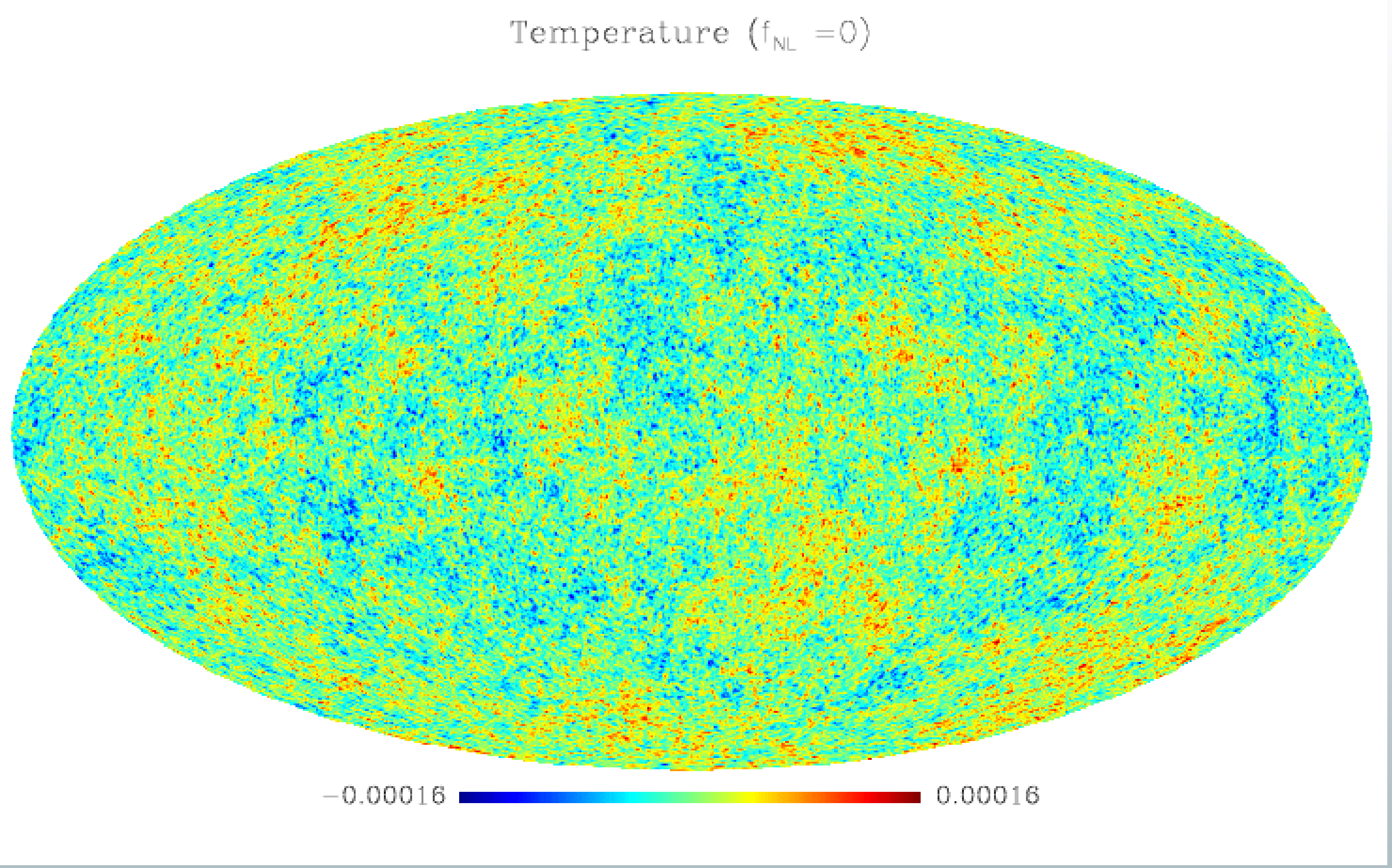

And...

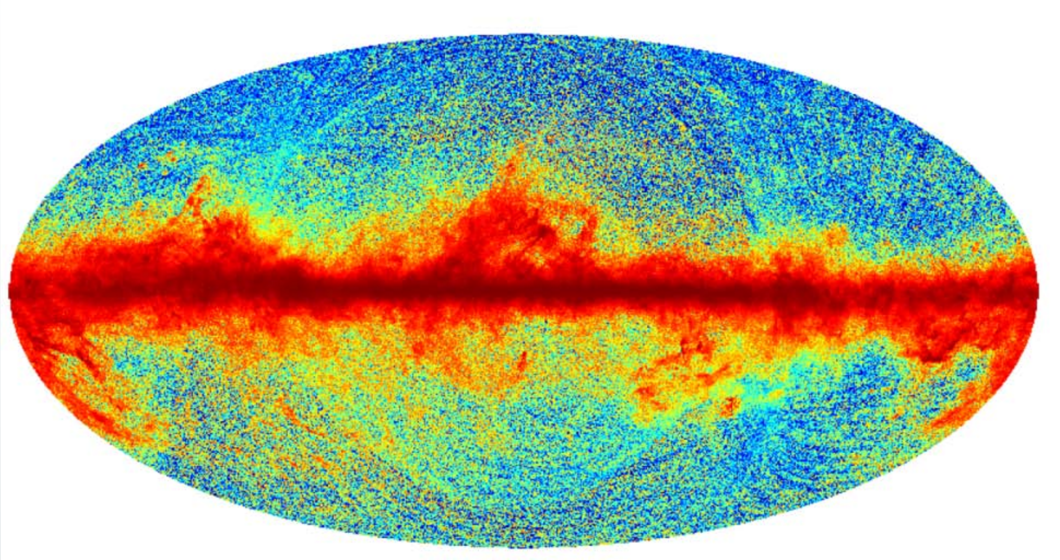

(143GHz)

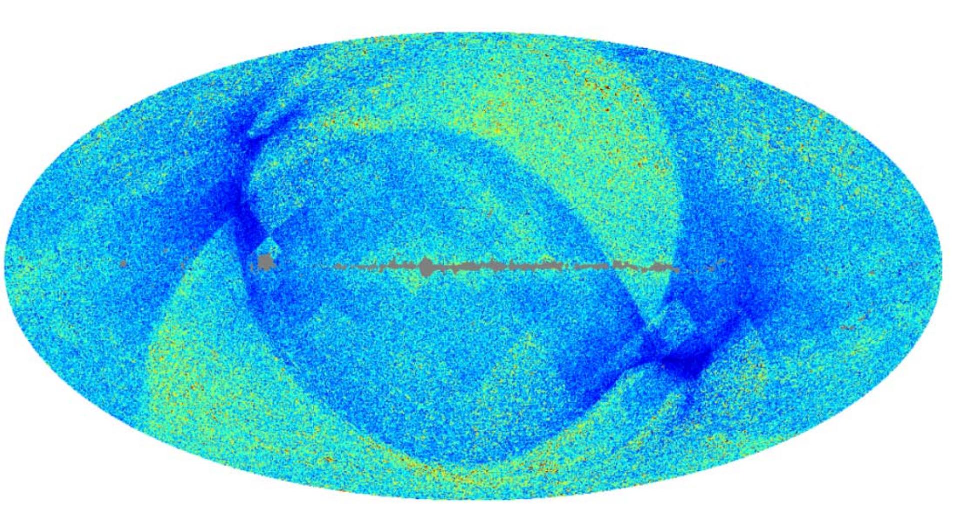

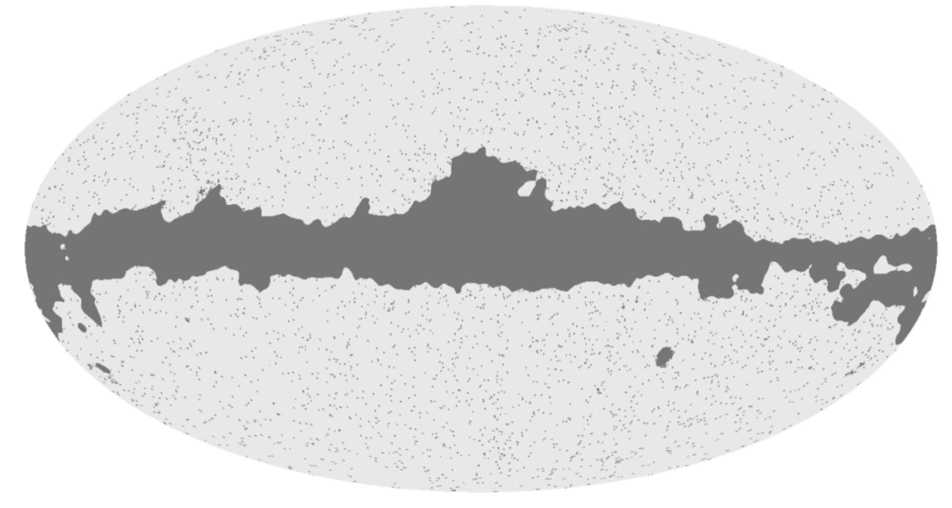

Estimators...

- Given a shape of the initial bispectrum (local, equil., etc), one can devise an unbiased minimum-variance estimator (taking derivatives of bispectrum wrt f_{nl})

$$\widehat{f_{NL}} = \frac{1}{N} \sum_{All\ell} \frac{B_{\ell_1\ell_2\ell_3} \widehat{B_{\ell_1\ell_2\ell_3}}}{C_{\ell_1} C_{\ell_2} C_{\ell_3}}, \text{with } N = \sum_{All\ell} \frac{(B_{\ell_1\ell_2\ell_3})^2}{C_{\ell_1} C_{\ell_2} C_{\ell_3}}$$

- This is $\propto$ $Npix^{5/2}$ (Planck Npix~5.10^7). One trick has been to look at factorisable F since then only $\propto$ $Npix^{3/2}$
- ... and debias it with MC to do it in practice, i.e. with a cut sky, inhomogeneous noise:
- In practice, this amounts to filter the maps before multiplying then summing them...

The (local) f_{NL} hunt

TABLE II: Summary of constraints on local non-Gaussianity

Year	data	Method	$f_{NL}^{local} \pm 2\sigma$ error	
2002	COBE	Bispectrum sub-optimal	$\|f_{NL}\| < 1500$	Komatsu et al. [222]
2003	MAXIMA	Bispectrum sub-optimal	$\|f_{NL}\| < 1900$	Santos et al. [223]
2003	WMAP 1-year	Bispectrum sub-optimal	39.5 ± 97.5	E. Komatsu et al. [23]
2004	VSA	Bispectrum sub-optimal	$f_{NL} < 5400$	Smith et al. [224]
2005	WMAP 1-year	Bispectrum sub-optimal-v1	47 ± 74	Creminelli et al. [25]
2006	WMAP 3-year	Bispectrum sub-optimal	30 ± 84	Spergel et al. [24]
2006	WMAP 3-year	Bispectrum sub-optimal-v1	32 ± 68	Creminelli et al. [26]
2007	WMAP 3-year	Bispectrum near-optimal	87 ± 62	Yadav and Wandelt [28]
2007	Boomerang	Minkowski Functionals	110 ± 910	De Troia et al. [225]
2008	WMAP 3-year	Minkowski Functionals	10.5 ± 80.5	C. Hikage et al. [195]
2008	WMAP 5-year	Bispectrum near-optimal	51 ± 60	Komatsu et al. [51]
2008	ARCHEOPS	Minkowski Functionals	70^{1075}_{-950}	Curto et al. 2008 [226]
2009	WMAP 3-year	Bispectrum optimal	58 ± 46	Smith et al. [131]
2009	WMAP 5-year	Bispectrum optimal	38 ± 42	Smith et al. [131]
2009	WMAP 5-year	Spherical Mexican hat wavelet	31 ± 49	Curto, A et. al. [206]
2009	BOOMERanG	Minkowski Functionals	-315 ± 705	P. Natoli et al. [227]
2009	WMAP 5-year	Skewness power spectrum	11 ± 47.4	Smidt, Joseph et al. [228]
2010	WMAP 7-year	Bispectrum optimal	32 ± 42	Komatsu et al. [132]

Minimum detectable f_{NL} versus l_{max}

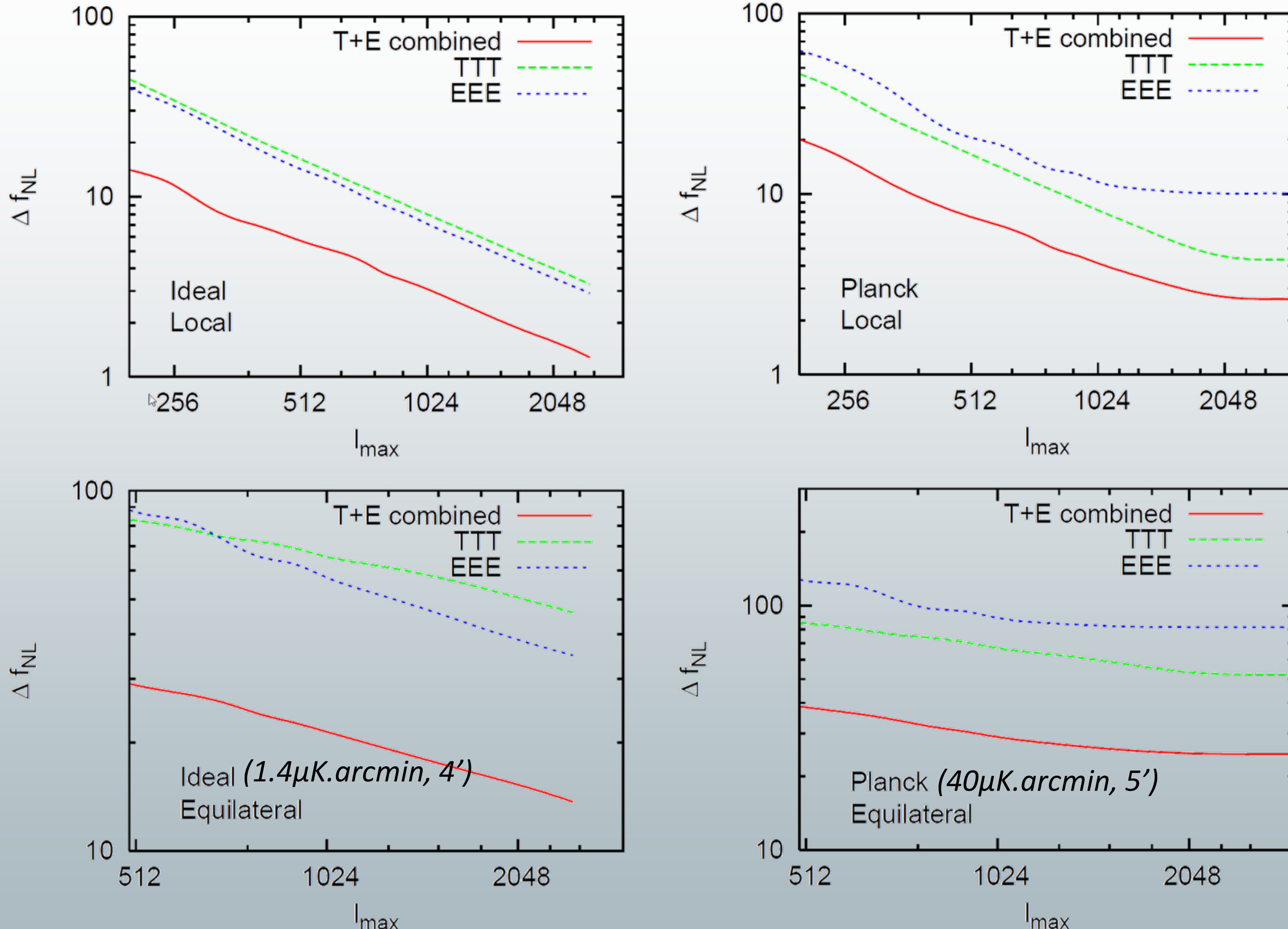

WMAP7
Δf_{NL}^{loc}~21 ←

Yadav & Wandelt 2010 1006.0275v3

Δf_{NL}^{local}~1 is the limit from the CMB; Cramer-Rao for Planck ~3!

Forecasts for scale-dependent f_{NL}

local

equilateral

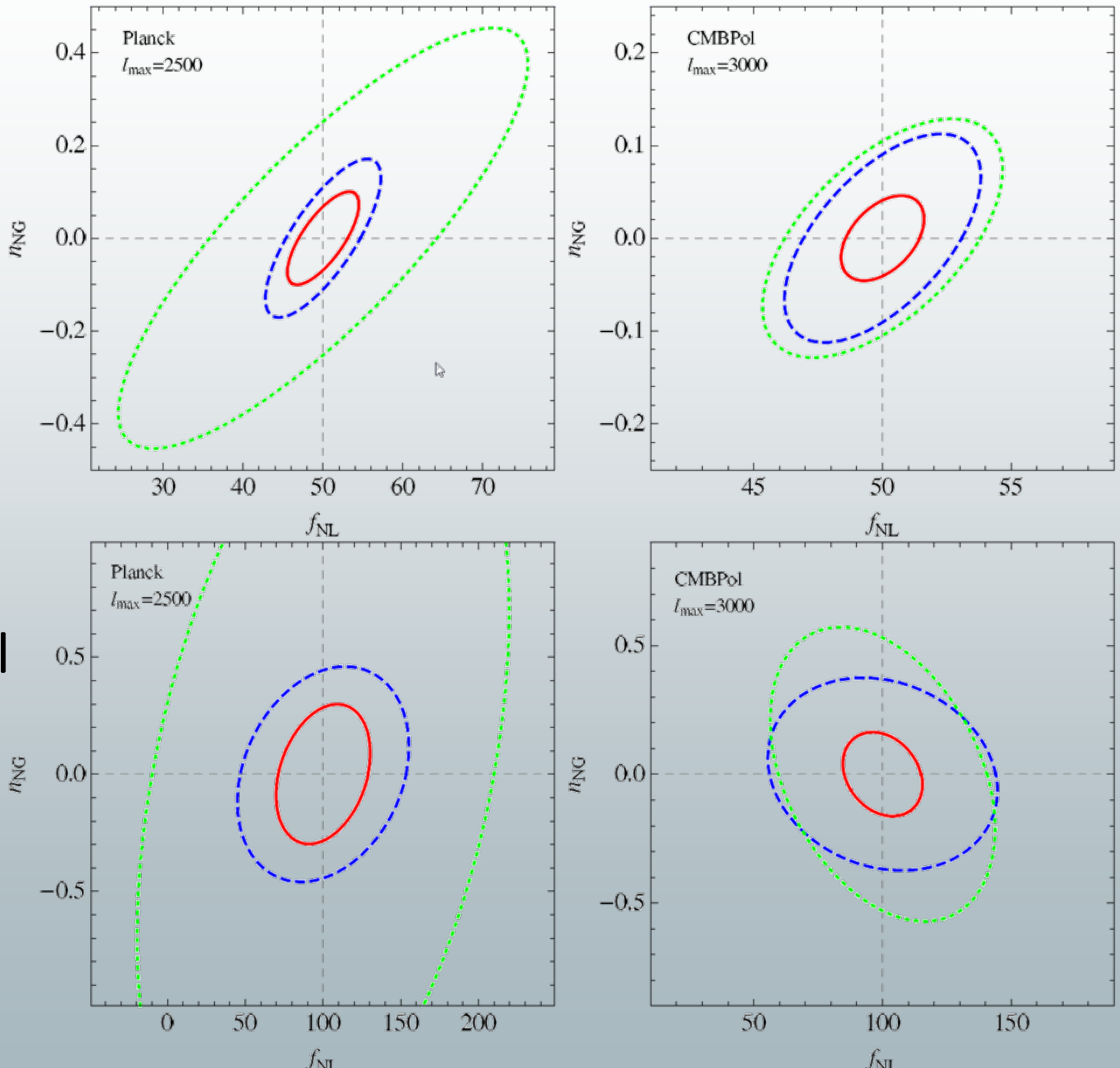

Green EE

Sefusatti et al. 2009

n is the exponent of the k dependence

Cramer-Rao bounds are just bounds

One need to look at all other sources of bispectra

- The largest one comes from ISW X lensing which would bias f_{NL} by ~9, if uncorrected.
- NB: 2nd order effects at LS surface have an equivalent f_{NL} of the order of 1 (~5?). No bispectrum template shape yet.
- And astrophysical foregrouns, in particular point sources... *Lacasa et al. 1107.2251v1* estimate (for noiseless full-sky maps without beam smoothing) that for Planck at 217 GHz, this may induce a negative bias , f_{NL}^{Local}=-6, coming from unresolved IR sources (assuming radio sources contribution has been well masked out). To be cont'd (including other foregrounds)...
- And the instrumental imperfections...
- Well, that's what we are busy doing... (Fortunately, not all sources project very well on all templates)

Modal bispectrum decomposition

Modal bispectrum decomposition (Fergusson, Liguori & Shellard 2010) has the advantage that no a priori assumption on bispectrum shape is required. Output in one go: primordial bispectrum reconstruction & fNL value for all known bispectrum shapes

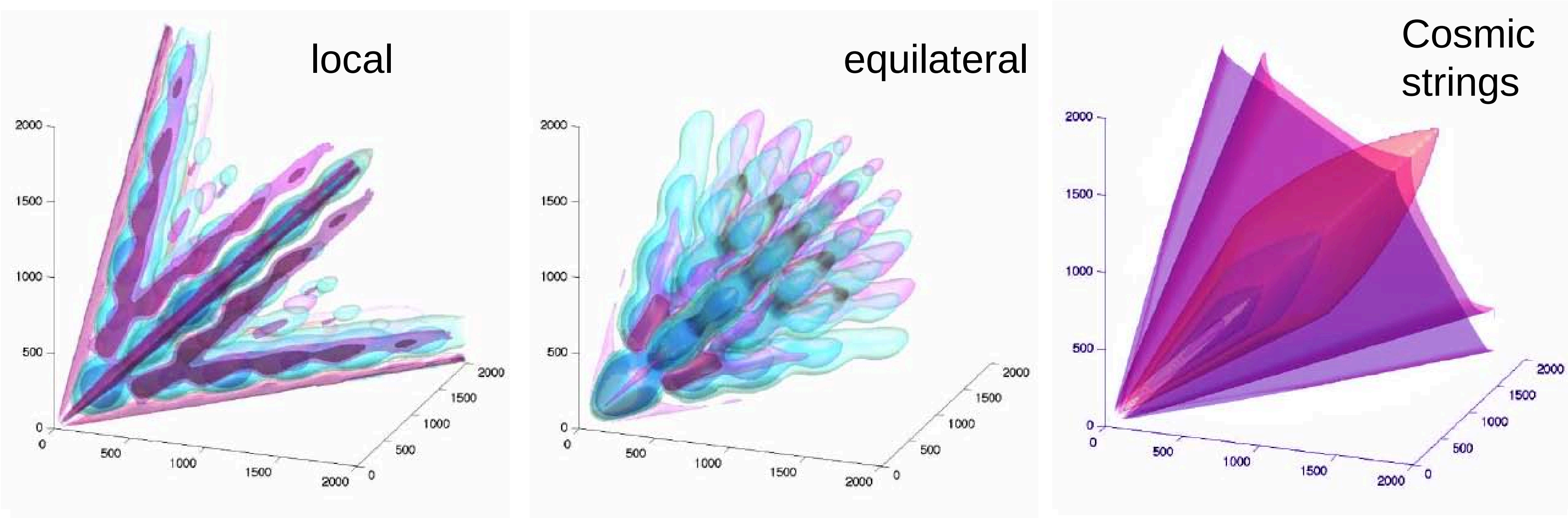

Fergusson and Shellard 2009

For the three most common bispectrum modes Planck will reduce the constrained volume by 70 compared to WMAP with a further factor of 20 possible for a next generation mission.

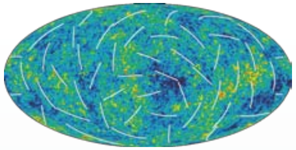

Trispectrum, and more...

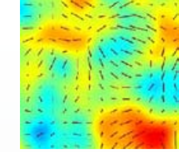

$$\langle a_{l_1m_1}a_{l_2m_2}a_{l_3m_3}a_{l_4m_4}\rangle = \sum_{LM}(-1)^M \begin{pmatrix} \ell_1 & \ell_2 & L \\ m_1 & m_2 & m_3 \end{pmatrix} \begin{pmatrix} \ell_3 & \ell_4 & L \\ m_1 & m_2 & m_3 \end{pmatrix} T^{l_1 l_2}_{l_3 l_4}(L)$$

WMAP5 trispectrum constraint on the local g_{NL} model is $-5.6 \times 10^5 < g_{NL} < 8.6 \times 10^5$
Fergusson, Regan& Shellard, 1012.6039;
See also Vielva & Sanz 2010, Smidt et al. 2010
But no optimal estimator (yet?)

$$T(k_1,k_2,k_3,k_4) = \tau_{\rm NL}[P_\zeta(k_{13})P_\zeta(k_3)P_\zeta(k_4) + (11 \text{ perms})] + \frac{54}{25} g_{\rm NL}[P_\zeta(k_2)P_\zeta(k_3)P_\zeta(k_4) + (3 \text{ perms})], (21)$$

$\tau_{\rm NL} = (6 f_{\rm NL}/5)^2$ for single field models

- Minkowski functionals (recently Hikage, Matsubara, etc)

$$V_k^{(d)}(\nu) = \frac{1}{(2\pi)^{(k+1)/2}} \frac{\omega_d}{\omega_{d-k}\omega_k} \left(\frac{\sigma_1}{\sqrt{d}\sigma_0}\right)^k e^{-\nu^2/2} \Big\{ H_{k-1}(\nu) + \Big[\frac{1}{6}S^{(0)}H_{k+2}(\nu) + \frac{k}{3}S^{(1)}H_k(\nu) + \frac{k(k-1)}{6}S^{(2)}H_{k-2}(\nu)\Big]\sigma_0 + \mathcal{O}(\sigma_0^2)\Big\},$$

$$S^{(0)} \equiv \frac{\langle f^3\rangle}{\sigma_0^4},$$

$$S^{(1)} \equiv -\frac{3}{4}\frac{\langle f^2(\nabla^2 f)\rangle}{\sigma_0^2\sigma_1^2},$$

$$S^{(2)} \equiv -\frac{3d}{2(d-1)}\frac{\langle(\nabla f)\cdot(\nabla f)(\nabla^2 f)\rangle}{\sigma_1^4},$$

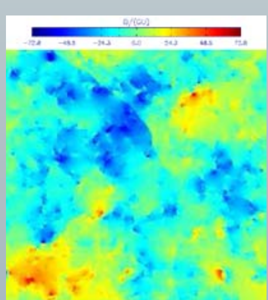

- And wavelets, needlets, etc (different weighting → cross-checks..)
- + Indicators specific to Strings, PMF, etc.

Variations of the fine structure constant

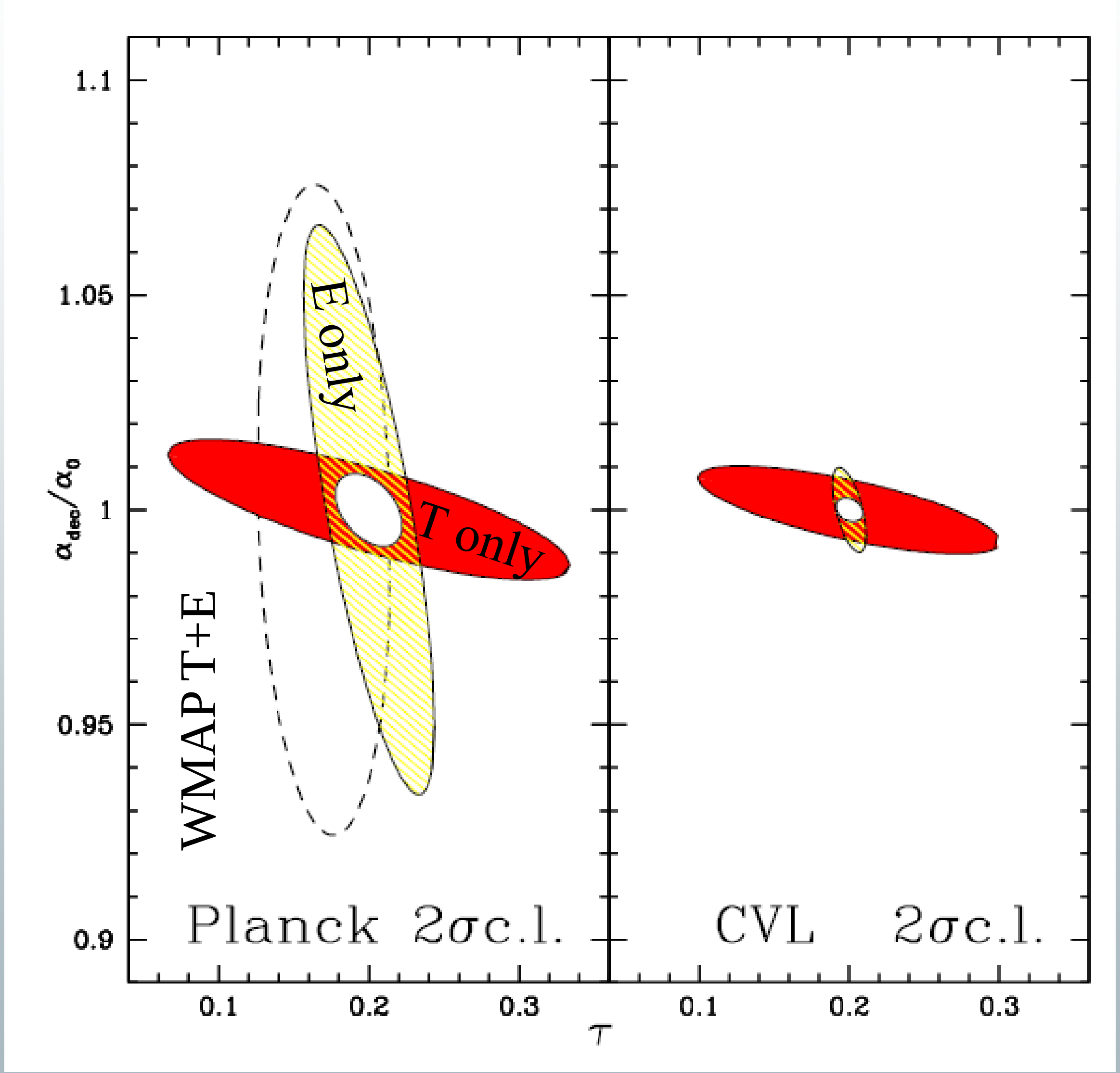

Planck will uniquely constrain the value of the fine structure constant at z~1000

And will go a long way towards extracting all the information CMB has to offer on this
(as expected progress will mostly be via E polarization measures)

Rocha et al. 2004

CORE

Cosmic ORigins Explorer

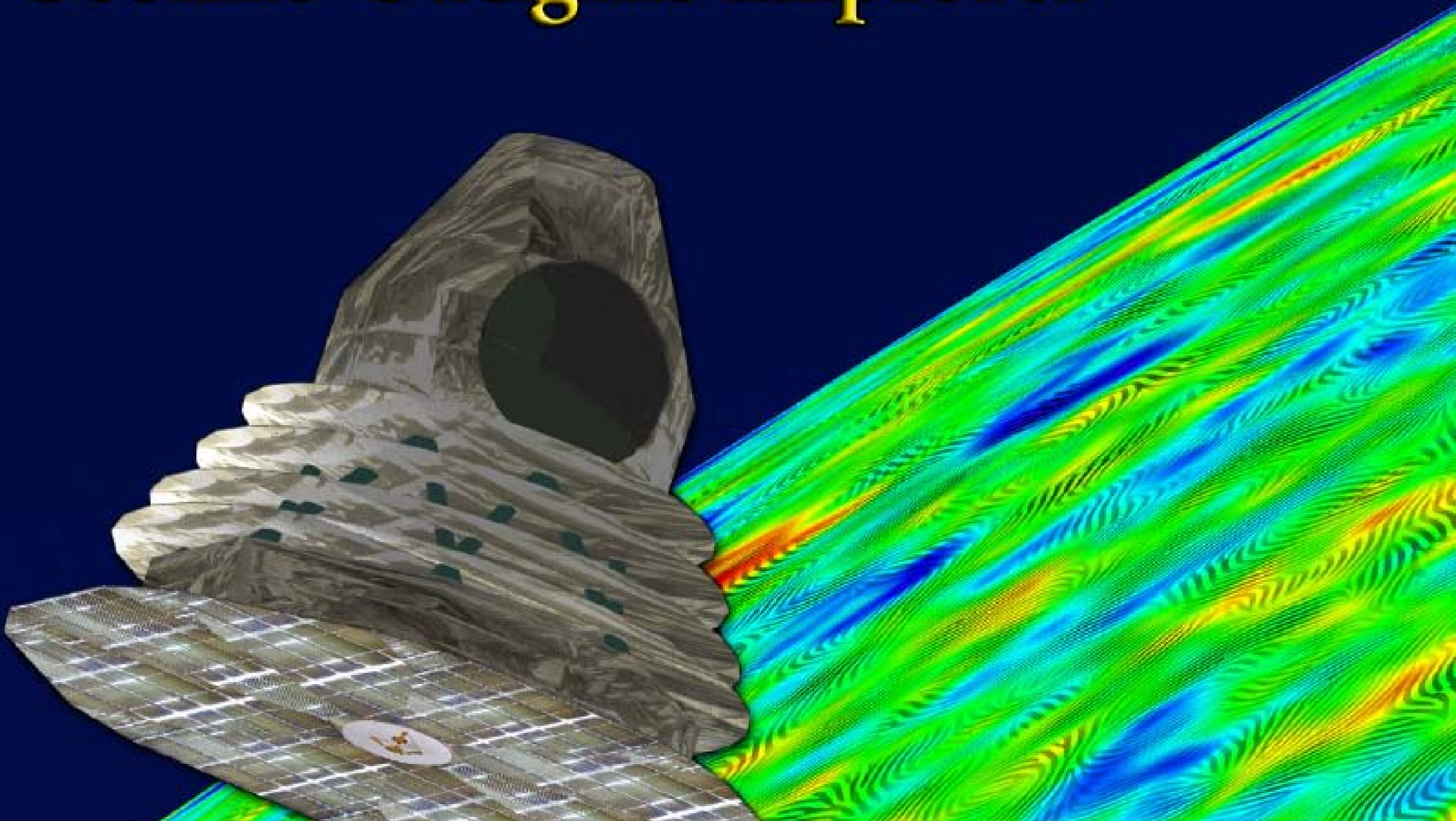

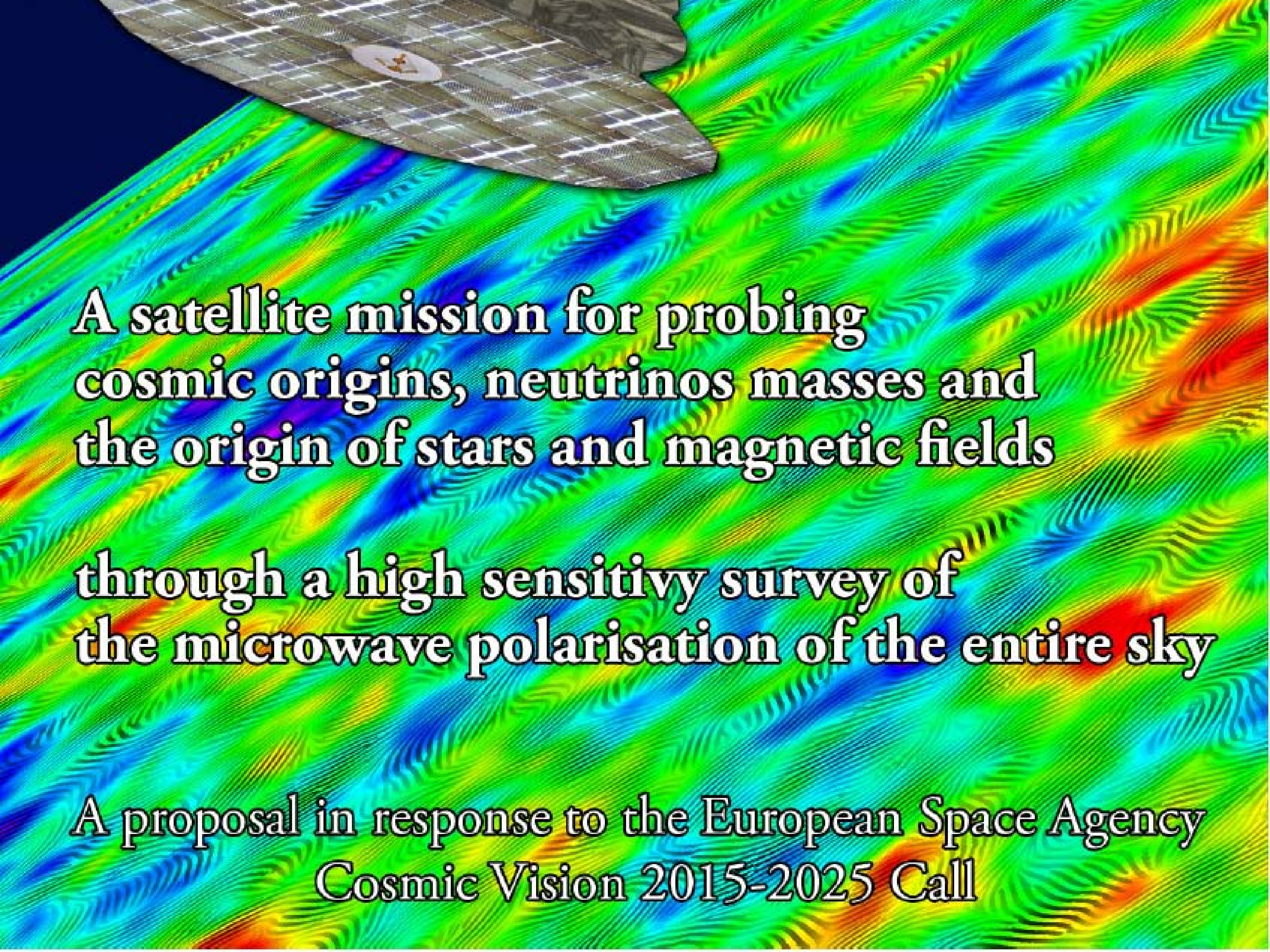
A satellite mission for probing
cosmic origins, neutrinos masses and
the origin of stars and magnetic fields
through a high sensitivy survey of
the microwave polarisation of the entire sky
A proposal in response to the European Space Agency
Cosmic Vision 2015-2025 Call

Performances summary

ν GHz	θ_{fwhm} arcmin	n_{det}	Temp (I) μK·arcmin RJ	Temp (I) μK·arcmin CMB	Pol (Q,U) μK·arcmin RJ	Pol (Q,U) μK·arcmin CMB
23	52.8	2	413	418	584	592
33	39.6	2	413	424	584	600
41	30.6	4	365	381	516	539
61	21.0	4	438	481	619	681
94	13.2	8	413	516	584	729

WMAP (9 year mission)

ν GHz	n_{unpol}	n_{pol}	θ_{fwhm} arcmin	Temp (I) μK·arcmin RJ	Temp (I) μK·arcmin CMB	Pol (Q,U) μK·arcmin RJ	Pol (Q,U) μK·arcmin CMB
30	4	4	32.7	198.5	203.2	280.7	287.4
44	6	6	27.9	228.0	239.6	322.4	338.9
70	12	12	13.0	186.5	211.2	263.7	298.7
100	8	8	9.9	23.9	31.3	33.9	44.2
143	11	8	7.2	11.9	20.1	19.7	33.3
217	12	8	4.9	9.4	28.5	16.3	49.4
353	12	8	4.7	7.6	107.0	13.2	185.3
545	3	0	4.7	6.8	1.1×10^3	—	—
857	3	0	4.4	2.9	8.3×10^4	—	—

PLANCK (30 month mission)

Sensitivity of Planck X20
Achieved through
durationX2, Inst.sensit.X2,
detector numberX100

ν GHz	$(\Delta\nu)$ GHz	n_{det}	θ_{fwhm} arcmin	Temp (I) μK·arcmin RJ	Temp (I) μK·arcmin CMB	Pol (Q,U) μK·arcmin RJ	Pol (Q,U) μK·arcmin CMB
45	15	64	23.3	4.98	5.25	8.61	9.07
75	15	300	14.0	2.36	2.73	4.09	4.72
105	15	400	10.0	2.03	2.68	3.50	4.63
135	15	550	7.8	1.68	2.63	2.90	4.55
165	15	750	6.4	1.38	2.67	2.38	4.61
195	15	1150	5.4	1.07	2.63	1.84	4.54
225	15	1800	4.7	0.82	2.64	1.42	4.57
255	15	575	4.1	1.40	6.08	2.43	10.5
285	15	375	3.7	1.70	10.1	2.94	17.4
315	15	100	3.3	3.25	26.9	5.62	46.6
375	15	64	2.8	4.05	68.6	7.01	119
435	15	64	2.4	4.12	149	7.12	258
555	195	64	1.9	1.23	227	3.39	626
675	195	64	1.6	1.28	1320	3.52	3640
795	195	64	1.3	1.31	8070	3.60	22200

COrE summary (4 year mission)

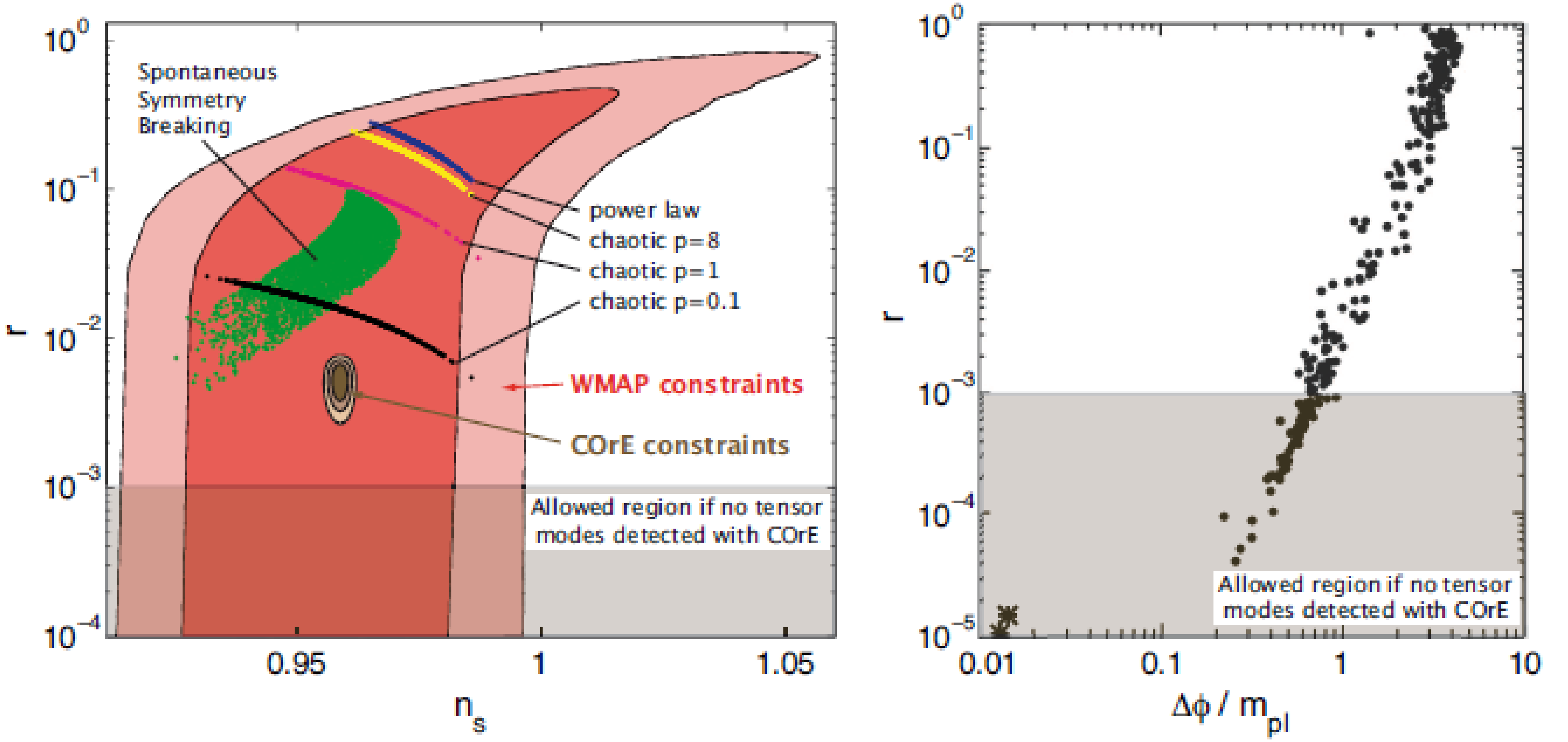

Spontaneous
Symmetry
Breaking
power law
chaotic p=8
chaotic p=1
chaotic p=0.1
WMAP constraints
COrE constraints
Allowed region if no tensor
modes detected with COrE
r
n_s
0.95
1
1.05
Allowed region if no tensor
modes detected with COrE
r
$\Delta\phi / m_{pl}$
0.01
0.1
1
10

Lensing: reconstruction noise

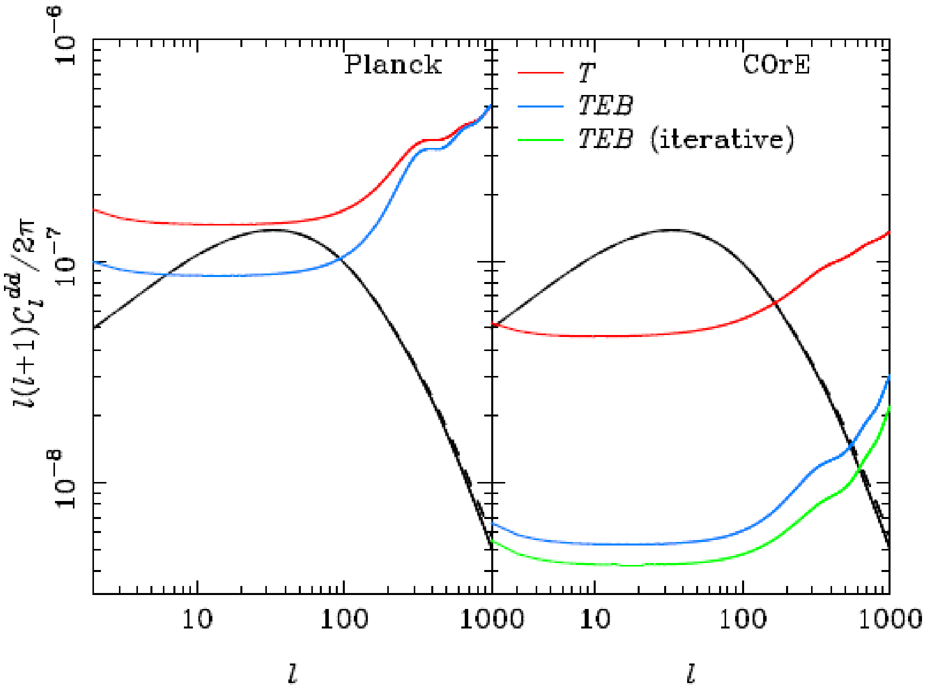

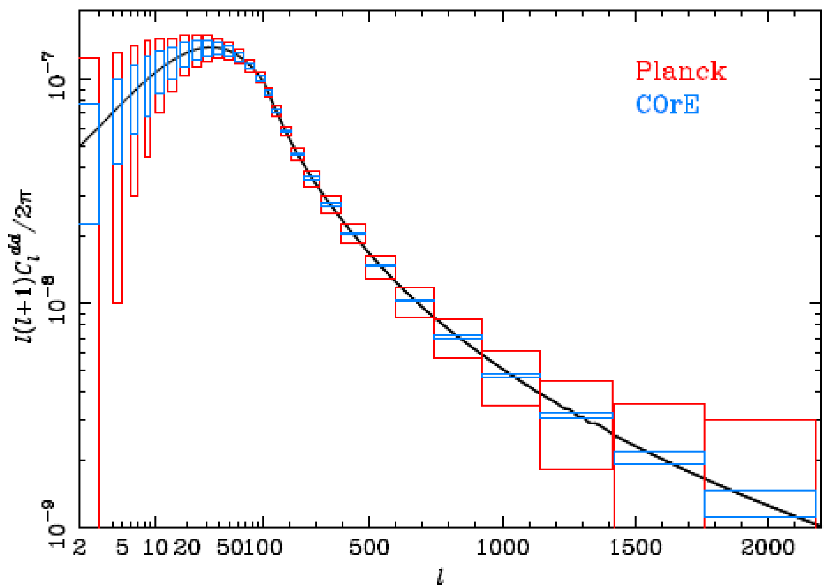

Conclusions 1/2

- Plain vanilla LCDM offers a good fit to all existing data
- Parameters are now determined with an accuracy at the per cent level:
  - *1.7% on Ω_B,*
  - *2.5% $\Omega c\ h^2$,*
  - *1.4% on Θ_S,*
  - *1% on n_s,*
  - *1.7% on τ,*
  - *4% on normalisation As*

Summary of t

Parameter	*WMAP* Seven-year ML[b]
$100\Omega_b h^2$	2.227
$\Omega_c h^2$	0.1116
Ω_Λ	0.729
n_s	0.966
τ	0.085
$\Delta^2_{\mathcal{R}}(k_0)$[d]	2.42×10^{-9}

- For the minimal model, using CMB+LSS (WMAP7+SPT+H0+BAO)
- No compelling indication of deviations (even though some are expected), nor of any anomalies

Search for extensions, expected or not

- WMAP7 fond none detectable yet

Table 2

Summary of the 95% Confidence Limits on Deviations From the Simple (Flat, Gaussian, Adiabatic, Power-law) ΛCDM Model Except for Dark Energy Parameters

Section	Name	Case	*WMAP* Seven-year	*WMAP*+BAO+SN[a]	*WMAP*+BAO+H_0
Section 4.1	Grav. wave[b]	No running ind.	$r < 0.36$[c]	$r < 0.20$	$r < 0.24$
Section 4.2	Running index	No grav. wave	$-0.084 < dn_s/d\ln k < 0.020$[c]	$-0.065 < dn_s/d\ln k < 0.010$	$-0.061 < dn_s/d\ln k < 0.017$
Section 4.3	Curvature	$w = -1$	N/A	$-0.0178 < \Omega_k < 0.0063$	$-0.0133 < \Omega_k < 0.0084$
Section 4.4	Adiabaticity	Axion	$\alpha_0 < 0.13$[c]	$\alpha_0 < 0.064$	$\alpha_0 < 0.077$
		Curvaton	$\alpha_{-1} < 0.011$[c]	$\alpha_{-1} < 0.0037$	$\alpha_{-1} < 0.0047$
Section 4.5	Parity violation	Chern–Simons[d]	$-5.^{\circ}0 < \Delta\alpha < 2.^{\circ}8$[e]	N/A	N/A
Section 4.6	Neutrino mass[f]	$w = -1$	$\sum m_\nu < 1.3\,\mathrm{eV}$[c]	$\sum m_\nu < 0.71\,\mathrm{eV}$	$\sum m_\nu < 0.58\,\mathrm{eV}$[g]
		$w \neq -1$	$\sum m_\nu < 1.4\,\mathrm{eV}$[c]	$\sum m_\nu < 0.91\,\mathrm{eV}$	$\sum m_\nu < 1.3\,\mathrm{eV}$[h]
Section 4.7	Relativistic species	$w = -1$	$N_{\rm eff} > 2.7$[c]	N/A	$4.34^{+0.86}_{-0.88}$ (68% CL)[i]
Section 6	Gaussianity[j]	Local	$-10 < f_{NL}^{\rm local} < 74$[k]	N/A	N/A
		Equilateral	$-214 < f_{NL}^{\rm equil} < 266$	N/A	N/A
	Gμ < 1 X 10-7 (ACT)	Orthogonal	$-410 < f_{NL}^{\rm orthog} < 6$	N/A	N/A

Komatsu et al. APJs, 192:18, 2011

See also lack of anomalies claimed in *Bennett et al., ApJs, 2011*

- Situation unchanged with most recent small scale data

	WMAP7	ACBAR+QUaD+WMAP7	ACT+WMAP7	SPT+WMAP7
r	< 0.7	< 0.33	< 0.25	< 0.21
$dn_s/d\ln k$	[-0.084, 0.020]	[-0.084, 0.003]	-0.034 ± 0.018	-0.024 ± 0.013
Y_p	< 0.51	0.326 ± 0.075	0.313 ± 0.044	0.296 ± 0.030
$N_{\rm eff}$	> 2.7	—	5.3 ± 1.3	3.85 ± 0.62

- Planck starts from this lack of surprises/detections...

Conclusions 2/2

- Planck works very well. HFI exceeds expectations.
- HFI survey data collection finishing. EOL Jan 15th, with about twice more data than the nominal 15months.

- First 10 months of data (Aug13th→Jun6th): (re)processing & characterising, producing ERCSC, performing first scientific analysis and publishing, all done in 7 months.
  - *ERCSC (~15 000 sources, 199 SZ clusters in ESZ, 915 in ECC) fulfills expectations; download available from the Planck legacy archive at ESA (and at IPAC too)*
  - *25 papers unveiled at Planck2011 in "La Cité des Sciences", Paris (& AAS) A&A special issue*

- Our model of the data is already good enough to enable some further CMB foregrounds analysis, but not yet fully "cosmology grade".
  - *Intermediate papers on foregrounds expected in early 2012, cosmology & 1st data release early 2013! (final in 2014)*

- PLANCK + ACTPOL/SPTPOL/... + LSS + LHC... + EUCLID! COrE?
- The coming years will continue to be fantastic!

A&A 520, A1 (2010)
DOI: 10.1051/0004-6361/200912983

Pre-launch status of the Planck mission

Astronomy & Astrophysics
Special feature

Planck pre-launch status: The *Planck* mission

J. A. Tauber[36], N. Mandolesi[45], J.-L. Puget[52], T. Banos[82], M. Bersanelli[32], F. R. Bouchet[51], R. C. Butler[45], J. Charra[52], G. Crone[37], J. Dodsworth[38], G. Efstathiou[90], R. Gispert[52], G. Guyot[52], A. Gregorio[93], J. J. Juillet[82], J.-M. Lamarre[66], R. J. Laureijs[36], C. R. Lawrence[61], H. U. Nørgaard-Nielsen[35], T. Passvogel[37], J. M. Reix[82], D. Texier[39], L. Vibert[52], A. Zacchei[46], P. A. R. Ade[6], N. Aghanim[52], B. Aja[18], E. Alippi[84], L. Aloy[37], P. Armand[82], M. Arnaud[7], A. Arondel[52], A. Arreola-Villanueva[61], E. Artal[18], E. Artina[84], A. Arts[37], M. Ashdown[89], J. Aumont[9], M. Azzaro[40], A. Bacchetta[83], C. Baccigalupi[5], M. Baker[37], M. Balasini[84], A. Balbi[33], A. J. Banday[67,12], G. Barbier[64], R. B. Barreiro[58], M. Bartelmann[67,95], P. Battaglia[84], E. Battaner[91], K. Benabed[51], J.-L. Beney[63], R. Beneyton[51], K. Bennett[36], A. Benoit[64], J.-P. Bernard[12], P. Bhandari[61], R. Bhatia[61], M. Biggi[74], R. Biggins[38], G. Billig[38], Y. Blanc[14], H. Blavot[52], J. J. Bock[61], A. Bonaldi[49], R. Bond[13], J. Bonis[63], J. Borders[61], J. Borrill[88], L. Boschini[84], F. Boulanger[52], J. Bouvier[64], M. Bouzit[52], R. Bowman[61], E. Bréelle[4], T. Bradshaw[77], M. Braghin[37], M. Bremer[36], D. Brienza[34], D. Broszkiewicz[4], C. Burigana[45], M. Burkhalter[73], P. Cabella[33], T. Cafferty[61], M. Cairola[83], S. Caminade[52], P. Camus[53], C. M. Cantalupo[65], B. Cappellini[32], J.-F. Cardoso[4], R. Carr[39], A. Catalano[4], L. Cayón[23], M. Cesa[83], M. Chaigneau[52], A. Challinor[90], A. Chamballu[43], J. P. Chambelland[82], M. Charra[52], L.-Y. Chiang[53], G. Chlewicki[83], P. R. Christensen[71], S. Church[24], E. Ciancietta[83], M. Cibrario[83], R. Cizeron[63], D. Clements[43], B. Collaudin[82], J.-M. Colley[4,51], S. Colombi[51], A. Colombo[37], F. Colombo[84], O. Corre[82], F. Couchot[63], B. Cougrand[52], A. Coulais[66], P. Couzin[82], B. Crane[52], B. Crill[61], M. Crook[77], D. Crumb[61], F. Cuttaia[45], U. Dörl[67], P. da Silva[51], R. Daddato[37], C. Damasio[37], L. Danese[5], G. d'Aquino[37], O. D'Arcangelo[60], K. Dassas[52], R. D. Davies[62], W. Davies[73], R. J. Davis[62], P. De Bernardis[34], D. de Chambure[37], G. de Gasperis[33], M. L. De la Fuente[18], P. De Paco[81], A. De Rosa[45], G. De Troia[33], G. De Zotti[49], M. Dehamme[63], J. Delabrouille[4], J.-M. Delouis[51], F.-X. Désert[64], G. di Girolamo[38], C. Dickinson[62], E. Doelling[38], K. Dolag[67], I. Domken[11], M. Douspis[52], D. Doyle[37], S. Du[63], D. Dubruel[82], C. Dufour[4], C. Dumesnil[52], X. Dupac[39], P. Duret[52], C. Eder[63], A. Elfving[37], T. A. Enßlin[67], P. Eng[52], K. English[61], H. K. Eriksen[10,56], P. Estaria[37], M. C. Falvella[2], F. Ferrari[84], F. Finelli[45], A. Fishman[61], S. Fogliani[46], S. Foley[38], A. Fonseca[61], G. Forma[82], O. Forni[12], P. Fosalba[87], J.-J. Fourmond[52], M. Frailis[46], C. Franceschet[32], E. Franceschi[45], S. François[52], M. Frerking[61], M. F. Gómez-Reñasco[57], K. M. Górski[61], T. C. Gaier[61], S. Galeotta[48], K. Ganga[4], J. García Lázaro[39], A. Garnica[61], M. Gaspard[63], E. Gavila[82], M. Giard[12], G. Giardino[36], G. Gienger[38], Y. Giraud-Heraud[4], J.-M. Glorian[12], M. Griffin[6], A. Gruppuso[45], L. Guglielmi[4], D. Guichon[82], B. Guillaume[37], P. Guillouet[4], J. Haissinski[63], F. K. Hansen[10,56], J. Hardy[61], D. Harrison[90], A. Hazell[76], M. Hechler[38], V. Heckenauer[52], D. Heinzer[38], R. Hell[67], S. Henrot-Versillé[63], C. Hernández-Monteagudo[67], D. Herranz[58], J. M. Herreros[57], V. Hervier[52], A. Heske[37], A. Heurtel[63], S. R. Hildebrandt[57], R. Hills[89], E. Hivon[51], M. Hobson[89], D. Hollert[61], W. Holmes[61], A. Hornstrup[35], W. Hovest[67], R. J. Hoyland[57], G. Huey[61], K. M. Huffenberger[92], N. Hughes[34], U. Israelsson[61], B. Jackson[37], A. Jaffe[43], T. R. Jaffe[62], T. Jagemann[39], N. C. Jessen[35], J. Jewell[61], W. Jones[22], M. Juvela[72], J. Kaplan[4], P. Karlman[61], F. Keck[38], E. Keihänen[21], M. King[61], T. S. Kisner[65], P. Kletzkine[37], R. Kneissl[67], J. Knoche[67], L. Knox[26], T. Koch[61], M. Krassenburg[37], H. Kurki-Suonio[21,42], A. Lähteenmäki[68], G. Lagache[52], E. Lagorio[64], P. Lami[52], J. Lande[12], A. Lange[61], F. Langlet[52], R. Lapini[74], M. Lapolla[84], A. Lasenby[89], M. Le Jeune[4], J. P. Leahy[62], M. Lefebvre[52], F. Legrand[51], G. Le Meur[63], R. Leonardi[27], B. Leriche[52], C. Leroy[52], P. Leutenegger[84], S. M. Levin[61], P. B. Lilje[10,56], C. Lindensmith[61], M. Linden-Vørnle[86], A. Loc[61], Y. Longval[52], P. M. Lubin[27], T. Luchik[61], I. Luthold[37], J. F. Macias-Perez[96], T. Maciaszek[14], C. MacTavish[43], S. Madden[37], B. Maffei[62], C. Magneville[8], D. Maino[32], A. Mambretti[84], B. Mansoux[63], D. Marchioro[84], M. Maris[46], F. Marliani[37], J.-C. Marrucho[63], J. Martí-Canales[37], E. Martínez-González[58], A. Martín-Polegre[37], P. Martin[82], C. Marty[12], W. Marty[12], S. Masi[34], M. Massardi[49], S. Matarrese[31], F. Matthai[67], P. Mazzotta[33], A. McDonald[38], P. McGrath[61], A. Mediavilla[18], P. R. Meinhold[27], J.-B. Mélin[8], F. Melot[96], L. Mendes[39], A. Mennella[32], C. Mervier[52], L. Meslier[52], M. Miccolis[84], M.-A. Miville-Deschenes[52], A. Moneti[51], D. Montet[82], L. Montier[12], J. Mora[61], G. Morgante[45], G. Morigi[45], G. Morinaud[52], N. Morisset[59], D. Mortlock[90], S. Mottet[51], J. Mulder[61], D. Munshi[90], A. Murphy[70], P. Murphy[61], P. Musi[83], J. Narbonne[12], P. Naselsky[71], A. Nash[61], F. Nati[34], P. Natoli[33], B. Netterfield[13], J. Newell[61], M. Nexon[12], C. Nicolas[52], P. H. Nielsen[85], N. Ninane[11], F. Noviello[52], D. Novikov[43], I. Novikov[71], I. J. O'Dwyer[61], P. Oldeman[37], P. Olivier[37], L. Ouchet[82], C. A. Oxborrow[35], L. Pérez-Cuevas[37], L. Pagan[84], C. Paine[61], F. Pajot[52], R. Paladini[80], F. Pancher[64], J. Panh[14], G. Parks[61], P. Parnaudeau[51], B. Partridge[41], B. Parvin[61], J. P. Pascual[18], F. Pasian[46], D. P. Pearson[61], T. Pearson[61], M. Pecora[84], O. Perdereau[63], L. Perotto[96], F. Perrotta[5], F. Piacentini[34], M. Piat[4], E. Pierpaoli[20], O. Piersanti[37], E. Plaige[63], S. Plaszczynski[63], P. Platania[60], E. Pointecouteau[12], G. Polenta[1], N. Ponthieu[52], L. Popa[54], G. Poulleau[52], T. Poutanen[21,42,68], G. Prézeau[61], L. Pradell[16], M. Prina[61], S. Prunet[51], J. P. Rachen[67], D. Rambaud[12], F. Rame[83], I. Rasmussen[37], J. Rautakoski[37], W. T. Reach[50], R. Rebolo[57], M. Reinecke[67], J. Reiter[61], C. Renault[96], S. Ricciardi[79], P. Rideau[82], T. Riller[67], I. Ristorcelli[12], J. B. Riti[82], G. Rocha[61], Y. Roche[82], R. Pons[12], R. Rohlfs[59], D. Romero[61], S. Roose[11], C. Rosset[63], S. Rouberol[51], M. Rowan-Robinson[43], J. A. Rubiño-Martín[57], P. Rusconi[84], B. Rusholme[50], M. Salama[61], E. Salerno[15], M. Sandri[45], D. Santos[96], J. L. Sanz[58], L. Sauter[51], F. Sauvage[82], G. Savini[75], M. Schmelzel[61], A. Schnorhk[37], W. Schwarz[61], D. Scott[19], M. D. Seiffert[61], P. Shellard[89], C. Shih[61], M. Sias[83], J. I. Silk[29], R. Silvestri[84], R. Sippel[3], G. F. Smoot[25], J.-L. Starck[8], P. Stassi[96], J. Sternberg[36], F. Stivoli[79], V. Stolyarov[90], R. Stompor[4], L. Stringhetti[45], D. Strommen[61], T. Stute[3], R. Sudiwala[6], R. Sugimura[61], R. Sunyaev[67], J.-F. Sygnet[51], M. Türler[59], E. Taddei[84], J. Tallon[61], C. Tamiatto[52], M. Taurigna[63], D. Taylor[39], L. Terenzi[45], S. Thuerey[37], J. Tillis[61], G. Tofani[44], L. Toffolatti[17], E. Tommasi[2], M. Tomasi[32], E. Tonazzini[15], J.-P. Torre[52], S. Tosti[52], F. Touze[63], M. Tristram[63], J. Tuovinen[69], M. Tuttlebee[38], G. Umana[47], L. Valenziano[45], D. Vallée[4], M. van der Vlis[37], F. Van Leeuwen[90], J.-C. Vanel[4], B. Van-Tent[51], J. Varis[69], E. Vassallo[38], C. Vescovi[64], F. Vezzu[64], D. Vibert[51], P. Vielva[58], J. Vierra[61], F. Villa[45], N. Vittorio[33], C. Vuerli[46], L. A. Wade[61], A. R. Walker[19], B. D. Wandelt[28], C. Watson[38], D. Werner[38], M. White[30], S. D. M. White[67], A. Wilkinson[62], P. Wilson[61], A. Woodcraft[6], B. Yoffo[4], M. Yun[61], V. Yurchenko[70], D. Yvon[8], B. Zhang[61], O. Zimmermann[64], A. Zonca[48], and D. Zorita[78]

(Affiliations can be found after the references)

Received 24 July 2009 / Accepted 12 November 2009

esa

planck

cnes

agenzia spaziale italiana

HFi PLANCK

PLANCK LFI

NASA

CNRS

DTU Space
National Space Institute

INAF ISTITUTO NAZIONALE DI ASTROFISICA

Science & Technology Facilities Council

CSIC
CONSEJO SUPERIOR DE INVESTIGACIONES CIENTÍFICAS

IAS orsay

IAP

INAF - IASF BO
ISTITUTO NAZIONALE DI ASTROFISICA
ISTITUTO DI ASTROFISICA SPAZIALE E FISICA COSMICA DI BOLOGNA

National Research Council of Italy

GOBIERNO DE ESPAÑA
MINISTERIO DE CIENCIA E INNOVACIÓN

CSA ASC

DLR
Deutsches Zentrum für Luft- und Raumfahrt e.V.

UK SPACE AGENCY

MAX-PLANCK-GESELLSCHAFT

A" Aalto University

APC

ioa

KICC Kavli Institute for Cosmology Cambridge

CAVENDISH ASTROPHYSICS

UNIVERSITY OF CAMBRIDGE

CARDIFF UNIVERSITY
PRIFYSGOL CAERDYDD

irfu cea saclay

cea
énergie atomique • énergies alternatives

CESR

CITA–ICAT

CNRS IN2P3
Les deux infinis

ipac
Infrared Processing and Analysis Center

HELSINKI INSTITUTE OF PHYSICS

INSTITUTO ASTROFISICA DE CANARIAS IAC

IFCA
Instituto de Física de Cantabria

Imperial College London

Università degli Studi di Milano

NÉEL institut

IPAG
Institut de Planétologie et d'Astrophysique de Grenoble

ISDC
DATA CENTRE FOR ASTROPHYSICS

JPL

LAL
LABORATOIRE DE L'ACCÉLÉRATEUR LINÉAIRE

l'Observatoire de Paris
LERMA

LPSC Grenoble
Laboratoire de Physique Subatomique et de Cosmologie

MANCHESTER 1824
The University of Manchester

MilliLab

Max-Planck-Institut für Astrophysik

NUI MAYNOOTH

INAF
OSSERVATORIO ASTRONOMICO DI PADOVA

UNIVERSITY OF OXFORD

Dipartimento di Fisica
SAPIENZA
Università di Roma

Science & Technology Facilities Council
Rutherford Appleton Laboratory

Università degli Studi di Roma
TOR VERGATA

OSSERVATORIO ASTRONOMICO TRIESTE

UBC

UC
UNIVERSIDAD DE CANTABRIA

UCSB

SISSA

ALMA

ESO

US
University of Sussex

esa

UNIVERSITY OF HELSINKI

UNIVERSITÉ DE GENÈVE

UNIVERSITY OF TORONTO

UNIVERSITÉ DE PARIS-SUD XI

ISTI
ISTITUTO DI SCIENZA E TECNOLOGIE DELL'INFORMAZIONE "A. FAEDO"

asdc
ASI Science Data Center

The first 25 (a to y)

Title ~250	Authors
Planck early results 01: The Planck mission	Planck Collaboration
Planck early results 02: The thermal performance of Planck	Planck Collaboration
Planck early results 03: First assessment of the Low Frequency Instrument in-flight performance	Mennella et al.
Planck early results 04: First assessment of the High Frequency Instrument in-flight performance	Planck HFI Core Team
Planck early results 05: The Low Frequency Instrument data processing	Zacchei et al.
Planck early results 06: The High Frequency Instrument data processing	Planck HFI Core Team
Planck early results 07: The Early Release Compact Source Catalogue	Planck Collaboration
The Explanatory Supplement to the Planck Early Release Compact Source Catalogue	Planck Collaboration
Planck early results 08: The all-sky early Sunyaev-Zeldovich cluster sample	Planck Collaboration
Planck early results 09: XMM-Newton follow-up for validation of Planck cluster candidates	Planck Collaboration
Planck early results 10: Statistical analysis of Sunyaev-Zeldovich scaling relations for X-ray galaxy clusters	Planck Collaboration
Planck early results 11: Calibration of the local galaxy cluster Sunyaev-Zeldovich scaling relations	Planck Collaboration
Planck early results 12: Cluster Sunyaev-Zeldovich optical scaling relations	Planck Collaboration
Planck early results 13: Statistical properties of extragalactic radio sources in the Planck Early Release Compact Source Catalogue	Planck Collaboration
Planck early results 14: Early Release Compact Source Catalogue validation and extreme radio sources	Planck Collaboration
Planck early results 15: Spectral energy distributions and radio continuum spectra of northern extragalactic radio sources	Planck Collaboration
Planck early results 16: The Planck view of nearby galaxies	Planck Collaboration
Planck early results 17: Origin of the submillimetre excess dust emission in the Magellanic Clouds	Planck Collaboration
Planck early results 18: The power spectrum of cosmic infrared background anisotropies	Planck Collaboration
Planck early results 19: All-sky temperature and dust optical depth from Planck and IRAS – constraints on the "dark gas" in our Galaxy	Planck Collaboration
Planck early results 20: New light on anomalous microwave emission from spinning dust grains	Planck Collaboration
Planck early results 21: Properties of the interstellar medium in the Galactic plane	Planck Collaboration
Planck early results 22: The submillimetre properties of a sample of Galactic cold clumps	Planck Collaboration
Planck early results 23: The Galactic cold core population revealed by the first all-sky survey	Planck Collaboration
Planck early results 24: Dust in the diffuse interstellar medium and the Galactic halo	Planck Collaboration
Planck early results 25: Thermal dust in nearby molecular clouds	Planck Collaboration